UNIVERSIDADE FEDERAL DE PERNAMBUCO

CENTRO DE CIÊNCIAS EXATAS E DA NATUREZA

PROGRAMA DE PÓS-GRADUAÇÃO EM FÍSICA

OSCAR HERNANDO BOHÓRQUEZ MARTÍNEZ

QUANTUM TRANSPORT IN DISORDERED SYSTEMS AND QUANTUM FEEDBACK IN QUBIT SYSTEMS

Recife

2018

OSCAR HERNANDO BOHÓRQUEZ MARTÍNEZ

QUANTUM TRANSPORT IN DISORDERED SYSTEMS AND QUANTUM FEEDBACK IN QUBIT SYSTEMS

Tese apresentada ao Programa de Pós-Graduação em Física do Departamento de Física da Universidade Federal de Pernambuco como parte dos requisitos para obtenção do título de Doutor em Física.

Área de concentração: Óptica-Informação Quântica.

Orientador: Prof. Dr. Antônio Murilo Santos Macêdo

Recife

2018

Catalogação na fonte
Bibliotecária Arabelly Ascoli CRB4-2068

B677q Bohórquez Martínez, Oscar Hernando
Quantum transport in disordered systems and quantum feedback in qubit systems / Oscar Hernando Bohórquez Martínez. – 2018.
137 f.: fig.

Orientador: Antônio Murilo Santos Macêdo.
Tese (Doutorado) – Universidade Federal de Pernambuco. CCEN. Física. Recife, 2018.
Inclui referências e apêndices.

1. Óptica. 2. Informação quântica. 3. Teoria da matriz aleatória. 4. Termodinâmica estocástica. I. Macêdo, Antônio Murilo Santos (orientador). II. Título.

535.2 CDD (22. ed.) UFPE-FQ 2019-28

OSCAR HERNANDO BOHÓRQUEZ MARTÍNEZ

QUANTUM TRANSPORT IN DISORDERED SYSTEMS AND QUANTUM FEEDBACK IN QUBIT SYSTEMS

Tese apresentada ao Programa de Pós-Graduação em Física do Departamento de Física da Universidade Federal de Pernambuco como parte dos requisitos para obtenção do título de Doutor em Física.

Aprovado em: 14/12/2018.

BANCA EXAMINADORA

Prof. Dr. Antônio Murilo Santos Macêdo
(Orientador)
Universidade Federal de Pernambuco

Prof. Dr. Bruno Gerarldo Carneiro da Cunha
(Examinador Interno)
Universidade Federal de Pernambuco

Prof. Dr. Renê Rodrigues Montenegro Filho
(Examinador Externo)
Universidade Federal de Pernambuco

Prof. Dr. André Maurício Conceição de Souza
(Examinador Externo)
Universidade Federal de Sergipe

Prof. Dr. Giovani Lopes Vasconcelos
(Examinador Externo)
Universidade Federal do Paraná

A mi madre y a mi abuela
por su infinito amor.

ACKNOWLEDGEMENTS

For the exciting discussions on so many physics topics. For their guidance and respect at times when efforts seemed to lead nowhere. For so much knowledge given so selflessly. My most sincere thanks to my thesis advisor Antônio Murilo Santos Macêdo.

To my mother and grandmother, for their endless love. To my father and my sisters, for their support when I needed it most. To my brothers-in-law, for the laughter and my nieces and nephews.

To my many friends that I still keep in spite of my neglected personality with such a priceless gift. In Colombia to Charles, Herneider, Dumar, Alejo, Juan Camilo, Juli, Carlitos, Dieguito, Murcia, the whole legion of "ángeles clandestinos", as Jattin wrote in his poem.

To the Colombian "galera" in Brazil. To Ivan and Melissa for welcoming me into their home. To Julian and Wilmer, for the good conversations and the coffee. And especially to Alejo, and to the "Nicolases", the physicist and the mathematician, for the beer and the many talks about physics, politics and amorous disappointments. To my Brazilian friends Yessica, Mariah and Nayara. For the undeserved affection and warm hospitality in that wonderful country.

To Viviana. Thank you for being there so long unconditionally.

To Hellen. Thank you for the intense and beautiful company at that time in Brazil.

To Carla. Thank you for so much care and so much selfless affection.

To the rural and urban workers of Colombia and Brazil, who with their effort sustained my studies and research projects through different scholarships granted by the respective governments.

To the research agencies of the Brazilian state CNPq ("Conselho Nacional de Desenvolvimento Científico e Tecnológico") and CAPES ("Coordenação de aperfeiçoamento de pessoal de nivel superior") that financed my doctorate.

ABSTRACT

In this work we study quantum transport phenomena in two different types of systems. The first type corresponds to so-called complex quantum systems, such as chaotic ballistic cavities and disordered quantum wires, which have a complex distribution of energy levels and transmission eigenvalues. This class of system does not admit a simple description in terms of a fixed Hamiltonian, and therefore we will make a statistical approach of its transport properties through Random Matrices Theory. We obtain exact expressions for the first three moments of the heat conductance of a quantum chain that crosses over from a superconducting quantum dot to a superconducting disordered quantum wire. Our analytic solution provides exact detailed descriptions of some smooth transitions that can be observed in the system as a function of its length, which include ballistic-metallic and metallic-insulating transitions. The two Bogolyubov de Gennes symmetry classes with time-reversal symmetry are accounted for. The striking effect of total suppression of the insulating regime in systems with broken spin-rotation invariance is observed at large length scales. For a single channel system, this anomalous effect can be interpreted as a signature of the presence of the elusive Majorana fermion in a condensed matter system. The second type of system corresponds to qubits, which, unlike complex systems, can be described by very simple Hamiltonians. In this case, we study the properties of open systems using master equations. We present a study of non-equilibrium thermodynamics of qubit systems submitted to quantum control. More specifically, we performed a comparative study of two types of simple two-level non-interacting quantum transport systems coupled to two bosonic and fermionic reservoirs respectively. Each system is submitted to a Wiseman-Milburn type feedback scheme in the formulation of stochastic thermodynamics. We see the effects of finite temperature and time delay on two specific feedback applications: a heat pump and a purification protocol. We observed a clear signature of the purity of the qubits in the Full Counting Statistics observed in the current flowing through the system.

Keywords: Quantum transport. Random Matrix Theory. Quantum feedback. Stochastic thermodynamics.

RESUMO

Neste trabalho estudamos fenômenos de transporte quântico em dois diferentes tipos de sistemas. O primeiro corresponde aos chamados sistemas quânticos complexos, como cavidades balísticas caóticas e fios quânticos desordenados, que possuem uma distribuição complexa de níveis de energia e de autovalores de transmissão. Estos sistemas não admitem uma descrição simples em termos de um hamiltoniano fixo, e portanto faremos uma abordagem estatística das propriedades de transporte através da teoria da matrizes aleatórias. Obtivemos expressões exatas para os três primeiros momentos da condutância térmica de uma cadeia quântica que interpola entre um ponto quântico supercondutor e um fio quântico desordenado supercondutor. Nossa solução analítica fornece descrições detalhadas exatas de algumas transições suaves que podem ser observadas no sistema em função de seu comprimento, que incluem transições balístico-metálico e metálico-isolante. As duas classes de simetria de Bogolyubov de Gennes com simetria de inversão de tempo são contabilizadas. O efeito marcante da supressão total do regime de isolamento em sistemas com invariância de rotação quebrada é observado em grandes escalas de comprimento. Para um sistema de canal único, esse efeito anômalo pode ser interpretado como uma assinatura da presença de um férmion de Majorana em um sistema de matéria condensada. O segundo tipo de sistema corresponde a qubits, que ao contrário dos sistemas complexos, podem ser descritos por hamiltonianos simples. Neste caso, estudamos propriedades de sistemas abertos usando equações mestras. Apresentamos um estudo da termodinâmica de não-equilíbrio de sistemas de qubits submetidos a controle quântico. Especificamente, fizemos um estudo comparativo de dois tipos de sistemas de transporte quântico simples não interagentes de dois níveis acoplados a dois reservatórios bosônicos e fermiônicos respectivamente. Cada sistema é submetido a um esquema de realimentação do tipo Wiseman-Milburn, no âmbito da formulação da termodinâmica estocástica. Vemos os efeitos da temperatura finita e do tempo de atraso em duas aplicações específicas do feedback: uma máquina de bombeamento e um protocolo de purificação. Observamos uma clara assinatura da pureza dos estados nos qubits na estatística de contagem observada na corrente que atravessa o sistema.

Palavras-chave: Transporte quântico. Teoria de matriz aleatória. Feedback quântico. Termodinâmica estocástica.

CONTENTS

1 INTRODUCTION

Research in quantum physics has been consolidated for almost a century as a broad and prolific field of theoretical, experimental, and even philosophical exploration, with surprising and outstanding results for science as a whole. Phenomena such as quantum entanglement at great distances, the tunneling effect, or quantum superposition in cases like the Schrödinger cat, just to mention a few of those that have become popular, continue to surprise not only the scientific community but also the general public, thanks to the effort of science communication via widespread media. All this is further enhanced by predictions about the possibilities of quantum technologies, some already realized, such as quantum cryptography and superconductivity-based magnetic levitation of trains; and others that are still under intensive research, such as perhaps the most awaited and spectacular of them all: the universal quantum computer.

In a nutshell, the general aim of quantum physics research is to rethink everything from the quantum perspective, which goes as far as to include a description of the fundamental units of both the physical systems (particles) and its information content (qubits). For example, there is not problem about the measurement in classical systems, since the act of measuring a physical property in a macroscopic system does not significantly alter the state of the system. However, when quantum effects are relevant, the act of measuring a physical observable does significantly affect the state of the system and this context dependence needs to be included explicitly in the theoretical construction. Much has been speculated and debated about the profound meaning of this state of affairs but no consensus has been reached yet, since it essentially involves a choice among several equally valid interpretations of quantum mechanics [Schlosshauer 2005, Burgos 2015]. The same applies to thermodynamics, which at the macroscopic level has an well established set of universal laws that have been consistently validated over the years through a huge amount of experiments in various regimes and appears to have a broad domain of validity that extends even beyond physics. Nevertheless, in the quantum domain the predictions of thermodynamics are valid

only on average, which is expected since the theory was constructed to describe macroscopic properties. This opens the possibility of extending the theory to describe quantum fluctuations of thermodynamic quantities, such as heat and work. Different interpretations of quantum thermodynamics have been advanced and include fundamental questions like: What is the meaning of quantum work? How can entropy and information be defined? [Talkner e Hänggi 2016, Funo e Quan 2018].

In this dissertation we address several issues related to the field of quantum transport, which was reformulated from the traditional classical approach to be understood in the framework of quantum physics. In this construction, fundamental questions were raised, such as: Is there a quantum of resistance or conductance? What is measured when you measure a resistance? [Stone e Szafer 1988] What about correlations and moments? Much progress has been made in answering these questions, but quantum transport remains a very active field of research with many open problems [Mello et al. 2004]. In this introduction we shall discuss some results related to these questions and in the process we will give the proper context to the subjects investigated in this work.

We start with the most basic physical transport phenomenon: the transfer of charge through a conductor. Ohm's law establishes that in metals, the electric current I is directly proportional to the applied voltage V

$$V = IR \quad \text{or} \quad I = GV, \tag{1.1}$$

where R and G are defined as the resistance and the conductance respectively, and $G = 1/R$. In a sample of length L, and constant cross section A, the conductance is given by

$$G = \frac{\sigma A}{L}, \tag{1.2}$$

where σ is the conductivity; an intensive quantity that depends on the microscopic characteristics of the material such as the electronic density and the mean free path. But what happens when the length of the material is very small? Can one expect an indefinitely large conductance and zero resistance? [Houten e Beenakker 2005, Beenakker e Houten 1991]

The answer came in 1988, when two groups reported the variation of conductance in steps defined in the form of a ladder, which suggested a quantization of conductance, and therefore of resistance [Wees et al. 1988, Wharam et al. 1988]. The experiment can be described as follows: A 2D electron gas, at the interface of a heterojunction of GaAs-AlGaAs is subjected to a potential difference between two contacts so that it passes through a small constriction of size of the same order as the Fermi wavelength λ_F of the electron gas. This allows there to be ballistic transport through the constriction, which can be studied by varying a gate voltage applied transversally. By varying the width W of the constriction through the gate voltage (see figure 1a) we can change the number of transverse modes that are connected to open transport channels. This kind of setup is called a quantum point contact. The experimental result obtained was that the conductance varies in steps of $2e^2/h$, as the gate voltage is increased, in temperatures near $0K$; and that the steps are flattened with the increase of the temperature, as shown in the figure 1b. This and other experiments defined the step or quantum of conductance and resistance, being

$$G_0 = \frac{2e^2}{h} = \frac{1}{12.5k\Omega}. \tag{1.3}$$

This result is theoretically justified by the Landauer formalism, and can be interpreted as an indication of the existence of a minimum of resistance in the ballistic conduction through a single channel, given by $12.5k\Omega$.

There are many systems in which the phenomenon of quantum transport can be studied. A paradigmatic one, for its simplicity, is the resonant double barriers, which consists of two potential barriers connecting two electron reservoirs through a conducting region called a quantum dot (see figure 2). As a quantum system, the dot has a specific amount of discrete energy levels, which can be in resonance with the transport modes of electrons passing through the structure. The potential barriers are characterized by the transition rates Γ_L, Γ_R that depend on the tunneling probabilities T_L, T_R of each barrier $\Gamma_{Ln,Rn} = \hbar\nu_n T_{L,R}$, where ν_n is the frequency of the n-th resonant level.

One of the most important theoretical result for this system states that the average current through the quantum dot, due to chemical potential gradients

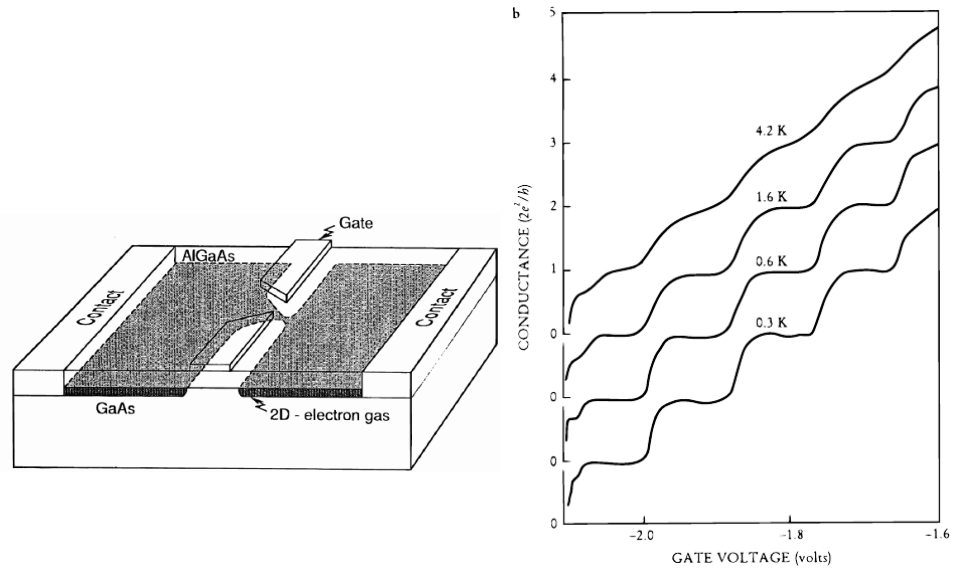

(a) (b)

Figure 1 – (a) Schematic representation of the conductance measurement experiment of a quantum point contact. Note that the flux is longitudinal, going from one contact to the other, and the transversal gate voltage controls the width W of the constriction. (b) Quantization of the conductance of an electron flux through a quantum point contact. As the negative voltage gate increases, so does the number of open channels in the constriction [Houten e Beenakker 2005].

between the reservoirs, at zero temperature, is

$$I = \frac{e}{\hbar} \sum_{n=1}^{N} \frac{\Gamma_{Ln}\Gamma_{Rn}}{\Gamma_{Ln} + \Gamma_{Rn}}. \tag{1.4}$$

This result can be derived both by using the Landauer formalism and via the master equation approach. It has been applied successfully, in its finite temperature version, to the analysis of experimental data of charge transport through molecules [Garrigues et al. 2016].

Another paradigmatic system with its transport properties widely studied are the ballistic cavities. The setup consists of cavities coupled to two or more electronic reservoirs, through waveguides that can transport a certain number of scattering modes. Within the cavity all scattering is caused by the boundaries,

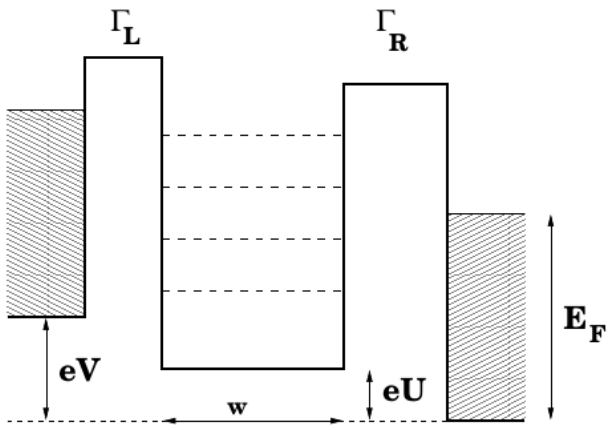

Figure 2 – Schematic view of a quantum dot isolated by two barriers connected to two reservoirs at different chemical potentials. The difference between these chemical potentials arises from the application of a voltage between the reservoirs [Blanter e Büttiker 2000].

so the electrons move in a ballistic way (see figure 3a). Random matrix theory predicts that the mean value and the variance of the conductance of a ballistic chaotic cavity with N scattering channels are given respectively by

$$\langle G \rangle = \frac{2e^2}{h}\left[\frac{N}{2} + \frac{\beta - 2}{4\beta} + \mathcal{O}\left(N^{-1}\right)\right], \quad \mathrm{var}(G) = \frac{e^4}{2\beta h^2}. \tag{1.5}$$

The first term of the mean conductance coincides with the value of the classical conductance, while the second term is a quantum correction, called weak localization, which results from coherent interferences between the optical paths of the electron wavefunction. The factor β is a constant that depends on some discrete symmetries of the system, as we will see later. Now we will only mention that if the system is invariant under time reversion, then $\beta = 1$ and thus the effect of weak location generates a decrease in conductance. This has indeed been corroborated experimentally by applying a weak magnetic field to the cavity, since it breaks the time-reversal symmetry [Keller et al. 1996].

In the figure 3b one can see that just when the magnetic field is zero, i.e. the only point at which time-reversal symmetry is preserved, a fall in conductance is observed, as can be deduced from the equation 1.5. The most remarkable feature of the variance is the fact that it depends only on universal constants and

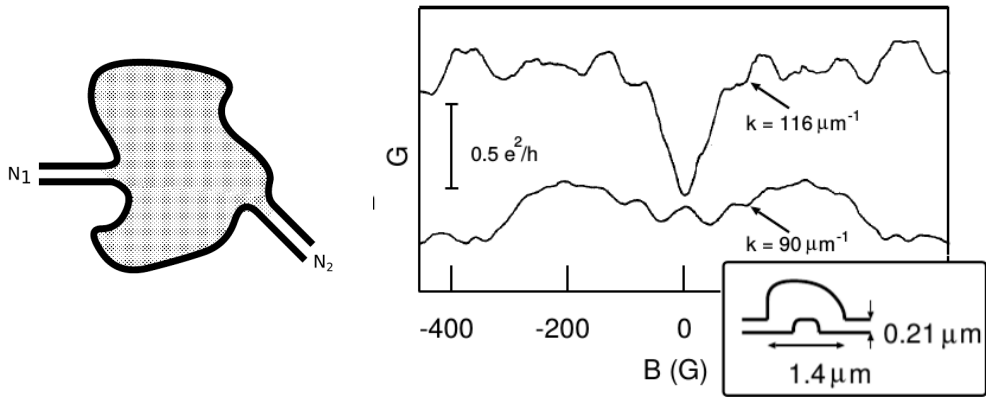

(a) (b)

Figure 3 – (a) Representation of a ballistic cavity coupled to two reservoirs, through two leads that sustain N_1 and N_2 scattering channels respectively [Brouwer 1997]. (b) Experimental variation of the conductance with respect to changes in an external magnetic field, applied to a cavity shaped like a "stomach" (inset) [Keller et al. 1996].

symmetry parameters. This phenomenon became known as universal conductance fluctuations, a hallmark of mesoscopic physics.

Introducing these devices helps us to contextualize the systems that will be dealt with in this work. On the one hand, there are complex systems, which, as in the case of ballistic cavities, have a complex distribution of energy levels and transmission eigenvalues, that do not admit of a simple description in terms of a fixed Hamiltonian. On the other hand, we have simple systems like the resonant double barriers with a configuration of energy levels that can be modeled by a simple Hamiltonian. Different types of systems need different approaches, so for quantum complex systems, we will use Random Matrix Theory (RMT) for the scattering matrix, since it can describe their universal properties, which in general, do not depend on their specific geometrical configuration. For simple systems, we will use the matrix density formalism of open systems, that is, the master equation formalism, which has a consistent thermodynamic construction in the regime of Markovianity, namely stochastic thermodynamics.

This Thesis is divided into two main parts. The first part, chapters 2 and 3, deals with complex systems. The second part, concerning simple two-level

systems, is dealt with in Chapters 5 and 6. In chapter 2 we briefly review RMT for scattering matrices in the framework of the Ten-Fold Way, which is a classification scheme in terms of all the ten possible general symmetries of physical systems. Then, we apply a classification scheme for the Brownian motion ensembles of random matrix theory, which together with a multivariate integral transform method, both introduced in [Macedo-Junior e Macêdo 2006], are used to solve analytically the problem presented in chapter 3.

In chapter 3 we employ RMT to study two classes of superconducting dot-wire systems. We obtain, in the continuum limit of a quantum chain with time-reversal symmetry, an exact description of thermal conduction of the crossover between a superconducting chaotic ballistic cavity (a quantum dot) and a disordered multichannel superconducting quantum wire. The calculations were guided by the classification scheme of RMT Brownian-motion ensembles and were performed by means of the multivariate integral transform method referred to in Chapter 2. More specifically, we obtain exact expressions for the first three moments of the heat conductance. The analytic solution describes in detail various types of smooth transitions as a function of the systems' length, which include ballistic-metallic and metallic-insulating transitions. If the system is realized as a single channel topological superconductor with broken spin-rotation invariance, we can interpret the total suppression of the insulating regime as a signature of the presence of a condensed matter Majorana fermion.

In chapter 4 we review the formalism of master equations for open quantum systems. More specifically, we study approximations that result in a Markovian master equation, or Lindblad equation. It allows for a consistent description of the thermodynamics of open quantum systems and is directly related to the stochastic thermodynamics approach of classical systems. Based on this formalism, we will describe a quantum control protocol that has been generically called Wiseman-Milburn feedback, and we shall include the technique of Full Counting Statistics in the formalism of master equations.

In chapter 5 we apply the formalism described in chapter 4 to a system that consists of a qubit coupled to two reservoirs and consider two types of reservoirs: fermionic and bosonic. These systems could physically correspond, in

the fermionic case, to a quantum dot coupled to two electronic reservoirs; and in the bosonic case, to a two-level system coupled to two reservoirs of photons (or phonons). On each system we consider the Wiseman-Milburn feedback quantum control operation to execute two tasks: a heat pump and a purification protocol. We make a comparative analysis of the efficiency of these tasks for each system and we obtain a clear signature on the Full Counting Statistics for the maximum efficency.

2 COHERENT QUANTUM TRANSPORT

The term “mesoscopic” was introduced in the early 1980s as a way to refer to systems whose size lies between extreme quantum systems and classical macroscopic systems [Nazarov e Blanter 2009]. These systems are large enough to generate robust universal statistics for their physical transport properties, but still small enough to preserve some relevant quantum effects. Typically, they consist of devices of the order of nanometers, although this characterization became somewhat restrictive since larger systems can also exhibit quantum coherence effects. As a matter of fact, transport properties of micron-scale contacts in semiconductor heterostructures have been shown to be the same as metallic contacts consisting of one or a few atoms. So, the study of quantum phenomena related to transport properties is now generically known as quantum transport and has become a broad and active field of both experimental and theoretical research [Mello et al. 2004, Nazarov e Blanter 2009].

When we refer to complex systems, we mean systems that have a complex distribution of energy levels and transmission eigenvalues. This property is shared by ballistic cavities and disordered systems. Disorder in a material generates multiple scatterings when particles are transported across its medium, defining its conduction properties. Two different types of disorder can be identified depending on the type of scattering [Khalaf 2017]. Static disorder arises from elastic scattering, since it preserves the coherence of the phase of the wave functions during collisions, even when averages are made over many realizations, thus in this type of disorder quantum coherence events will survive. This type of disorder is characterized by the mean free path l_e, which broadly is the average distance between scattering centers, therefore it depends on the concentration of disorder in the material. The other type of disorder is generated from inelastic scattering coming from thermal excitations or interactions between different degrees of freedom of the system. This disorder generates randomness in the wave function phase each time a collision occurs, which in turn generates a loss of coherence as more and more collisions occur. We can characterize this type of disorder by the

dephasing length l_ϕ, which is the characteristic length for coherence loss. Thus, for distances greater than l_ϕ, the system behaves quasi classically. Unlike the mean free path, the dephasing length depends on several parameters of the system and normally decreases with temperature. Therefore, it is expected that at low temperatures there are two well separated intrinsic scales in the system, $l_\phi \gg l_e$, and then there will be quantum effects associated with coherence phenomena, such as the weak localization effect and universal conductance fluctuations.

There are other quantities that help us characterize transport regimes in complex quantum systems. For instance, the disorder parameter $\delta_p = 1/k_F l_e$ for a metallic system of Fermi wave-vector magnitude k_F, has a critical value above which Anderson localization sets in and the system becomes an insulator. It is worth noting that δ_p is used as an effective expansion parameter in many-body diagrammatic perturbation theory of weakly disordered systems [Altshuler 1985, Lee e Stone 1985]. One could also consider the diffusion constant $D_e = v_F l_e/3$ (for 3D systems), where $v_F = \hbar k_F/m$ is the Fermi velocity, which together with the dephasing time $\tau_\phi = l_\phi/v_F$, defines the Thouless length $L_T = (D_e\tau_\phi)^{1/2} \equiv \sqrt{(1/3)l_\phi l_e}$. The length L_T corresponds to the distance through which a particle diffuses before losing its phase coherence. Again, at low temperatures we usually have $l_e < L_T < l_\phi$.

In terms of these length scales, different limits or coherent transport regimes can be defined depending on the relative value of the length L of the sample (for weak disorder $\delta_p = 1/k_F l_e \ll 1$) [Mello et al. 2004]. We give below a short list of the most common transport regimes.

- Ballistic: $L \ll l_e, l_\phi$. In this regime, the particles propagate ballistically, i.e. without scattering of any kind in the bulk of the sample. There is scattering only at the boundaries and thus coherence effects are relevant. This is valid, for instance, in chaotic cavities or quantum dots defined on high-mobility heterostructures.

- Diffusive: $l_e \ll L < L_T$. In this regime, the particles diffuse through the sample undergoing elastic collisions, or even a few inelastic scattering,

so that coherent transport is prevalent. Disordered quantum wires are prototypical examples of systems with this kind of transport.

- Macroscopic: $l_e \ll L_T \ll L$. Due to the increase of inelastic collisions, it is generally expected that the transport will eventually lose its coherent properties as the length increases, so in this regime the system will behave quasi classically.

There are other interesting quantities that help characterize quantum transport: in the diffusive regime the ergodic time $\tau_{erg} = L^2/2D_e$ is defined as the time it takes a particle to diffuse throughout the entire sample. In the ballistic regime we have $\tau_{erg} \sim L/v_F$, and is defined the dwell time, which is the time during which a confined particle remains in the system: $2\pi\hbar/\tau_{dwell} = \delta \sum_n T_n$, where δ is the mean level spacing, and T_n is the tunnel probability of mode n [Beenakker 1997].

2.1 From classical to quantum phase coherent transport

The Drude model [Ashcroft e Mermin 1976] was the first transport model to successfully describe conductance phenomena in materials. Proposed in 1900 as an application of classical kinetic theory, it interprets transport of a particle through a sample as a succession of random scatterings due to disorder, between which the particle moves freely (see figure 4). Of course, the particle's trajectory was assumed to be purely classical. This model can be summarized as follows:

The equation of motion of an electron subject to an electric field $\mathbf{E}$ and scattered at random times, with τ being the average time between scattering events, is

$$\dot{\mathbf{p}} = -e\mathbf{E} - \frac{\mathbf{p}}{\tau}. \tag{2.1}$$

The average time, also called relaxation time is related to the mean free path through $l_e = v\tau$, where v is the average electron velocity, which in a low temperature metal is very close to the Fermi velocity. In the steady state, $\dot{\mathbf{p}} = 0$, and

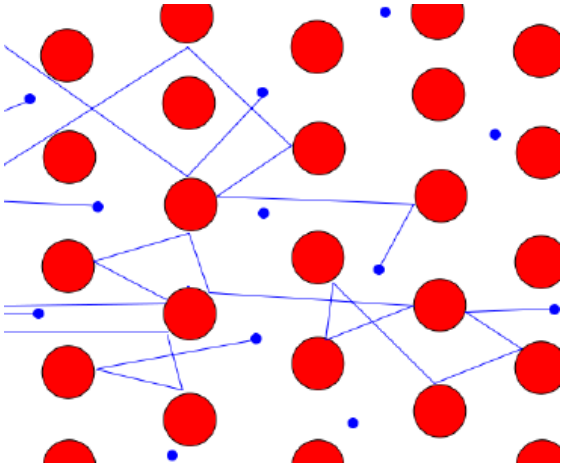

Figure 4 – Schematic representation of the Drude model. Particles are diffused throughout the medium between scatterers and have free movement between impurities [Wikipedia contributors 2018].

we have $\mathbf{p} = -e\mathbf{E}\tau$. Using the definition of current density $\mathbf{J} = -en_e\mathbf{v}$, where n_e denotes the electronic density, one obtains Ohm's law

$$\mathbf{J} = \sigma\mathbf{E}, \quad \sigma = \frac{e^2 n_e \tau}{m}. \tag{2.2}$$

The main feature of this equation is the prediction that the conductivity σ is proportional to the relaxation time, or equivalently, to the mean free path. Other approaches, such as the Boltzmann equation, which is also classical [Emary 2009], or the Sommerfeld model [Ashcroft e Mermin 1976], which incorporates quantum statistics, also predict Ohm's law with Drude's conductivity, albeit the interpretation of τ is model dependent.

As discussed above, in quantum systems it is necessary to take into account the quantum effects associated with partial wave interferences between the different optical paths of the particle in its transport process. This is the case of the weak localization effect, in which the self-interference between the forward scattering and backscattering trajectories of a particle, besides the interference with other particles, generates quantum corrections to the expected classical conductance that goes beyond a simple renormalization of Drude's formula. To see this in a simple argument, note first that quantum mechanics establishes that the probability of a particle to be transported between two points, is the square

norm of the sum of the amplitudes of all possible paths connecting the two points

$$P = \left| \sum_{\text{paths } P} A_P \right|^2 = \sum_{\text{paths } P,P'} A_P A_{P'}^* = \sum_{\text{paths } P} |A_P|^2 + \sum_{\text{paths } P \neq P'} A_P A_{P'}^*. \quad (2.3)$$

The first term in the right hand side of the latter equation corresponds to the classical probability, and the second term is the quantum correction coming from wave interference. Many particles subject to multiple scatterings will have completely random phases, so on average, these interference terms will be canceled out, which leads to a classical Drude-like behavior. However, a few trajectories will have backscattering contributions, as shown in figure 5.

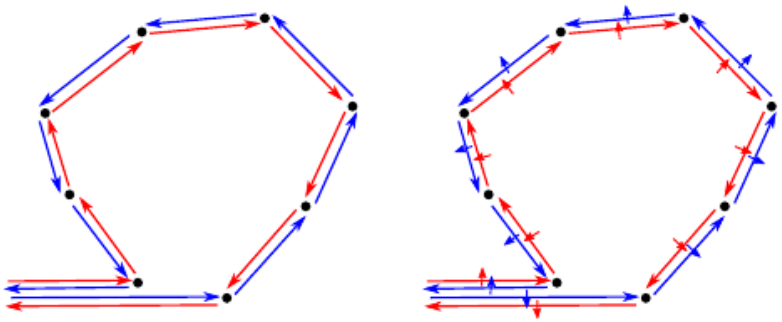

Figure 5 – Schematic representation of a scattering trajectory self-interfering coherently. To the left (right) there is presence (absence) of spin-orbit coupling in the material [Khalaf 2017].

Let us assume that the system has time reversal symmetry. If the material has spin rotation symmetry, the forward scattering and backscattering trajectories will interfere with the time reversal trajectories in such a way that they will reinforce the probability of backscattering (left of the figure 5), which generates a negative contribution to conductance, since it provides a tendency for the particle to localize as it was shown in the equation 1.5 for $\beta = 1$. This is the phenomenon known as the weak localization effect. In the case of materials that have significant spin-orbit coupling (as we will see later this corresponds to a symmetry factor $\beta = 4$), the electron spin direction is coupled to the momentum direction, as we see from the scheme on the right of the figure 5. Trajectories with opposite

spin generate destructive interference, leading a negative sign in the quantum correction of the equation 2.3, so that the backscattering effect is canceled, and the conductance increases implying a weak anti-localization effect [Bergmann 1984]. When time reversal symmetry is broken (symmetry factor $\beta = 2$), e.g. by applying a magnetic field, these localization effects are lost. Therefore these interference effects are highly sensitive to magnetic fields, as was discussed for ballistic cavities in the introduction. The phenomena of weak localization can be understood as a precursor of the "strong" Anderson localization.

The Anderson localization phenomenon [Evers e Mirlin 2008] is the effect by which the diffusion of a particle is totally suppressed in a random potential, on account of quantum interferences. Also known as strong localization, in general it depends on the degree of disorder in the material. Qualitatively, although this effect is predicted for 1D and 2D materials in any degree of disorder, for 3D materials there is a critical disorder at which the transition from conductor to insulator happens. The phenomena predicted by Anderson in 1958 [Anderson 1958], only had a systematic and consistent description in the seminal papers [Edwards e Thouless 1972, Abrahams et al. 1979] where the scaling theory of localization is introduced, describing the conductance in a material in terms of the sample size length L

$$\beta(G(L)) = \frac{d \ln G(L)}{d \ln L}. \tag{2.4}$$

The $\beta(G)$ function provides a good phenomenological model for different conduction regimes in various dimensions, but a rigorous description requires the full language of renormalization group theory. In the diffusive regime, Ohm's law establishes that the conductance varies as $G(L) = \sigma L^{d-2}$, which implies that $\beta(G) = d-2$ when the Thouless parameter $t \equiv \ln G(L)$ is long. On the other hand, in the Anderson localization regime, when the conductance falls exponentially $G \propto e^{-L/\xi}$ in a localization length ξ, the $\beta(G)$-function is $\beta(G) = \ln(G) \propto -L/\xi$, leading to the shape of the graph shown in the figure 6. It can be shown that when the $\beta(G)$-function vanishes, the renormalization-group flow has an unstable fixed point and the system exhibits a metal-insulating transition. For 1D and 2D systems we see that there is no such transition, i.e. these systems always have Anderson localization. For 3D systems there is a critical value $\beta(G) = 0$ at which

the Anderson transition occurs and the system may exhibit metallic diffusive behavior.

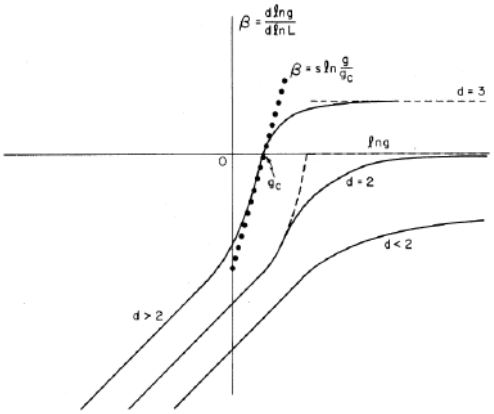

Figure 6 – $\beta(G)$-function of the scaling theory of localization for $d = 1, 2, 3$ dimensions. [Abrahams et al. 1979].

Another effect that has its origin in quantum coherence and which has no classical analogue, is the universal conductance fluctuations [Lee, Stone e Fukuyama 1987]. It was found for mesoscopic samples that, when an external parameter is varied, such as a magnetic field or the Fermi energy, the fluctuations of the measured conductance have approximately the same value for different systems, of the order of e^2/h. Furthermore, when the number of samples of a given measurement is varied, the fluctuations present the same value. In the figure 7 we show typical fluctuations for three different systems. Note that similar behavior is observed for fluctuations in the same sample by varying different parameters, thus showing its universal character. Of course, outside the quantum regime, as the size increases, the fluctuations decrease, until eventually, at the thermodynamic limit, they become insignificant.

Despite the good qualitative description of the Anderson localization transition provided by the phenomenological single parameter scaling theory, it is desirable to have a full fledged microscopic theory that explains transport phenomena in all regimes and provides non-perturbative quantitative results that can be tested experimentally. One important approach in this direction is scattering matrix theory.

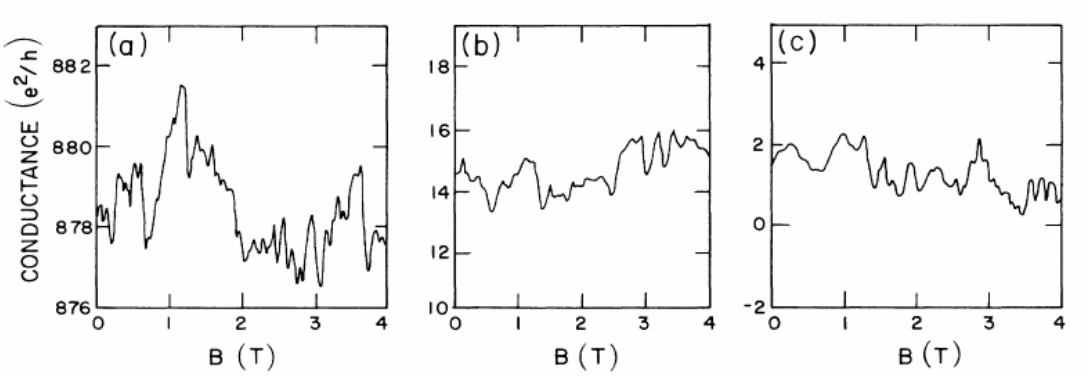

Figure 7 – Comparison of conductance fluctuations for three different samples [Lee, Stone e Fukuyama 1987].

2.2 Scattering Matrix Theory

The scattering matrix formalism provides a natural framework for the description of phase-coherence transport properties in quantum systems, since it allows a description in terms of the probabilities of transmission of the electron wave functions through the sample [Datta 1997]. It brings a quantum treatment that accounts for the interferences between wave functions to describe transport phenomena with phase coherence.

Consider a disordered region, through which electrons are propagated, due to the difference in temperature and/or chemical potential between two electronic reservoirs, connected to the sample via ideal leads

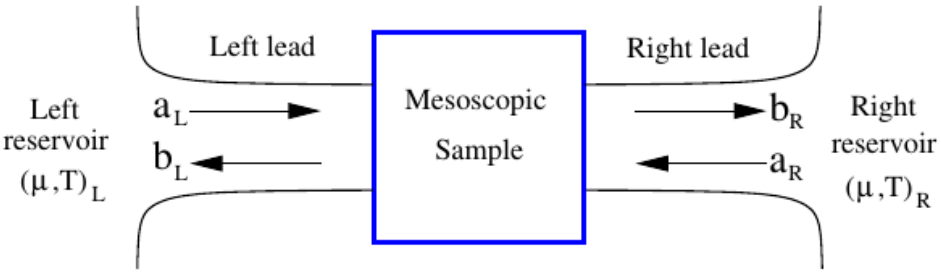

Figure 8 – Mesoscopic sample over which electrons are scattered. The amplitudes of the scattering channels are indicated as $a_{L,R}$, $b_{L,R}$ according to their direction of propagation [Emary 2009].

The wave function of an electron in a lead is

$$\psi_n^{\pm} \sim \chi_n \exp(ik_n x) \tag{2.5}$$

where χ_n is the transverse component, and defines the propagation modes, or quantized scattering channels $n = 1, 2, ..., N$; k_n is the longitudinal moment along of the longitudinal direction of the lead. The wave functions of the incident and reflected particles can be written on the basis of the amplitudes of each of the N_L and N_R modes on the left (L) and right (R) leads (see figure 8). Let us collect the incident and the reflected wave functions in two vectors, respectively

$$\mathbf{a} = (a_{L1}, ..., a_{LN_L}, a_{R1}, ..., a_{RN_R})^T \quad \text{and} \quad \mathbf{b} = (b_{L1}, ..., b_{LN_L}, b_{R1}, ..., b_{RN_R})^T. \tag{2.6}$$

The scattering $\boldsymbol{S}$-matrix relates these vectors

$$\mathbf{b} = \boldsymbol{S}\mathbf{a}, \tag{2.7}$$

and can be written in a block structure

$$\boldsymbol{S} = \begin{pmatrix} \boldsymbol{r} & \boldsymbol{t} \\ \boldsymbol{t}' & \boldsymbol{r}' \end{pmatrix}, \tag{2.8}$$

where the matrices $\boldsymbol{r}$ and $\boldsymbol{r}'$ contain the probability amplitudes for a particle to be reflected on the right or the left of the sample; and the matrices $\boldsymbol{t}'$ and $\boldsymbol{t}$, the probability amplitudes for the transmission from the left to the right and vice-versa, respectively. The $\boldsymbol{S}$-matrix is unitary due to the conservation of the probability current and has dimension $(N_L + N_R) \times (N_L + N_R)$.

The electron reservoirs are considered macroscopically large, in thermal equilibrium, and are characterized by their temperature T and their chemical potential μ. The distribution of the thermalized electrons in the reservoirs correspond to the Fermi distribution

$$f(E) = \frac{1}{\exp((E - \mu)/k_B T) + 1}. \tag{2.9}$$

2.2.1 Landauer-Büttiker formalism

The Landauer-Büttiker formalism makes use of scattering matrix theory to describe quantum transport phenomena [Datta 1997]. Originally developed

by Landauer for the two terminals problem, it was generalized by Buttiker for N terminals [Stone e Szafer 1988]. In the second quantization formalism, the amplitudes in the equation 2.6 are related to the creation $\hat{a}^{\dagger}_{Ln_L}$, $\hat{b}^{\dagger}_{Ln_L}$ and annihilation $\hat{a}_{Ln_L}$, $\hat{b}_{Ln_L}$ electron operators, in such a way that

$$\hat{\mathbf{b}} = \hat{\boldsymbol{S}}\hat{\mathbf{a}}, \tag{2.10}$$

$$\hat{\mathbf{a}} = (\hat{a}_{L1}, ..., \hat{a}_{LN_L}, \hat{a}_{R1}, ..., \hat{a}_{RN_R})^T, \quad \hat{\mathbf{b}} = (\hat{b}_{L1}, ..., \hat{b}_{LN_L}, \hat{b}_{R1}, ..., \hat{b}_{RN_R})^T. \tag{2.11}$$

Using the standard form of the probability current operator

$$\hat{I}_{\mathrm{L}}(z,t) = \frac{\hbar e}{2\mathrm{i}m}\int \mathrm{d}\boldsymbol{r}_{\perp}\left[\hat{\Psi}^{\dagger}_{\mathrm{L}}(\boldsymbol{r},t)\frac{\partial}{\partial z}\hat{\Psi}_{\mathrm{L}}(\boldsymbol{r},t) - \left(\frac{\partial}{\partial z}\hat{\Psi}^{\dagger}_{\mathrm{L}}(\boldsymbol{r},t)\right)\hat{\Psi}_{\mathrm{L}}(\boldsymbol{r},t)\right], \tag{2.12}$$

and the field operators of the second-quantization formalism

$$\hat{\Psi}_{\mathrm{L}}(\boldsymbol{r},t) = \int \mathrm{d}E\mathrm{e}^{-\mathrm{i}Et/\hbar}\sum_{n=1}^{N_{\mathrm{L}}(E)}\frac{\chi_{\mathrm{Ln}}(\boldsymbol{r}_{\perp})}{(2\pi\hbar v_{\mathrm{Ln}}(E))^{1/2}}\left[\hat{a}_{\mathrm{Ln}}\mathrm{e}^{\mathrm{i}k_{\mathrm{Ln}}z} + \hat{b}_{\mathrm{Ln}}\mathrm{e}^{-\mathrm{i}k_{\mathrm{Ln}}z}\right], \tag{2.13}$$

with $k_{\mathrm{Ln}} = (2m(E - E_{\mathrm{Ln}}))^{1/2}/\hbar$ and $v_{\mathrm{Ln}} = \hbar k_{\mathrm{Ln}}/m$, can be shown [Blanter e Büttiker 2000] that the probability current operator through one of the leads (the left in this case and away from the sample, see figure 8), is given by

$$\hat{I}_L(t) = \frac{e}{2\pi\hbar}\sum_n \int dE(\hat{n}^{+}_{Ln}(E,t) - \hat{n}^{-}_{Ln}(E,t)), \tag{2.14}$$

where $\hat{n}^{\pm}_{Ln}(E,t)$ are the time-dependent occupation numbers for incident and reflected electrons in the mode n on the left lead. It is quite intuitive to have the probability current as the difference between the occupations of the incoming and outgoing electrons. Taking the average of the probability current operator, one can find its relation with the non-diagonal blocks of the scattering matrix

$$\langle\hat{I}_L(t)\rangle = \frac{e}{2\pi\hbar}\sum_n \int dE\,\mathrm{Tr}\big[\boldsymbol{t}^{\dagger}(E)\boldsymbol{t}(E)\big](f_L(E,t) - f_R(E,t)). \tag{2.15}$$

Assuming small bias and temperature (linear response), it was shown that the electrical conductance is given by

$$G = G_0\,\mathrm{Tr}\big[\boldsymbol{t}^{\dagger}\boldsymbol{t}\big] = G_0\sum_i T_i, \quad \text{where} \quad G_0 = \frac{e^2}{h} \tag{2.16}$$

is the quantum of the electrical conductance. Note that this latter expression was written in terms of the eigenvalues T_i of the matrix $\boldsymbol{t}^\dagger\boldsymbol{t}$, which is basis independent. In the same way, assuming the same chemical potential in the two reservoirs, and a small difference of temperatures δT; the thermal conductance can be expressed as

$$G = G_0 \operatorname{Tr}\left[\boldsymbol{t}^\dagger\boldsymbol{t}\right] = G_0 \sum_i T_i, \quad \text{where} \quad G_0 = \frac{\pi^2 k_B T}{3h} \tag{2.17}$$

is the quantum of the thermal conductance. We will designate the electrical and thermal conductance with the same letter G meaning in normal systems, electrical conductance, and in superconducting systems, thermal conductance, since in the latter, we will study heat transport phenomena since the charge transport is not well defined. For the RMT of superconducting systems (samples with normal-superconducting junctions), it is necessary to add new degrees of freedom corresponding to the creation of holes in Andreev reflections [Beenakker 1992, Beenakker et al. 2011, Beenakker 2005], as we will see in the next section. So, the reflection matrix acquires a new block structure

$$\boldsymbol{r} = \begin{pmatrix} \boldsymbol{r}_{ee} & \boldsymbol{r}_{eh} \\ \boldsymbol{r}_{he} & \boldsymbol{r}_{hh} \end{pmatrix}, \tag{2.18}$$

where the diagonal blocks $\boldsymbol{r}_{ee(hh)}$ represent the usual electron (hole) reflection and the off-diagonal blocks $\boldsymbol{r}_{eh(he)}$ describe the Andreev reflections [Stenberg 2007]. In a superconducting systems the electrical conductance is not conserved; nevertheless, the electrical Andreev conductance through a normal-superconducting junction is

$$G = 2G_0 \operatorname{Tr}\left[\boldsymbol{r}_{he}^\dagger \boldsymbol{r}_{he}\right]. \tag{2.19}$$

Because heat is conserved, the thermal conductance in superconducting systems is given by the equation 2.17 with an additional factor $1/2$ to account for new the degrees of freedom [Dahlhaus, Béri e Beenakker 2010].

2.3 Andreev reflection and Majorana fermions

Quantum transport analysis can be extended to superconducting systems, in which scattering phenomena at the normal-superconducting interface (NS)

play a relevant role. This is the case of so-called Andreev reflection, which has no classical analog but can nevertheless be understood in comparison with a classical reflection in a normal-normal interface. Figure 4 presents an outline of the two types of reflection. In a normal reflection, for example from a metal to an insulator, an electron is scattered at an angle equal to the incident angle, both measured from the normal line to the surface. When an electron with an energy close to Fermi energy is reflected on the N-S interface, it is backscattered as a hole, with opposite velocity and the same moment since the velocity of a hole is opposite to its moment. The backscatter of the hole arises because, on the superconducting side, the electron is absorbed along with another available electron, in the form of a Cooper pair.

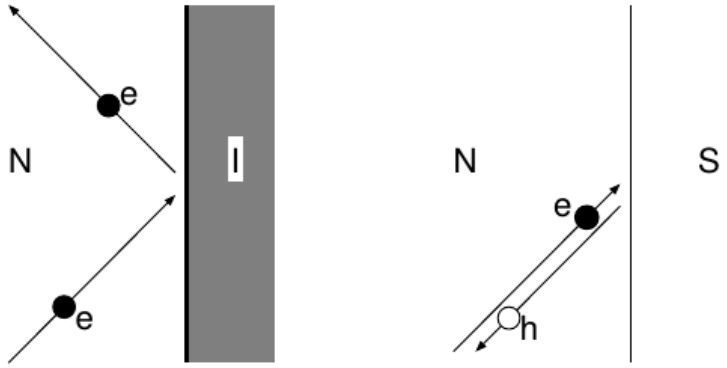

Figure 9 – Normal reflection vs. Andreev reflection. In the first one there is a dispersion from a normal metal (N) on an insulating surface (I). In the second, reflection occurs at the N-S interface. In a normal reflection, the charge is conserved but not the moment; in a Andreev reflection, the moment is conserved but not the charge [Beenakker 2005].

In a normal reflection the electric charge is conserved but not the moment, in contrast in an Andreev reflection the charge is not conserved but the moment is, so in a superconducting system, rather than analyzing the transport of charge, the transport of heat will be analyzed.

It has been theorized that Andreev reflections should generate the appearance of quasi-particles called Majorana fermions in condensed matter [Elliott e Franz 2015]. As is known, Majorana fermions take their name from their predic-

tor [Majorana 1937], and are a kind of fermionic particles, which are at the same time their own antiparticle. This in contrast to Dirac fermions which are not their own antiparticle. To understand how Majorana fermions appear in condensed matter, we retake the anticommutation relations of electrons in second quantization formalism, in which an electron characterized by the quantum numbers j can be created by the $c_j^\dagger$ operator, and annihilated with the c_j operator

$$\left\{c_i^\dagger, c_j^\dagger\right\} = \{c_i, c_j\} = 0, \quad \left\{c_i^\dagger, c_j\right\} = \delta_{ij}. \tag{2.20}$$

It is possible to rewrite these operators in the "Majorana basis" as follows

$$c_j = \frac{1}{2}\left(\gamma_{j1} + i\gamma_{j2}\right), \quad c_j^\dagger = \frac{1}{2}\left(\gamma_{j1} - i\gamma_{j2}\right), \tag{2.21}$$

or equivalently

$$\gamma_{j1} = c_j^\dagger + c_j, \quad \gamma_{j2} = i\left(c_j^\dagger - c_j\right). \tag{2.22}$$

The decomposition of the fermionic operators in the "Majorana basis" is a canonical transformation of the Hamiltonian in second quantization, that without loss of generality, can be written in terms of $c_j^\dagger$ and c_j, or the new operators $\gamma_{j\alpha}$. This and can be understood as a rewriting in terms of a real part and an imaginary part that fulfills the following algebra

$$\{\gamma_{i\alpha}, \gamma_{j\beta}\} = 2\delta_{ij}\delta_{\alpha\beta}, \quad \gamma_{i\alpha}(E) = \gamma_{i\alpha}^\dagger(-E). \tag{2.23}$$

The last relation precisely accounts for the creation of pairs of electrons with energy E above the Fermi level, and holes with energy $-E$ below the Fermi level, in a Andreev reflection. In fact, according to equation 2.22, an isolated Majorana fermion can be understood as a superposition of a electron and a hole. From the perspective of the "Majorana basis", any electron could be understood as consisting of two fermions of Majorana, however, making this separation for two Majorana fermions that are not spatially separated does not make much sense, and only complicates things. However there is a class of materials called topological superconductors [Avron, Osadchy e Seiler 2003, Khalaf 2017, Elliott e Franz 2015, Beenakker 2015] where the spatial separation of two Majorana fermions to form an electron is clearly manifested. In such materials, the "Majorana basis" is the only way to describe the a situation. Such is the case of the Kitaev chain [Kitaev

2001], in which the topological phases of matter are most simply evidenced, and where it is has predicted, along with several other systems, the appearance of Majorana fermions zero modes, i.e. fermions which are their particle and their antiparticle at the same time. These fermions can only manifest when they are at Fermi level; this is

$$\gamma_{i\alpha}(0) = \gamma_{i\alpha}^{\dagger}(0). \tag{2.24}$$

Note that it is implicitly being assumed that the charge conjugation operation corresponds to the complex conjugate operation. Later we will see that the symmetries of temporal reversal and charge conjugation will be determinant in classifying the materials.

2.4 Random Matrix Theory

Random Matrix Theory provides a natural framework for the study of complex systems [Beenakker 1997], for which the description of the microscopic details is outside the scope of a simple Hamiltonian. This happens because if the complexity is large enough, the Hamiltonian description can be replaced by a statistical approach in terms of an ensemble of random matrices, over which the basic symmetries of the system are imposed, and from which universal properties can be derived. It is well known that under certain conditions, the behavior of complex quantum systems do not depend on microscopic details such as the position of the impurities. Likewise, transport properties ballistic chaotic cavities do not depend on the shape of the boundaries. Then, a random matrix ensemble corresponding to a Hamiltonian can also describe closed ballistic chaotic cavities, while a random matrix ensemble corresponding to a scattering matrix can describe open ballistic chaotic cavities coupled to reservoirs. A random matrix ensemble of transfer matrices is convenient to describe disordered quasi-one-dimensional systems, as will see later [Brouwer 1997].

The symmetries of the system are imposed on the random matrices, and these determine the functional form of their distributions. Since translation and rotation symmetries are broken in a complex system; the theory deals only with the time-reversal (TR) and spin rotation (SR) symmetries, plus the particle-hole symmetry (PH) in superconducting systems.

The random matrix ensembles, introduced by Wigner to study the nucleus of heavy atoms, were classified by Dyson according to the inherent symmetry of the corresponding Hamiltonian [Mehta 2004], in what became known as the Three-Fold Way. A Wigner-Dyson (WD) ensemble is an ensemble of hermitian matrices $\boldsymbol{H}$ with a Gaussian distribution, such that the matrix-values distribution function has the form

$$P(\boldsymbol{H}) = c\exp\{(-\beta \boldsymbol{V})\}, \tag{2.25}$$

where $\boldsymbol{V} \propto \boldsymbol{H}^2$, c is a constant and β depends on the symmetry of the system.

2.4.1 Symmetries in RMT: The three fold way

Random matrices are characterized by the presence or absence of time-reversal symmetry

$$\boldsymbol{H}\mathcal{T} = \mathcal{T}\boldsymbol{H} \Rightarrow \boldsymbol{H} = \mathcal{T}\boldsymbol{H}\mathcal{T}^{-1} \tag{2.26}$$

where $\mathcal{T}$ is the time reversal operator. It is known that $\mathcal{T}$ is antiunitary and [Haake 2013]

$$\mathcal{T} = \begin{cases} \mathcal{K} \quad \text{for integer spin,} \quad \mathcal{T}^2 = 1, \\ i\boldsymbol{\sigma_y}\mathcal{K} \quad \text{for half-integer spin,} \quad \mathcal{T}^2 = -1, \end{cases} \tag{2.27}$$

with $\mathcal{K}$ the operator of complex conjugation. It can be shown that if the system has time-reversal symmetry, the Hamiltonian can be represented by real elements, which corresponds to an ensemble with $\beta = 1$. For systems with broken time-reversal symmetry, the Hamiltonian must be represented by complex elements, and its ensemble has $\beta = 2$. In the same way, for systems with broken spin rotation symmetry, the Hamiltonian can be represented by quaternions, and its ensemble has $\beta = 4$. Note that β matches the number of degrees of freedom of the Hamiltonian elements (see table 1).

We know that an Hermitian matrix $\boldsymbol{H}$ has eigenvalues $E_1, E_2, ..., E_M$, corresponding to the eigenvector matrix U that is orthogonal (unitary, simpletic), for $\beta = 1(2, 4)$ respectively. To find the joint probability distribution of the eigenvalues, it is first necessary to find the Jacobian that connects the volume element dH and the volume element $dU \prod_i^M dE_j$. The partial volume element dU is the invariant measure, or Haar measure of the respective group of the eigenvector

matrix U (orthogonal, unitary or simpletic) and this group gives the name to each one of the ensembles GOE (Gaussian Ortogonal Ensemble), GUE (Unitary), GSE (Simpletic). One can show that

$$dH = dU J(\{E_j\}) \prod_i^M dE_j, \quad J(\{E_j\}) = \prod_{i<j}^M |E_i - E_j|^\beta. \tag{2.28}$$

Then the equation 2.25 becomes

$$P(\{E_j\}) \propto \prod_{i<j}^M |E_i - E_j|^\beta \prod_j^M e^{-\beta V(E_j)}. \tag{2.29}$$

These ensembles describes physical systems when the size of the Hermitian matrix $\boldsymbol{H}$ is very large $M \to \infty$. In this regime the correlation functions between energy levels do not depend on the heuristic confining potential V. Dyson also studied the so-called circular ensembles, which are formed by unitary matrices, and therefore can be applied to the scattering $\boldsymbol{S}$-matrix, which is intrinsically unitary. The same analysis of the time reversal symmetry of the scattering matrix

$$\boldsymbol{S}(E)\mathcal{T} = \mathcal{T}\boldsymbol{S}^{-1}(E) \Rightarrow \boldsymbol{S}(E) = \mathcal{T}\boldsymbol{S}^\dagger(E)\mathcal{T}^{-1} \tag{2.30}$$

shows that for systems with TR and SR symmetries ($\beta = 1$) the $\boldsymbol{S}$-matrix must be symmetric (Circular Ortogonal Ensemble COE). For systems without TR symmetry ($\beta = 2$) there are no restrictions ($\boldsymbol{S}$-matrix must always be unitary, CUE); and for systems without spin rotation, $\boldsymbol{S}$-matrix must be self-dual (CSE). This is summarized in the table 1, with the first column indicating the name of the Cartan classification of the respective compact symmetric spaces [Caselle e Magnea 2004].

An ensemble of scattering matrices $\boldsymbol{S}$ of size $2N \times 2N$ has eigenvalues e^{ϕ_j} where the eigenphase is $0 \leq \phi \leq 2\pi$ and $j = 1, ..., 2N$. This eigenvalues form a circular ensemble (note that eigenvalues form a circle in the complex plane). Thus, in the same way as the equation 2.29, the uniform distribution of the scattering matrices ensemble has the form

$$P(\{\phi_j\}) \propto \prod_{i<j} |e^{\phi_i} - e^{\phi_j}|^\beta. \tag{2.31}$$

On the other hand, the polar decomposition of the scattering matrix [Beenakker 1997] allows to write it in terms of the transmission eigenvalues $T_1, ..., T_N$ of the matrix $tt^\dagger$

$$\boldsymbol{S} = \begin{pmatrix} u & 0 \\ 0 & v \end{pmatrix} \begin{pmatrix} -\sqrt{1-\boldsymbol{T}} & \sqrt{\boldsymbol{T}} \\ \sqrt{\boldsymbol{T}} & \sqrt{1-\boldsymbol{T}} \end{pmatrix} \begin{pmatrix} u' & 0 \\ 0 & v' \end{pmatrix}, \tag{2.32}$$

with u, u',v,v' $N \times N$ unitary matrices and $\boldsymbol{T}$ the diagonal matrix of eigenvalues. Again, the joint probability distribution is obtained by the Jacobian that connects the volume elements dS to the products of du, du', dv, dv' and $\prod_i^N dT_i$ [Baranger e Mello 1994, Jalabert, Pichard e Beenakker 1994]

$$dS = dudu'dvdv' \prod_{i<j}^{N} |T_j - T_i|^\beta \prod_j^N T_j^{-1+\beta/2} dT_j, \tag{2.33}$$

We then conclude that

$$P(T_1, ..., T_N) \propto \prod_{i<j}^{N} |T_j - T_i|^\beta \prod_j^N T_j^{-1+\beta/2}. \tag{2.34}$$

Table 1 – Wigner Dyson ensembles. The tick mark indicates the presence or absence of the respective symmetry and the columns of $\boldsymbol{H}$ and $\boldsymbol{S}$ indicate the structure of the matrix components. β is the symmetry factor.

	TRS($\mathcal{T}^2$)	SRS	β	$\boldsymbol{H}$	$\boldsymbol{S}$
A	1	$\surd$	1	real symmetric	complex unitary symmetric
AI	$\times$	$\surd/\times$	2	complex hermitian	complex unitary
AII	-1	$\times$	4	quaternion self-dual	complex unitary self-dual

Note that the construction of the joint probability distribution for the energy levels 2.29, and the transmission eigenvalues 2.34, are completely analogous, with the difference that, in the case of the hermitian matrix, the probability distribution only makes physical sense when the number of eigenvalues is very large. By contrast, for the construction from the scattering matrix, the distribution makes sense for an arbitrary number of transmission eigenvalues, including $N = 1$.

2.4.2 The ten fold way

Random matrix ensembles beyond the Wigner Dyson ones have also been studied, since they can account for the properties of superconducting and chiral systems. The particle-hole (PH) symmetry becomes essential, which together with the TR symmetry and the SR symmetry, define these ensembles. The new classification, introduced by Altland and Zirnbauer [Altland e Zirnbauer 1997, Zirnbauer 2010] extends the Three-fold way in a Ten-fold way of classification when all symmetries are accounted for. In particular, when the ensembles describe superconducting systems, they are called Bogoliubov-De Gennes (BG) ensembles. Here we briefly review their features. Starting from the mean field theory for superconductors whose Hamiltonian is

$$\boldsymbol{\mathcal{H}} = \hat{\Psi}^\dagger \boldsymbol{H} \hat{\Psi}, \quad \hat{\Psi} = (\hat{\psi}, \hat{\psi}^\dagger) = (\hat{\psi}_\uparrow, \hat{\psi}_\downarrow, \hat{\psi}_\uparrow^\dagger, \hat{\psi}_\downarrow^\dagger), \tag{2.35}$$

$$\boldsymbol{H} = \begin{pmatrix} \boldsymbol{H_0} - E_F & -i\boldsymbol{\sigma_y}\Delta \\ i\boldsymbol{\sigma_y}\Delta^* & E_F - \boldsymbol{H_0} \end{pmatrix}, \quad \Delta = V_o \langle \hat{\psi}_\uparrow \hat{\psi}_\downarrow \rangle. \tag{2.36}$$

Both $\boldsymbol{\mathcal{H}}$ and Ψ are represented in the second quantization formalism. In the first quantization, $\boldsymbol{H}$ can be interpreted as the Hamiltonian of the dynamics of the Bogoliubov quasi-particles.

$$\boldsymbol{H}\Psi(\mathbf{r}, t) = -i\hbar \frac{\partial}{\partial t} \Psi(\mathbf{r}, t), \tag{2.37}$$

$$\Psi = (\psi_e, \psi_h) = (\psi_{e\uparrow}, \psi_{e\downarrow}, \psi_{h\uparrow}, \psi_{h\downarrow}). \tag{2.38}$$

These are the Bogoliubov-de Gennes equation that couples electrons e and holes h with opossite spin $\uparrow\downarrow$ through the pair potential Δ. PH symmetry can be expressed by the charge conjugation operator

$$\mathcal{C} = \begin{cases} i\tau_y \mathcal{K} & \text{for integer spin}, \quad \mathcal{C}^2 = -1, \\ \tau_x \mathcal{K} & \text{for half-integer spin}, \quad \mathcal{C}^2 = 1, \end{cases} \tag{2.39}$$

which is antiunitary, but unlike the time reversion operator, it anti-commutes with $\boldsymbol{H}$, then $\boldsymbol{H} = -\mathcal{C}\boldsymbol{H}\mathcal{C}^{-1}$. In the "Majorana basis" $\mathcal{C} = \mathcal{K}$ [Beenakker 2015] (see

equation 2.24). This symmetry together with the presence or absence of TR and SR symmetry defines four new classes which are summarized in table 2, where we used the notation

$$\boldsymbol{H} = \begin{pmatrix} \boldsymbol{W} & \boldsymbol{Z} \\ \boldsymbol{Z}^\dagger & -\boldsymbol{W} \end{pmatrix} \tag{2.40}$$

to establish the symmetries on the Hamiltonian of equation 2.36.

Making an analysis similar to the one done for the Wigner Dyson ensembles, was obtain the joint probability distribution of the energy levels of this classes as [Beenakker 2015]

$$P(\{E_j\}) \propto \prod_{i<j}^{M} |E_i^2 - E_j^2|^{\beta_E} \prod_{j}^{M} |E_j|^{\gamma_E} e^{-\beta_E V(E_j)}. \tag{2.41}$$

There are two differences with equation 2.29: the factor $|E_i^2 - E_j^2|^{\beta_E} = |E_i - E_j|^{\beta_E}|E_i + E_j|^{\beta_E}$ that emerges form the PH symmetry, causing the repulsion between $\pm E$ levels; and the factor $|E_j|^{\gamma_E}$, which acts like a repulsion from the Fermi energy.

Again from the polar decomposition of the $\boldsymbol{S}$-matrix, one can obtain the joint probability distribution of the transmission values

$$P(\{T_j\}) \propto \prod_{i<j} |T_i - T_j|^{\beta_T} \prod_{i} T_i^{\beta_T/2-1}(1-T_i)^{\gamma_T/2}. \tag{2.42}$$

Note that the α's and β's in the equations 2.41 and 2.42 are different and are specified in the tables 2 and 3.

Finally, the picture is completed by the chiral (CH) symmetry, which is the composition of the TR and PH symmetry $\boldsymbol{H} = -\mathcal{T}\mathcal{C}\boldsymbol{H}\mathcal{C}^{-1}\mathcal{T}^{-1}$. This is unitary, anti-commutes with $\boldsymbol{H}$ and defines Hamiltonians of the form

$$\boldsymbol{H} = \begin{pmatrix} 0 & \boldsymbol{Z} \\ \boldsymbol{Z}^\dagger & 0 \end{pmatrix}. \tag{2.43}$$

Systems like the hexagonal carbon lattice of graphene [Macedo-Junior e Macêdo 2002], or superconductors with symmetrical spectrum around ε_F, satisfy this type of Hamiltonian. In fact, in table 2 there are already classes with the presence of this symmetry ($\boldsymbol{W} = 0$). In table 3 the remaining classes are shown.

Table 2 – Bogoliubov de Gennes ensembles. The numbers of the symmetries are indicated in the equations 2.27 and 2.39, the $\boldsymbol{H}$ structure is referred to the equation 2.43, and the symmetry factor β and γ are different for the $\boldsymbol{H}$ and $\boldsymbol{S}$ ensembles.

	PH($\mathcal{C}^2$)	TR($\mathcal{T}^2$)	SR	β_E	γ_E	$\boldsymbol{H}$	β_T	γ_T	$\boldsymbol{S}$
D	1	$\times$	$\times$	2	0	$\boldsymbol{Z}$ complex skew	1	-1	real ortogonal
DIII	1	-1	$\times$	4	1	$\boldsymbol{Z}$ complex skew, $\boldsymbol{W}=0$	2	-1	real ortogonal symmetric
C	-1	$\times$	$\surd$	2	2	$\boldsymbol{Z}$ complex symmetric	4	2	sympletic
CI	-1	1	$\surd$	1	1	$\boldsymbol{Z}$ complex symmetric, $\boldsymbol{W}=0$	2	1	sympletic symmetric

Table 3 – Chiral ensembles. These are defined when the symmetry number TR and PH are equal.

	CH	PH($\mathcal{C}^2$)	TR($\mathcal{T}^2$)	β_E	γ_E	$\boldsymbol{H}$	β_T	γ_T	$\boldsymbol{S}$
BDI	$\surd$	1	1	1	0	$\boldsymbol{Z}$ real $\boldsymbol{W}=0$	1	-1	real ortogonal
AIII	$\surd$	$\times$	$\times$	2	1	$\boldsymbol{Z}$ complex $\boldsymbol{W}=0$	2	-1	complex unitary
CII	$\surd$	-1	-1	4	3	$\boldsymbol{Z}$ quaternion $\boldsymbol{W}=0$	4	-1	sympletic

2.5 RMT for quasi-zero and quasi-one dimensional systems

Typically, ensembles of hermitian random matrices are used to describe the universal statistical properties of closed systems, such as ballistic chaotic cavities and metallic grains. This is justified as long as the difference between the energy levels in the cavity is not greater than the inverse of the ergodic time $\hbar/\tau_{erg}$. Otherwise, the universality of the statistical properties breaks down. Similarly, ensembles of scattering random matrices can describe universal transport properties of in open ballistic cavities if the dwell time τ_{dwell}, defined as the time that an electron remains within the cavity, is much greater than the ergodic time $\tau_{dwell} \gg \tau_{erg}$ [Brouwer 1997].

Since a ballistic chaotic cavity is an effective quasi-zero dimensional system,

the next natural step was to establish a RMT for quasi-one-dimensional systems, namely, for quantum wires in which the length of the system is much greater than the width. These systems are ergodic in the transverse direction, and since they are theoretically constructed as the composition of many small slices as we will see later, the central limit theorem guarantees that the transport properties of the system are universal, i.e., like the slices, the transport properties do not depend on the shape of the system [Brouwer 1997]. The natural framework is the formalism of the transfer matrix, due to its multiplicative composition property that is not true for the scattering matrix. Unlike the latter, the transfer matrix relates incident and transfer modes, or equivalently, the left and the right modes of the sample. This is, on the basis of amplitudes of each mode (Figure 8)

$$\boldsymbol{\psi}_{left} = (a_{L1}, ..., a_{LN_l}, b_{L1}, ..., b_{LN_L})^T \quad , \quad \boldsymbol{\psi}_{right} = (a_{R1}, ..., a_{RN_R}, b_{R1}, ..., b_{RN_R})^T, \tag{2.44}$$

the transfer matrix $\boldsymbol{M}$ is

$$\boldsymbol{\psi}_{left} = \boldsymbol{M}\boldsymbol{\psi}_{right}. \tag{2.45}$$

So it is natural for a chain of N samples to obtain the multiplicative composition property $\boldsymbol{M} = \boldsymbol{M}_1\boldsymbol{M}_2...\boldsymbol{M}_N$. Again the polar decomposition relates $\boldsymbol{M}$ with the transmission eigenvalues $T_1, ..., T_N$

$$\boldsymbol{M} = \begin{pmatrix} v & 0 \\ 0 & v'^{\dagger} \end{pmatrix} \begin{pmatrix} \sqrt{\boldsymbol{T}^{-1}} & \sqrt{\boldsymbol{T}^{-1} - 1} \\ \sqrt{\boldsymbol{T}^{-1}} & \sqrt{\boldsymbol{T}^{-1}} \end{pmatrix} \begin{pmatrix} u' & 0 \\ 0 & u^{\dagger} \end{pmatrix}; \tag{2.46}$$

where u, u',v,v' are $N \times N$ unitary matrices and $\boldsymbol{T}$ the diagonal matrix of eigenvalues of $\boldsymbol{t}\boldsymbol{t}^{\dagger}$. Taking $\lambda_i = (1 - T_i)/T_i$ the Jacobian that connects the volume elements dM and the products of du, du', dv, dv' and $\prod_i^N d\lambda_i$ is

$$dM = J(\{\lambda_j\})dudu'dvdv' \prod_i^N d\lambda_i \Rightarrow J(\{\lambda_j\}) = \prod_{i<j}^M |\lambda_i - \lambda_j|^{\beta}. \tag{2.47}$$

The calculation of the joint probability distribution for the T_i's was done in the following way. Assuming that the distribution for a wire of length L is known, a small slice of size L_o is added to the wire to calculate the variation of the distribution (Figure 10). Each transmission eigenvalue is modeled as a random variable in the form of a Brownian motion, so one obtains the equation for the

evolution of the distribution as a function of the sample's length L. The calculation is made assuming that the added slice has a weak disorder ($l_e \gg \lambda_F$ were λ_F is the Fermi wave length of the electron) and is thick enough to be considered macroscopic, but is sufficiently thin to make the calculations in a perturbative way ($\lambda_F \ll L_o \ll l_e$).

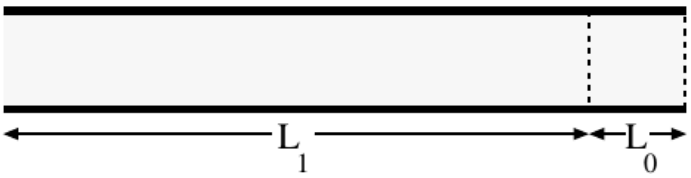

Figure 10 – Small slice of size L_o added to a quantum wire. This scaling scheme leads to a Brownian motion of the transmission eigenvalues [Beenakker 1997].

2.5.1 The DMPK equation

Using the perturbation theory at second order in terms of $1-T_o = \mathcal{O}(L_o/l_e)$, being T_0 the diagonal matrix of eigenvalues of the tiny slice, and averaging over the different ensembles of the matrix $\boldsymbol{M}$, we obtain the first two moments of the transmission eigenvalues of the added slice δT_i expanded to the first order of $\delta s = L_o/l_e$

$$\begin{aligned}
\frac{\langle \delta T_i \rangle}{\delta s} &= -T_i + \frac{2T_i}{\beta N + 2 - \beta}\left(1 - T_i + \frac{\beta}{2}\sum_{j\neq i}\frac{T_i + T_j - 2T_iT_j}{T_i - T_j}\right), \\
\frac{\langle \delta T_i \delta T_j \rangle}{\delta s} &= \delta_{ij}\frac{4T_i^2(1-T_i)}{\beta N + 2 - \beta}.
\end{aligned} \tag{2.48}$$

Then, from the Fokker Plank equation for the Brownian motion

$$\frac{\partial P}{\partial s} = \frac{1}{\delta s}\sum_{i=1}^{N}\frac{\partial}{\partial T_i}\left(-\langle \delta T_i \rangle P + \frac{1}{2}\sum_{j=1}^{N}\frac{\partial}{\partial T_j}\langle \delta T_i \delta T_j \rangle P\right), \tag{2.49}$$

and inserting equation 2.48 into 2.49, was derived the DMPK equation for the WD classes

$$l_e\frac{\partial P}{\partial L} = \frac{2}{\beta N + 2 - \beta}\sum_{i=1}^{N}\frac{\partial}{\partial \lambda_i}\lambda_i(1+\lambda_i)J\frac{\partial}{\partial \lambda_i}\frac{P}{J}. \tag{2.50}$$

The DMPK equation for the WD classes was deduced by Dorokhov for $\beta = 2$ [Dorokhov 1982], and by Mello, Pereyra and Kumar for $\beta = 1$ [Mello, Pereyra e Kumar 1988], with the extension for $\beta = 4$ made by Macêdo and Chalker [Macêdo, Chalker et al. 1992]. This equation has been extensively and successfully used to study transport properties in quasi one-dimensional systems with weak disorder. The extension for chiral and BG classes was then done by Brouwer et al. [Brouwer et al. 1998, Brouwer et al. 2000]. The Fokker Planck equation for all classes can be written more compactly in terms of the variable $T_i = \text{sech}^2(q_i)$

$$\frac{\partial P}{\partial L} = \frac{1}{2\gamma l_e} \sum_i^N \frac{\partial}{\partial q_i} J \frac{\partial}{\partial q_i} \frac{P}{J}, \tag{2.51}$$

with

$$J = \prod_i \sinh^{\alpha}(2q_i) \prod_{j<i} \prod_{\pm} \sinh^{\beta_{\pm}}(q_i \pm q_j), \tag{2.52}$$

where we defined $\gamma = (\beta_+ + \beta_-)(N-1)/2 + 1 + \alpha$. For the WD and BG classes $\beta_+ = \beta_- = \beta$ and for the chiral classes $\beta_+ = 0, \beta_- = \beta$. A further generalization of the DMPK equation was proposed by Muttalib et al [Muttalib e Gopar 2002, Gopar, Muttalib e Wölfle 2002], to take into account strong disorder and systems beyond the quasi one-dimensionality. However, it has the disadvantage that, unlike the DMPK equation, is not a single parameter scaling equation.

2.5.2 Ten fold way for quasi one-dimensional systems

Table 4 shows the values of the indices of equation 2.52 for all ten classes defined in the Cartan classification for the $\boldsymbol{S}$ and $\boldsymbol{M}$ matrices, together with some universal results that we will discuss below.

Brouwer et al. [Brouwer et al. 1998, Brouwer et al. 2000] predicted that for chiral classes (for odd N) and for superconductors of classes D and DIII, there is no exponential localization, in contrast with the standard classes. In the limit of long distances $L \gg N l_e$, the average conductance falls as $1/\sqrt{L}$, in a kind of super-ohmic behavior where the conductance falls even slower than in the ohmnic case (or equivalently $-\overline{\ln g} \propto \sqrt{L}$ as is shown in the table 4) This anomalous behavior is known as delocalization. They also found that in these classes the

Table 4 – Then fold way for quasi unidimensional quantum wires. The table shows the Cartan classification for the $\boldsymbol{S}$ and $\boldsymbol{M}$ matrices, the Jacobian indices (equation 2.52) of the Fokker Planck equation, $-\overline{\ln g}$ for the limit $L \gg Nl_e$, the DOS when $\varepsilon \to 0$ and the number ν of topologically protected zero modes. The results for $-\overline{\ln g}$ and $\rho(\varepsilon)$ are valid for N even. For odd N the results are the same as for class D [Brouwer et al. 2005].

Class	$\boldsymbol{S}$	M	β	α	$-\overline{\ln g}$	$\rho(\varepsilon)$ for $\varepsilon \to 0$	ν
WD	AI	CI	1	1	$2L/(\gamma l)$	ρ_0	0
	A	AIII	2	1	$2L/(\gamma l)$	ρ_0	0
	AII	DIII	4	1	$2L/(\gamma l)$	ρ_0	0
Chiral	BDI	AI	1	0	$2\beta L/(\gamma l)$	$\rho_0 \lvert \ln \lvert \varepsilon\tau_c \rvert \rvert$	$\mathbb{Z}$
	AIII	A	2	0	$2\beta L/(\gamma l)$	$\pi\rho_0 \lvert \varepsilon\tau_c \ln \lvert \varepsilon\tau_c \rvert \rvert$	$\mathbb{Z}$
	CII	AII	4	0	$2\beta L/(\gamma l)$	$\frac{1}{3}\pi\rho_0 \lvert (\varepsilon\tau_c)^3 \ln \lvert \varepsilon\tau_c \rvert \rvert$	$\mathbb{Z}$
BdG	CI	C	2	2	$2\alpha L/(\gamma l)$	$\frac{1}{2}\pi\rho_0 \lvert \varepsilon\tau_c \rvert$	0
	C	CII	4	3	$2\alpha L/(\gamma l)$	$\rho_0 \lvert \varepsilon\tau_c \rvert^2$	0
	DIII	D	2	0	$4\sqrt{L/(2\pi\gamma l)}$	$\pi\rho_0/\lvert \varepsilon\tau_c \ln^3 \lvert \varepsilon\tau_c \rvert \rvert$	$\mathbb{Z}_2$
	D	BDI	1	0	$4\sqrt{L/(2\pi\gamma l)}$	$\pi\rho_0/\lvert \varepsilon\tau_c \ln^3 \lvert \varepsilon\tau_c \rvert \rvert$	$\mathbb{Z}_2$

behavior of the density of states (DOS) diverges as

$$\rho(\varepsilon) \sim \frac{1}{|\varepsilon\tau_c \ln^3(\varepsilon\tau_c)|}, \tag{2.53}$$

as the energy $\varepsilon \to 0$ and $\tau_c \sim N^2 l_e/v_F$ is the time that the particle needs to diffuse through a wire of length $\sim Nl_e$. This singularity had already been found by Dyson in the analysis of disordered linear chains [Dyson 1953] and is known as the Dyson divergence. On the other hand, Motrunich et al. [Motrunich, Damle e Huse 2001] found, through an analysis of strong-disorder renormalization group (RG), that generically, systems of classes D and DIII present localization like the WD classes, and the DOS diverges as a power law $\rho(E) \sim |\varepsilon\tau_c|^{\delta+1}$ with $\delta > 0$. However, at certain critical points of fine-tuning disorder, they observed that delocalization and Dyson divergence are present. They were also the first to relate this criticality with transitions between topological phases and to point out the possibility of

having Majorana zero modes at the ends of the wire. Gruzberg et al. [Gruzberg, Read e Vishveshwara 2005] confirmed the localization results deducing a generalized Fokker Plank equation and claimed that the delocalization at critical points is well described by the DMPK equation for superconductors (see equation 2.51). Furthermore, they proposed a "superuniversality" between the chiral and superconducting classes D and DIII, since these have equal characteristics at the critical points, like delocalization and Dyson divergence. Remarkably, in the thick wire limit, where $N \gg 1$, it is predicted that there will always be delocalization, regardless of the degree of disorder.

Later, Mudry [Mudry 2017] argued that the diverging nature of the density of states at the band center for five of the ten symmetry classes is a signature of topologically protected zero modes bound to point defects (see the last column in the table 4). For quantum wires, these modes are tied to their ends, and in the superconducting cases, these modes correspond to Majorana fermions [Fulga et al. 2013]. In conclusion, there is a correspondence between delocalization, Dyson divergence and topologically protected zero modes common to chiral classes with odd N and superconducting classes D and DIII (see table 4).

2.6 Brownian-motion ensembles of random matrix theory

2.6.1 A classification scheme

Macedo-Junior and Macêdo constructed a classification scheme for the Brownian motion ensembles of RMT based on the general theory of Markovian stochastic processes and on the multivariable generalization of classical orthogonal polynomials [Macedo-Junior e Macêdo 2006, Macedo-Junior e Macêdo 2007]. Given a set of correlated random variables $a \leq x_i \leq b$ $(i = 1, ..., N)$, an equation for the evolution of the joint distribution was obtained under the following assumptions: (i) path continuity; (ii) homogeneity; (iii) equilibrium distribution given by classical random matrix ensembles and (iv) a complete set of generalized multivariate classical polynomials as eigenfunctions.

Under these conditions, they concluded that the only equation that satisfies

these assumptions is a Fokker-Planck equation

$$\frac{\partial P}{\partial t} = \mathcal{L}_{FP} P, \tag{2.54}$$

where

$$\mathcal{L}_{FP} = \sum_i^N \frac{\partial}{\partial x_i}\left(J_B w_N s(x_i) \frac{\partial}{\partial x_i} \frac{1}{J_B w_N} \right) \tag{2.55}$$

is the Fokker-Planck operator with

$$J_B(\{x\}) = |\Delta_N(\{x\})|^\beta, \quad \Delta_N(\{x\}) = \prod_{i<j}(x_i - x_j), \quad \text{and} \quad w_N(\{x\}) = \prod_i^N w(x_i). \tag{2.56}$$

The steady solution of the Fokker Planck equation is

$$P_{st}(\{x\}) = C_N J_\beta(\{x\}) w_N(\{x\}) \tag{2.57}$$

which reproduces the joint probability distribution of orthogonal polynomial ensembles (Hermite, Laguerre and Jacobi ensembles) of RMT. The usual constraints from the theory of classical orthogonal polynomials were imposed by construction [Dennery e Krzywicki 2012]: given the interval $[a, b]$, the auxiliary function $s(x)$ must be a real polynomial with real roots of degree no greater than 2; $s(x) = s_0 + s_1 x + s_2 x^2$ and using the weight function $w(x)$, we define a function

$$r(x) = \frac{1}{w(x)} \frac{d}{dx}(w(x)s(x)), \tag{2.58}$$

that must be a polynomial of degree 1, and it must satisfy the boundary condition

$$w(a)s(a) = 0 = w(b)s(b). \tag{2.59}$$

These functions will be specified later. In the case of circular ensembles, this classification can reproduce the joint probability distribution of the eigenvalues in $\boldsymbol{S}$-matrix ensembles, and will be useful to describe transport properties in ballistic chaotic cavities. In general, a Fokker Planck equation in its standard form reads

$$\frac{\partial P}{\partial t} = \sum_i^N \left(-\frac{\partial}{\partial x_i} D_i^{(1)} + \frac{\partial^2}{\partial^2 x_i} D_i^{(2)} \right) P. \tag{2.60}$$

It can be shown that the drift and diffusion coefficients in the above classification scheme are given respectively by

$$D_i^{(1)} = r(x_i) + \beta \sum_{j(\neq i)} \frac{s(x_i)}{x_i - x_j} \quad \text{and} \quad D_i^{(2)} = s(x_i). \tag{2.61}$$

The average of any observable in the form of a function $F(x_1, ..., x_N)$ can be calculated as

$$\langle F \rangle = \int d^N x F(\{x\}) P(\{x\}, t), \tag{2.62}$$

and its "time" evolution will be

$$\frac{d}{dt}\langle F \rangle = \langle \mathcal{L}_{FP}^{\dagger} F \rangle, \tag{2.63}$$

where $\mathcal{L}_{FP}^{\dagger}$ is the adjoint Fokker–Planck operator

$$\mathcal{L}_{FP}^{\dagger} = \sum_i^N \frac{1}{J_B w_N} \frac{\partial}{\partial x_i} \left(J_B w_N s(x_i) \frac{\partial}{\partial x_i} \right). \tag{2.64}$$

The central idea of this classification scheme is the realization that a concrete matrix representation of the ensembles becomes unnecessary and the scheme provides an alternative to the Ten Fold Way classification of RMT.

It is possible to solve the Fokker Planck equation 2.54 by performing the Sutherland similarity transformation

$$P(\{x\}, t) = w_N J_\beta \Psi(\{x\}, t), \tag{2.65}$$

which maps the Fokker Planck equation onto a Schrödinger equation with imaginary time

$$\frac{\partial \Psi}{\partial t} = -\mathcal{H}\Psi, \tag{2.66}$$

with an effective Hamiltonian of the form

$$\mathcal{H} = -\sum_i^N \frac{1}{w(x_i)} \frac{\partial}{\partial x_i} \left(w(x_i) s(x_i) \frac{\partial}{\partial x_i} \right) + \frac{\beta(\beta - 2)}{4} \sum_{i \neq j} \frac{s(x_i)}{(x_i - x_j)^2} + V_0, \tag{2.67}$$

where

$$V_0 = \frac{\beta N(N-1)}{12} (s_2 \beta (N-2) + 3r_1), \tag{2.68}$$

and the factors s_2 and r_1 correspond to the coefficients of the polynomials $s(x) = s_0 + s_1 x + s_2 x^2$ and $r(x) = r_0 + r_1 x$. The Hamiltonian of this mapping corresponds to a quantum-type Calogero-Shuterland system, which describes a system of N non-relativistic particles on a line, interacting with a pairwise inverse-square potential [Calogero 2008]. The exact eigenfunctions and eigenvalues of $\mathcal{H}$ can be obtained via the transformation $\Psi = J_\beta \Phi$. For the classical random-matrix ensembles the function Φ yields Jack-type multivariate extensions of the classical orthogonal polynomials.

In this Thesis we use the functions referred to in the table 5, which characterize and summarize in a complete way the Brownian-motion ensembles classification scheme of RMT.

Table 5 – Functions of the classification scheme of the Brownian-motion ensembles of RMT for the orthogonal polynomial ensembles, $\boldsymbol{S}$-matrix ensembles and transfer $\boldsymbol{M}$ matrix ensembles

Ensemble	$w(x)$	$s(x)$	$r(x)$	$Interval$
Hermite	e^{-x^2}	1	$-2x$	$(-\infty, \infty)$
Laguerre	$x^\nu e^{-x}$ $(\nu > -1)$	x	$1 + \nu - x$	$[0, \infty)$
Jacobi	$(1-x)^\nu (1+x)^\mu$ $(\nu, \mu > -1)$	$1 - x^2$	$\mu - \nu - (2 + \mu + \nu)x$	$[-1, 1]$
SM-WD	$x^{\beta/2-1}$	$x(1-x)$	$\beta(1-x)/2 - x$	$[0, 1]$
SM-Chiral	$(1-x^2)^{\beta/2-1}$	$1 - x^2$	$-\beta x$	$[-1, 1]$
SM-BdG	$x^{\beta/2-1}(1-x)^{\gamma/2}$ $(\gamma = -1, 1)$	$x(1-x)$	$\beta(1-x)/2 - x(\gamma/2 + 1)$	$[0, 1]$
TM-WD	1	$x^2 - 1$	$2x$	$[1, \infty)$
TM-Chiral	$x^{[(1-N)\beta-2]/2}$	x^2	$[1 - \beta(N-1)/2]x$	$[1, \infty)$
TM-BdG	$(x^2-1)^{(\alpha-1)/2}$ $(\alpha = 0, 2)$	$x^2 - 1$	$(1 + \alpha)x$	$[1, \infty)$

2.6.2 An integral transform method

In reference [Macedo-Junior e Macêdo 2006], Macedo-Junior and Macêdo introduced a multidimensional integral transform which will allow us to solve the Fokker Planck equation in an image space ν for the $\boldsymbol{S}$-matrix and $\boldsymbol{M}$-matrix ensembles. Making use of a Sutherland similarity transformation we will be able

to obtain a ν-space Calogero-Shuterland model. The integral transform is defined as

$$W(\{\nu\},t) = \langle \Omega_\beta(\{x\},\{\nu\})\rangle = \int d^N x\ \Omega_\beta(\{x\},\{\nu\}) P(\{x\},t), \tag{2.69}$$

with the kernel chosen as the ratio of products of spectral determinants

$$\Omega_\beta(\{x\},\{\nu\}) = \frac{\prod_{k=1}^{n_0}\det(X-\nu_{0k}1_N)}{\prod_{l=1}^{n_1}\det^{\beta/2}(X-\nu_{1l}1_N)} = \prod_{i=1}^{N}\frac{\prod_{k=1}^{n_0}(x_i-\nu_{0k})}{\prod_{l=1}^{n_1}(x_i-\nu_{1l})^{\beta/2}}, \tag{2.70}$$

where n_0 and n_1 are positive integers satisfying $\beta n_1 = 2n_2$. Such integral transform can be interpreted as a map transforming the joint distribution $P(\{x\},t)$, in x-space, into the joint distribution $W(\{\nu\},t)$ in ν-space. This is a powerful tool to uncouple the hierarchic relations of the n-point correlation function. In the target space, the time evolution of $W(\{\nu\},t)$ is

$$\begin{aligned}
\frac{\partial}{\partial t}W(\{\nu\},t) &= \int d^N x\ \Omega_\beta(\{x\},\{\nu\})\frac{\partial}{\partial t}P(\{x\},t) \\
&= \int d^N x\ \Omega_\beta(\{x\},\{\nu\})\ \mathcal{L}_x P(\{x\},t) \\
&= \int d^N x\ P(\{x\},t)\ \mathcal{L}_x^\dagger \Omega_\beta(\{x\},\{\nu\}).
\end{aligned} \tag{2.71}$$

The advantage of working in the image ν-space, is that the number of variables to be treated, unlike the x-space space, is independent of N, which represents an effective reduction of variables both in the analytical work and in the numerical analysis. The fundamental premise of the method is the assumption of the existence of a Fokker-Planck operator $\mathcal{M}_\nu^\dagger$ acting in the space ν that satisfies the relation

$$\mathcal{M}_\nu^\dagger \Omega_\beta(\{x\},\{\nu\}) = \mathcal{L}_x^\dagger \Omega_\beta(\{x\},\{\nu\}). \tag{2.72}$$

From equations 2.71 and 2.72 it follows that the time evolution of $W(\{\nu\},t)$ is

$$\left(\frac{\partial}{\partial t} - \mathcal{M}_\nu^\dagger\right) W(\{\nu\},t) = 0, \tag{2.73}$$

with the Fokker Planck operator $\mathcal{M}_\nu^\dagger$ given by

$$\mathcal{M}_\nu^\dagger = \sum_{k=1}^{n_0}\left(D_{0,k}^{(1)}\frac{\partial}{\partial\nu_{0,k}} + D_{0,k}^{(2)}\frac{\partial^2}{\partial\nu_{0,k}^2}\right) + \sum_{l=1}^{n_1}\left(D_{1,l}^{(1)}\frac{\partial}{\partial\nu_{1,l}} + D_{1,l}^{(2)}\frac{\partial^2}{\partial\nu_{1,l}^2}\right), \tag{2.74}$$

where the drift and diffusion coefficients are

$$D_{0k}^{(1)} = -\frac{\beta}{2}\frac{1}{VB}\frac{\partial\left(s(\nu_{0k})VB\right)}{\partial\nu_{0k}}, \quad D_{1l}^{(1)} = \frac{1}{VB}\frac{\partial\left(s(\nu_{1l})VB\right)}{\partial\nu_{1l}} \tag{2.75}$$

and

$$D_{0k}^{(2)} = -\frac{\beta}{2}s(\nu_{0k}), \quad D_{1l}^{(2)} = s(\nu_{1l}) \tag{2.76}$$

respectively. With these coefficients, we can regroup the terms of the equation 2.74 in order to write in a compact form

$$\mathcal{M}_{\nu}^{\dagger} = \frac{1}{VB}\left[\sum_{l=1}^{n_1}\frac{\partial}{\partial\nu_{1l}}\left(s(\nu_{1l})VB\frac{\partial}{\partial\nu_{1l}}\right) - \frac{\beta}{2}\sum_{k=1}^{n_0}\frac{\partial}{\partial\nu_{0k}}\left(s(\nu_{0k})VB\frac{\partial}{\partial\nu_{0k}}\right)\right], \tag{2.77}$$

where we introduced the functions

$$V \equiv \prod_{k=1}^{n_0} w_0(\nu_{0k}) \prod_{l=1}^{n_1} w_1(\nu_{1l}), \tag{2.78}$$

and

$$B \equiv \prod_{k<k'} |\nu_{0k} - \nu_{0k'}|^{4/\beta} \prod_{l<l'} |\nu_{1l} - \nu_{1l'}|^{\beta} \prod_{k,l} |\nu_{0k} - \nu_{1l}|^{-2}, \tag{2.79}$$

where the functions $w_0(\nu)$ and $w_1(\nu)$ related to $w(\nu)$ and $s(\nu)$ of Table 5 through

$$w_0(\nu) = w^{2/\beta}(\nu)s^{2/\beta-1}(\nu), \tag{2.80}$$

$$w_1(\nu) = \frac{s^{\beta/2-1}(\nu)}{w(\nu)}. \tag{2.81}$$

In reference [Macedo-Junior e Macêdo 2007] the authors studied the connection between Calogero-Sutherland-type quantum systems and the Sutherland similarity transformation in x-space 2.65, in the framework of the classification scheme of Brownian-motion ensembles. Since these quantum systems have been extensively studied, mapping the Fokker Planck equation onto a Calogero-Sutherland-type Hamiltonian allows analytical solutions to different properties of relevant observables in quantum transport problems. More specifically, the n-point correlation function can be explicitly calculated. In reference [Macedo-Junior 2006] a similar analysis was performed in the image space, completing the mapping scheme represented in the figure 11.

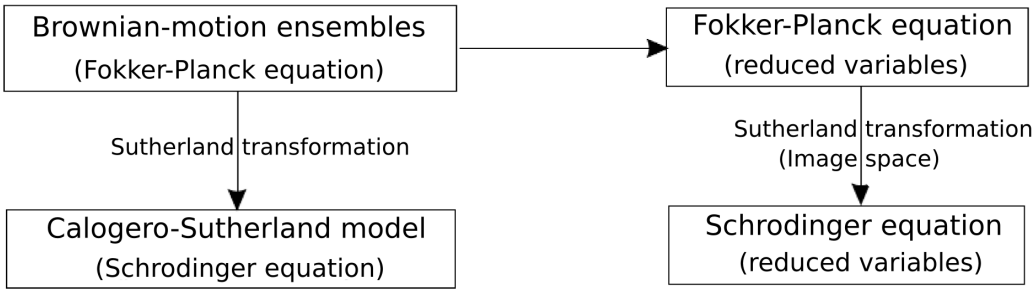

Figure 11 – Schematic representation of integral transform method and the mappings in the x-space and the ν-space [Macedo-Junior 2006].

The corresponding Sutherland transformation in image space is given by

$$W(\{\nu\},t) = B^{-1/2}\Psi(\{\nu\},t), \tag{2.82}$$

which maps the Fokker-Planck equation onto a Schrödinger equation with imaginary time

$$\frac{\partial\Psi}{\partial t} = -\mathcal{H}_\nu\Psi, \tag{2.83}$$

where the Hamiltonian is defined by

$$\mathcal{H}_\nu = B^{1/2}\mathcal{M}_\nu^\dagger B^{-1/2}. \tag{2.84}$$

Writing explicitly the Hamiltonian, we see that it is related to $\mathcal{M}_\nu$, plus the addition of a term that depends on B, the latter defined in the equation 2.79.

$$\mathcal{H}_\nu = \mathcal{M}_\nu^\dagger + \sum_{\alpha=0}^{1}\sum_{j=1}^{n_\alpha}\left\{-\frac{1}{2}D_{\alpha,j}^{(1)}\frac{\partial \ln B}{\partial\nu_{\alpha,j}} + D_{\alpha,j}^{(2)}\left[\frac{1}{4}\left(\frac{\partial \ln B}{\partial\nu_{\alpha,j}}\right)^2 - \frac{1}{2}\frac{\partial^2 \ln B}{\partial\nu_{\alpha,j}^2} - \frac{\partial \ln B}{\partial\nu_{\alpha,j}}\frac{\partial}{\nu_{\alpha,j}}\right]\right\}. \tag{2.85}$$

Calculating the indicated derivatives of

$$\ln B = \frac{4}{\beta}\sum_{k<k'}\ln|\nu_{0k}-\nu_{0k'}| + \beta\sum_{l<l'}\ln|\nu_{1l}-\nu_{1l'}| - 2\sum_{k,l}\ln|\nu_{0k}-\nu_{1l}|, \tag{2.86}$$

and grouping the terms, one obtains the final form of the Hamiltonian as the sum of a non-interacting and an interacting term respectively given by

$$\mathcal{H}_\nu = \mathcal{H}_0 + \mathcal{V}. \tag{2.87}$$

The non-interacting part is

$$\begin{aligned}\mathcal{H}_0 &= \sum_{l=1}^{n_1}\left[s(\nu_{1l})\frac{\partial^2}{\partial\nu_{1l}^2}+\left(\frac{\beta+2}{2}s'(\nu_{1l})-r(\nu_{1l})\right)\frac{\partial}{\partial\nu_{1l}}\right]\\ &\quad-\frac{\beta}{2}\sum_{k=1}^{n_0}\left[s(\nu_{0k})\frac{\partial^2}{\partial\nu_{ok}^2}+\frac{2}{\beta}r(\nu_{0k})\frac{\partial}{\partial\nu_{0k}}\right],\end{aligned} \tag{2.88}$$

which can be written in a way similar to its correspondent term in x-space (see equation 2.67). Then, from the functions $w_0(\nu)$ and $w_1(\nu)$ defined in the equations 2.80 and 2.81, we get

$$\mathcal{H}_0=\sum_{l=1}^{n_1}\frac{1}{w_1(\nu_{1l})}\frac{\partial}{\partial\nu_{1l}}\left(w_1(\nu_{1l})s(\nu_{1l})\frac{\partial}{\partial\nu_{1l}}\right)-\frac{\beta}{2}\sum_{k=1}^{n_0}\frac{1}{w_0(\nu_{0k})}\frac{\partial}{\partial\nu_{0k}}\left(w_0(\nu_{0k})s(\nu_{0k})\frac{\partial}{\partial\nu_{0k}}\right). \tag{2.89}$$

The interaction term is given by

$$\mathcal{V}=\frac{2-\beta}{\beta}\sum_{k\neq k'}\frac{s(\nu_{0k})}{(\nu_{0k}-\nu_{0k'})^2}+\frac{\beta(2-\beta)}{4}\sum_{l\neq l'}\frac{s(\nu_{1l})}{(\nu_{1l}-\nu_{1l'})^2}+\frac{\beta-2}{2}\sum_{k,l}\frac{s(\nu_{0k})+s(\nu_{1l})}{(\nu_{0k}-\nu_{1l'})^2}+\mathcal{V}_0, \tag{2.90}$$

where

$$\mathcal{V}_0=\frac{1}{12}(\beta+2)\big((\beta+4)s_2-3r_1\big)n_1. \tag{2.91}$$

The full Hamiltonian represents a system with two types of particles: $\nu_{0,1},\ldots,\nu_{0,n_0}$ and $\nu_{1,1},\ldots,\nu_{1,n_1}$, interacting with each other. For $\beta=2$, the Hamiltonian simplifies to the non-interacting case

$$\mathcal{H}_0=\sum_{l=1}^{n}w(\nu_{1l})\frac{\partial}{\partial\nu_{1l}}\left(\frac{s(\nu_{1l})}{w(\nu_{1l})}\frac{\partial}{\partial\nu_{1l}}\right)-\sum_{k=1}^{n}\frac{1}{w(\nu_{0k})}\frac{\partial}{\partial\nu_{0k}}\left(w(\nu_{0k})s(\nu_{0k})\frac{\partial}{\partial\nu_{0k}}\right). \tag{2.92}$$

In deriving this equation we used the fact that $n_0=n_1=n$ from the above condition $\beta n_1=2n_2$, and the definitions of the functions $w_1(\nu)=1/w(\nu)$ and $w_0(\nu)=w(\nu)$ (see equations 2.80 and 2.81). In the next chapter we will use this similarity transformation to solve analytically a quantum transport problem in superconducting systems in the case where the symmetries of the system fix the value $\beta=2$.

3 HEAT TRANSPORT AND MAJORANA FERMIONS IN A SUPERCONDUCTING QUANTUM CHAIN: AN EXACT SOLUTION

Random-matrix theory (RMT) has been widely used in the study of phase-coherent complex quantum systems and has been particularly successful in uncovering universal properties of quantum transport in chaotic and disordered systems [Beenakker 1997]. Much of the success of RMT in quantum transport is due to the strong correspondence between the statistical properties of random-matrix ensembles and the fluctuations of measured observables of complex quantum systems as a function of some control parameter, such as energy or magnetic field. The universality of transport properties, such as the moments of the conductance, lies in their independence of microscopic details of the scattering source. Nevertheless, random-matrix ensembles are sensitive to certain intrinsic symmetries of the system, such as time reversal (TR), spin rotation (SR), particle-hole (PH) and chiral (Ch). It has been established that these symmetries lead to a classification of RMT ensembles into ten universal classes (the ten-fold way) [Altland e Zirnbauer 1997, Caselle 1996], which are divided into three categories: (i) Wigner Dyson (WD, three classes), appropriate to describe normal disordered conductors, (ii) Chiral (CH, three classes), appropriate for systems with a purely off-diagonal disorder, and (iii) Bogoliubov-de Gennes (BdG, four classes), appropriate for normal-superconducting (NS) hybrid systems.

From the perspective of quantum transport, phase coherent mesoscopic systems can be classified into two types: (I) disordered conductors, in which impurities generate multiple elastic scatterings with an associated mean free path l_e that is less than the system's dimensions and (II) ballistic cavities, where l_e is greater than the system's dimensions and thus the dominant scattering mechanism is reflection at the border of the cavity. Remarkably, RMT can efficiently describe both types of systems since universal transport properties do not depend on the details of either the impurity potential (for disordered systems) or the shape of the cavity (for ballistic systems) [Beenakker 1997]. This insensitivity to microscopic details goes as far as to allow an identification, under certain conditions, of a

multichannel disordered quantum wire with a chain of ballistic cavities [Brouwer e Altland 2008].

Besides RMT, there are other well-developed approaches to quantum transport in both disordered wires and chaotic ballistic cavities: the field theoretic non-linear sigma-model [Efetov 1999] and the trajectory-based semiclassical approach [Richter e Sieber 2002] are the most well known. These three approaches have many advantages and pitfalls, but since they are constructed from different and somewhat unrelated statistical hypothesis on the behavior of the underlying degrees of freedom, they may be considered a complementary, albeit equivalent, physical description of the system. Notwithstanding, a full fledged mathematical proof of the equivalence of these three approaches is still missing, in spite of much effort and some successes in particular systems, such as quantum dots with ideal couplings to external leads [Berkolaiko e Kuipers 2012, Macedo-Junior e Macêdo 2014].

In superconducting systems, quantum transport has very striking and different features in comparison with their normal counterpart, which in part is due to what is known as Andreev reflections (AR). The most remarkable phenomenon is probably the possibility of a condensed matter realization of Majorana fermions as protected bound states at the ends of topological superconducting wires [Elliott e Franz 2015]. Transport observables in these systems, such as the electrical conductance, can give information about topological invariants and topological quantum numbers. The thermal conductance, on the other hand, although it may not contain direct information of topological invariants, as can be seen from their random matrix description [Dahlhaus 2012], can still provide valuable information about topological phase transitions [Beenakker 2015].

3.1 The Scattering Problem

Consider a confined quantum system ideally coupled to two electron reservoirs via point contacts with N_1 and N_2 open scattering channels respectively. As we saw in the section 2.4, according to the Landauer-Büttiker scattering formalism [Datta 1997], coherent particle transfer through such a device can be

efficiently described by its scattering matrix, which can be generically written as

$$\boldsymbol{S} = \begin{bmatrix} \boldsymbol{r}_{N_1\times N_1} & \boldsymbol{t}_{N_1\times N_2} \\ \boldsymbol{t}'_{N_2\times N_1} & \boldsymbol{r}'_{N_2\times N_2} \end{bmatrix}, \tag{3.1}$$

where $\boldsymbol{r}$, $\boldsymbol{r}'$ are reflection matrices and $\boldsymbol{t}$, $\boldsymbol{t}'$ are transmission matrices. The subscripts denote the matrix dimensions and the matrices $\boldsymbol{t}\boldsymbol{t}^\dagger$ and $\boldsymbol{t}'\boldsymbol{t}'^\dagger$ are hermitian and have the same set of non-zero transmission eigenvalues $(T_1, ..., T_N) \in [0,1]^N$. Transport observables can be conveniently written in terms of these transmission eigenvalues. For instance, the thermal conductance of a superconducting system, at low temperature T, is given by [Dahlhaus, Béri e Beenakker 2010],

$$G = G_0 d \sum_i^N T_i, \tag{3.2}$$

where $G_0 = \pi^2 k_B^2 T/6h$, $N = \mathrm{m}in(N_1, N_2)$ and d is the spin and/or particle-hole degeneracy.

In ballistic chaotic cavities the transmission eigenvalues are strongly correlated random variables, which because of assumption of ergodic dynamics are well described by RMT. According to RMT, the scattering matrix of a ballistic chaotic cavity with ideal contacts is uniformly distributed over its manifold, and thus the probability density is only restricted by the presence or absence of certain symmetries. For the BdG classes the corresponding joint distribution of transmission eigenvalues is given by [Dahlhaus, Béri e Beenakker 2010]

$$P(\{\tau\}) = C_N \prod_{i<j} |T_i - T_j|^\beta \prod_i T_i^{\beta(\mu+1)/2-1} (1-T_i)^{\gamma/2}, \tag{3.3}$$

where $\mu = |N_1 - N_2|$ and C_N is a normalization constant. The values of the parameters β and γ are solely determined by the symmetries, as shown in the table 2. Note that this equation is more general than equation 2.42 since it includes the asymmetry between the numbers of channels N_1 and N_2 (see figure 3). Here we shall consider only systems in the presence of TR symmetry, which implies $\beta = 2$. Moreover, we must set $\gamma = 1$ for systems in the presence of SR symmetry and $\gamma = -1$ for systems with broken SR symmetry. According to the ten-fold way of classifying random matrix ensembles, these classes are denoted CI and DIII

respectively. We remark that the system described by the equation 3.3 differs from a normal ballistic cavity, because, in addition to the two normal contacts coupling to the reservoirs, the cavity is geometrically defined by a normal-superconducting interface, which generates Andreev reflections [Beenakker 1997]. As a matter of fact, this type of cavity is also known as an Andreev quantum dot [Dahlhaus, Béri e Beenakker 2010]. We remark that if we set $\gamma = 0$ in the equation 3.3 we recover the Wigner Dyson AI class for normal systems with broken TR symmetry (see table 1), which turns out to be a useful way to compare our exact expressions for the moments of the thermal conductance with known results of the literature.

We proceed by combining Andreev quantum dots in a chain geometry, as shown in Figure 12. In such a setup the excitation gap induced by the proximity effect in the inner region is closed by adjusting the superconducting boundaries to have a phase difference of π, which also ensures that there is no breaking of TR symmetry [Beenakker 2015, Dahlhaus, Béri e Beenakker 2010]. The RMT description of the system can be obtained by appropriately combining the scattering matrices of the Andreev quantum dots, or from the corresponding product of random transfer matrices, see [Sena-Junior, Almeida e Macêdo 2014, Pedrosa et al. 2015] for more details. An equivalent description using the supersymmetric non-linear sigma model is also possible [Iida, Weidenmüller e Zuk 1990]. Since we want to obtain exact analytical results, we follow reference [Macêdo 2000, Duarte-Filho, Macedo-Junior e Macêdo 2007] and take the continuum limit which leads to a Fokker-Planck equation for the evolution, with the sample's length, of the joint probability distribution of transmission eigenvalues with a zero-length initial condition given by the RMT description of an Andreev quantum dot. See reference [Iida, Weidenmüller e Zuk 1990, Duarte-Filho, Macedo-Junior e Macêdo 2007] for the corresponding problem with normal quantum dots.

The Fokker-Planck equation of a disordered Andreev quantum wire of length L, with N open scattering channels, is given by (see equation 2.51) [Brouwer et al. 2000]

$$\frac{\partial P}{\partial s} = \sum_{i}^{N} \frac{\partial}{\partial q_i} J \frac{\partial}{\partial q_i} \frac{P}{J}, \tag{3.4}$$

where $s = L/[2l_e(\beta N - \beta + \alpha + 1)]$ is an adimensional length and

$$J = \prod_{i<j} |\cosh(2q_i) - \cosh(2q_j)|^{\beta} \prod_{i}^{N} \sinh^{\alpha}(2q_i). \tag{3.5}$$

The variables q_i are related to the transmission eigenvalues through the relation $T_i = \text{sech}^2(q_i)$ and since we are considering superconducting TR-symmetric systems, we must set $\beta = 2$. The parameter α can take the values $\alpha = 2$ (in the presence of SR symmetry) and $\alpha = 0$ (in the absence of SR symmetry). The WD class is obtained by setting $\alpha = 1$ and assuming that TR symmetry is broken (table 4).

The problem has thus been reduced to solving the equation 3.4 with an initial condition given by the equation 3.3, which is the joint probability distribution of transmission eigenvalues of an Andreev quantum dot. Remarkably, an exact analytical solution can be constructed using an integral transform method [Macedo-Junior e Macêdo 2006] which provides a complete description of the smooth crossover of the thermal conductance moments as a function of the system's length, covering all transport regimes: ballistic, metallic and insulating. For a related study of a normal dot-wire system (WD class) with broken TR symmetry, see [Macêdo 2000].

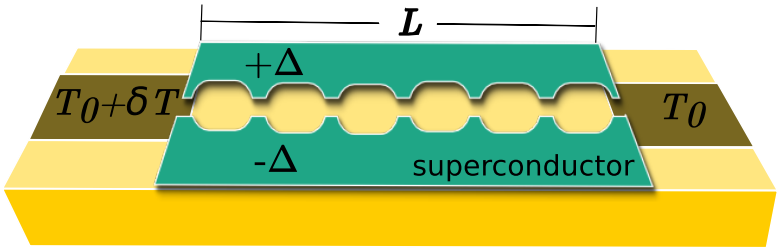

Figure 12 – Chain of Andreev quantum dots. By varying the sample's length L, we can go from a quantum dot to a chain of dots, which in the continuous limit is a quantum wire. The conducting device is bounded by superconductors with a phase difference of π (order parameters given by $\pm\Delta$) and connected to electron reservoirs with different temperatures via ideal contacts.

3.2 The Integral Transform Method

In the section 2.6 we study a powerful way to represent the probability distributions of the RMT ensembles is to employ a classification scheme based on matrix valued Brownian motion ensembles [Macedo-Junior e Macêdo 2006]. In this section were defined the following functions

$$J_\beta(\{x\}) = \prod_{i<j}^{N} |x_i - x_j|^\beta \quad \text{and} \quad \omega_N(\{x\}) = \prod_{i}^{N} \omega(x_i), \tag{3.6}$$

where the random variables x_i are related to the transmission eigenvalues T_i via a simple procedure described in [Macedo-Junior e Macêdo 2006]. For a ballistic cavity we may follow the reference [Souza e Macedo-Junior 2015] and take $x_i = T_i$ and write the joint distribution as the stationary solution of the corresponding Brownian motion. We thus get

$$P^{(0)}(\{x\}) = C_N J_\beta(\{x\})\omega_N(\{x\}), \tag{3.7}$$

where the function $\omega(x)$ is given in the table 6. The equation 3.7 will be used as the initial condition of our crossover problem. On the other hand, for a quasi-one-dimensional quantum wire we may follow the reference [Macedo-Junior e Macêdo 2007] and take $x_i = \cosh(2q_i) = (2 - T_i)/T_i$ and write the corresponding Fokker-Planck equation as

$$\frac{\partial P}{\partial s} = \sum_{i}^{N} \frac{\partial}{\partial x_i} s(x_i)\omega_N J_\beta \frac{\partial}{\partial x_i} \frac{P}{\omega_N J_\beta}, \tag{3.8}$$

where the functions $\omega(x)$ and $s(x)$ are also given in the table 6.

Table 6 – Classification of Brownian motion ensembles for the BdG class

RMT	random variable	$\omega(x)$	$s(x)$	a	b
dot	$x_i = T_i$	$x^{\beta(\mu+1)/2-1}(1-x)^{\gamma/2}$	$x(1-x)$	0	1
wire	$x_i = 2/T_i - 1$	$(x^2-1)^{(\alpha-1)/2}$	x^2-1	1	∞

Instead of directly solving the Fokker-Plank equation 3.8 with initial condition 3.7, we employ an integral transform method that effectively maps equation

3.8 onto a much simpler Fokker-Planck problem in an image space of smaller dimension. The multidimensional integral transform was defined in the subsection 2.6.2 as [Macedo-Junior e Macêdo 2006]

$$W(\{\vartheta\}, s) = \int d^N x \; \Omega_\beta(\{x\}, \{\vartheta\}) P(\{x\}, s), \tag{3.9}$$

where the kernel Ω_β is chosen to have only two $\{\vartheta\}$ variables, which is the minimal number of image variables that allows the exact calculation of the first three heat conductance moments. We thus define (analogously to the equation 2.70)

$$\Omega_\beta(\{x\}, \{\vartheta\}) = \prod_i^N \frac{x_i - \vartheta_{0,1}}{x_i - \vartheta_{1,1}}. \tag{3.10}$$

The Fokker-Planck equation in image space $\{\vartheta\}$ is given by

$$\left(\frac{\partial}{\partial s} - \mathcal{M}_\vartheta^\dagger \right) W(\{\vartheta\}, s) = 0, \tag{3.11}$$

where

$$\mathcal{M}_\vartheta^\dagger = \frac{1}{VB} \sum_{i=0}^{1} (-1)^{1+i} \frac{\partial}{\partial \vartheta_{i,1}} \left(s(\vartheta_{i,1}) VB \frac{\partial}{\partial \vartheta_{i,1}} \right) \tag{3.12}$$

and we defined

$$V = \frac{\omega(\vartheta_{0,1})}{\omega(\vartheta_{1,1})} \quad \text{and} \quad B = \frac{1}{(\vartheta_{0,1} - \vartheta_{1,1})^2}, \tag{3.13}$$

in the same way as section 2.6.2. We can now perform the transformation

$$W(\{\vartheta\}, s) = 1 + \omega(\vartheta_{1,1}) B^{-1/2} \Psi(\{\vartheta\}, s) \tag{3.14}$$

that maps equation 3.11 onto a Schrödinger equation in imaginary time ($s \to it$). Choosing $\vartheta_{0,1} = -\vartheta_0$ and $\vartheta_{1,1} = -\vartheta_1$:

$$\frac{\partial \Psi}{\partial t} + \mathcal{H} \Psi = 0, \tag{3.15}$$

where

$$\mathcal{H} = \sum_{i=0}^{1} (-1)^i \frac{1}{\omega(\vartheta_i)} \frac{\partial}{\partial \vartheta_i} \left(\omega(\vartheta_i) s(\vartheta_i) \frac{\partial}{\partial \vartheta_i} \right) \tag{3.16}$$

is a free particle Hamiltonian in image space.

We proceed by calculating the initial condition $W(\{\vartheta\},0)$ using the joint distribution of the Andrev quantum dot (see equation 3.7). Here we may again use the integral transform method with the following modified kernel

$$\Omega_{\beta}^{(0)}(\{\tau\},\{\vartheta\}) = \left(\frac{1-\vartheta_0}{1-\vartheta_1}\right)^N \prod_i^N \frac{T_i - 2/(1-\vartheta_0)}{T_i - 2/(1-\vartheta_1)}, \tag{3.17}$$

where $T_i = x_i$. The choice of kernel is motivated from the connection between the supersymmetric non-linear sigma model and RMT [Macêdo 2000]. From the stationary solution of the corresponding Fokker-Planck equation, we find (see the appendix A)

$$W(\{\vartheta\},0) = 1 + (\vartheta_0 - \vartheta_1)\sum_{l=0}^{N-1} \frac{(1-\vartheta_0)^l}{(1-\vartheta_1)^{l+1}}(f_{N-l-1}(\vartheta_0)g_{N-l-1}(\vartheta_1) - 1), \tag{3.18}$$

where

$$\begin{aligned} f_n(\vartheta_0) &= F[-n, -n-\mu; -2n-\mu-\frac{\gamma}{2}; \frac{1-\vartheta_0}{2}], \\ g_n(\vartheta_1) &= F[n+1, n+1+\mu; 2n+\mu+\frac{\gamma}{2}+2; \frac{1-\vartheta_1}{2}], \end{aligned} \tag{3.19}$$

and $F[a,b;c;z]$ denotes the hypergeometric function.

We are now in position to unify the notations for the symmetry indices γ and α of the quantum dot and the quantum wire respectively. For that, we introduce the new index

$$\nu = \frac{\alpha - 1}{2} = \frac{\gamma}{2}, \tag{3.20}$$

which can have two values: $\nu = 1/2$ (system with TR and SR symmetry) or $\nu = -1/2$ (systems with TR symmetry and no SR symmetry). In the ten-fold way of S-matrix classification, these classes correspond to CI and DIII respectively. We remark that $\nu = 0$ corresponds to the Wigner-Dyson AI class (systems with no TR symmetry).

3.3 Exact Solution for the Dot-Wire System

We can now address the full problem and solve the equation 3.11, which describes a superconducting quantum wire, with a quantum dot initial condition

given by the equation 3.18. It will prove convenient to use the kernel 3.10 with the choices $\vartheta_{0,1} = -\vartheta_0$ and $\vartheta_{1,1} = -\vartheta_1$, so that we may write

$$\Omega_\beta(\{x\},\{\vartheta\}) = \prod_i^N \frac{x_i + \vartheta_0}{x_i + \vartheta_1}. \tag{3.21}$$

Note that after using the relation $x_i = 2/T_i - 1$ we recover the equation 3.17.

Following the procedure introduced in [Macedo-Junior e Macêdo 2006] and [Macêdo 2000] we can find the eigenvalues of the Hamiltonian $\mathcal{H}$, shown in the equation 3.16. We start by specifying the domains of the variables ϑ_0 and ϑ_1. Inspired by the supersymmetry calculations of the reference [Macêdo 2000], we set $-1 \leq \vartheta_0 \leq 1$ and $1 \leq \vartheta_0 \leq \infty$. The eigenvalues of $\mathcal{H}$ are $\varepsilon_{nk} = k^2 + (n+\nu+1/2)^2$ and the corresponding eigenfunctions are (see appendix B):

$$\varphi_{nk}(\vartheta_0,\vartheta_1) = \frac{A_k^{(-\nu)}}{(h_n^{(\nu)})^{1/2}} P_n^{(\nu)}(\vartheta_0) \frac{F_k^{(-\nu)}(\vartheta_1)}{\omega(\vartheta_i)}, \tag{3.22}$$

where $h_n^{(\nu)}$ and $A_k^{(\nu)}$ are normalization constants of the Jacobi polynomials $P_n^{(\nu)}(\vartheta_0) \equiv P_n^{(\nu,\nu)}(\vartheta_0)$ and the hypergeometric function $F_k^{(\nu)}(\vartheta_1) = F[\nu + \frac{1}{2} + ik, \nu + \frac{1}{2} - ik; \nu + 1; \frac{1-\vartheta_1}{2}]$ respectively (see Appendices A and B).

We can now construct the Green's function by using its spectral resolution in terms of the eigenfunctions and the eigenvalues of $\mathcal{H}$. We find

$$G(\{\vartheta\},\{\vartheta'\},s) = (1-\vartheta_0'^2)^\nu (\vartheta_1'^2 - 1)^\nu \sum_{n=0}^{\infty} \int_0^\infty dk \varphi_{nk}(\vartheta_0,\vartheta_1)\varphi_{nk}(\vartheta_0',\vartheta_1') e^{-\varepsilon_{nk}s}. \tag{3.23}$$

From the completeness of the eigenfunctions, it follows immediately that

$$G(\{\vartheta\},\{\vartheta'\},0) = \delta(\vartheta_0 - \vartheta_0')\delta(\vartheta_1 - \vartheta_1') \tag{3.24}$$

Using the equation 3.23, we can write 3.14 as

$$W(\{\vartheta\},s) = 1 + (\vartheta_0 - \vartheta_1)\omega(\vartheta_1) \int_{-1}^1 d\vartheta_0' \int_1^\infty d\vartheta_1' G(\{\vartheta\},\{\vartheta'\},s) \frac{W(\vartheta',0)}{(\vartheta_0' - \vartheta_1')\omega(\vartheta_1')} e^{-\varepsilon_{nk}s} \tag{3.25}$$

Inserting the equation 3.23 into 3.25, we get

$$W(\{\vartheta\},s)=1+(\vartheta_0-\vartheta_1)\sum_{n=0}^{\infty}\int_0^{\infty}dk\frac{(A_k^{(-\nu)})^2}{h_n^{(\nu)}}e^{-\varepsilon_{nk}s}P_n^{(\nu)}(\vartheta_0)F_k^{(-\nu)}(\vartheta_1)\sum_{l=0}^{N-1}(I_{nl}^{(1)}J_{kl}^{(1)}-I_{nl}^{(0)}J_{kl}^{(0)}), \tag{3.26}$$

where $I_{nl}^{(i)}$ and $J_{kl}^{(i)}$, $i\in\{0,1\}$, are obtained from the following integrals

$$\begin{aligned}
I_{nl}^{(0)}&=\int_{-1}^{1}d\vartheta_0(1-\vartheta_0^2)^{\nu}P_n^{(\nu)}(\vartheta_0)(1-\vartheta_0)^l,\\
J_{kl}^{(0)}&=\int_{1}^{\infty}d\vartheta_1\frac{F_k^{(-\nu)}(\vartheta_1)}{(\vartheta_1^2-1)^{\nu}(1-\vartheta_1)^{l+1}},\\
I_{nl}^{(1)}&=\int_{-1}^{1}d\vartheta_0(1-\vartheta_0^2)^{\nu}P_n^{(\nu)}(\vartheta_0)(1-\vartheta_0)^l f_{N-l-1}(\vartheta_0),\\
J_{kl}^{(1)}&=\int_{1}^{\infty}d\vartheta_1\frac{F_k^{(-\nu)}(\vartheta_1)}{(\vartheta_1^2-1)^{\nu}(1-\vartheta_1)^{l+1}}g_{N-l-1}(\vartheta_1).
\end{aligned} \tag{3.27}$$

The integrals are calculated in the Appendix C in terms of the number of open channels N_1 and N_2. Note that the information about the number of channels is encoded in the functions $f_n(\vartheta_0)$ and $g_n(\vartheta_1)$ (see equation 3.19). The final result is presented in the following theorem

Theorem 1. *The solution of the Fokker Planck equation 3.11 with initial condition given by 3.18, in the space of the coordinates $\{\vartheta\}$, is given by*

$$W(\{\vartheta\},s)=1+2(\vartheta_0-\vartheta_1)\sum_{n=0}^{N-1}\frac{P_n^{(\nu)}(\vartheta_0)P_n^{(\nu)}(1)}{h_n^{(\nu)}}\int_0^{\infty}d\mu_{nk}c_{nk}^{(\nu)}(N_1)c_{nk}^{(\nu)}(N_2)F_k^{(-\nu)}(\vartheta_1)e^{-\varepsilon_{nk}s}, \tag{3.28}$$

where $d\mu_{nk}=dk|\Gamma(1/2-\nu+ik)|^2/(|\Gamma(ik)|^2\varepsilon_{nk})$ and

$$c_{nk}^{(\nu)}(N)=\frac{|\Gamma(N+\nu+1/2+ik)|^2}{(N-n-1)!\Gamma(N+n+2\nu+1)}. \tag{3.29}$$

This theorem is the central result of this work. It can be used as a generating function to find the first three moments of the thermal conductance. A noteworthy feature of the exact result is the the separation of the left-right boundary conditions in the form of the product $c_{nk}^{(\nu)}(N_1)c_{nk}^{(\nu)}(N_2)$, which as we will see later allows a straightforward identification of different conducting regimes.

3.4 Application: Moments of the Heat Conductance

As an application of the equation 3.28 we calculate the first three moments of the heat conductance. The Landauer formula for the dimensionless thermal conductance is

$$g = \sum_{i}^{N} T_i = \sum_{i}^{N} \frac{2}{1+x_i}. \tag{3.30}$$

From the equations 3.9, 3.21 and 3.30 it is straightforward to verify that the first three moments of thermal conduction can be obtained from the generating function as

$$\langle g \rangle = \left.\frac{2\partial W}{\partial \vartheta_0}\right|_{\vartheta_0=1=\vartheta_1} \quad \langle g^2 \rangle = -\left.\frac{4\partial^2 W}{\partial\vartheta_0\partial\vartheta_1}\right|_{\vartheta_0=1=\vartheta_1} \text{ and}$$
$$\langle g^3 \rangle = 4\left.\left(\frac{\partial^3 W}{\partial\vartheta_0\partial\vartheta_1^2} - \frac{\partial^3 W}{\partial\vartheta_1\partial\vartheta_0^2}\right)\right|_{\vartheta_0=1=\vartheta_1}. \tag{3.31}$$

From the equation 3.28 we get

$$\langle g^m \rangle = 4\sum_{n=0}^{N-1} \frac{(P_n^{(\nu)}(1))^2}{h_n^{(\nu)}} \int_0^\infty d\mu_{nk} g_{nk}^{(m)} c_{nk}^{(\nu)}(N_1) c_{nk}^{(\nu)}(N_2) e^{-\varepsilon_{nk}s}, \tag{3.32}$$

where

$$g_{nk}^{(1)} = 1, \quad g_{nk}^{(2)} = \frac{k^2+(1/2-\nu)^2}{(1-\nu)} + \frac{n(n+2\nu+1)}{(1+\nu)},$$
$$g_{nk}^{(3)} = \frac{(k^2+(1/2-\nu)^2)(k^2+(3/2-\nu)^2)}{2(2-\nu)(1-\nu)} + \frac{2n(n+2\nu+1)(k^2+(1/2-\nu)^2)}{(1+\nu)(1-\nu)}$$
$$+\frac{n(n-1)(n+2\nu+1)(n+2\nu+2)}{2(1+\nu)(2+\nu)}. \tag{3.33}$$

Equation 3.32 is a very general exact result. It is valid for any number of channels N_1 and N_2, and for any value of the dimensionless length of the quantum wire s. It is the central application of this paper and as it stands it can serve as a useful tool to compare with results from other non-perturbative approaches, such as the trajectory-based semiclassical technique and field-theoretic methods.

In the figure 13 we show the behavior of the first three cumulants (denoted with double brackets) of the thermal conductance, as a function of the system's length, of both the WD (full line) and BdG classes DIII (dashed line) and CI

(dotted line) for the case of a single channel in each lead. This case is particularly interesting, since as shown in the reference [Dahlhaus, Béri e Beenakker 2010] the class DIII can be realized using Majorana modes of topological superconductors. Therefore, the unusual behavior of the heat conductance moments in this class can be interpret as a signature of the presence of Majorana fermions in the system.

It was, in the study of disordered quantum wires that evidences of the presence of condensed matter Majorana modes emerged most clearly. These can be traced back to the prediction [Brouwer et al. 2000] that for quantum wires in the chiral classes (for odd N open scattering channels) and in the superconducting D and DIII classes there is no exponential localization, since, unlike its behavior in the standard classes, the average conductance falls off in the limit of long distances $L \gg Nl$ as $1/\sqrt{L}$, which is a kind of super-ohmic behavior. They also found that in these special classes the average density of states (DOS) diverges logarithmically, $\rho(\varepsilon) \sim 1/|\varepsilon\tau \ln^3(\varepsilon\tau)|$, as energy $\varepsilon \to 0$ (where $\tau = N^2 l$ and the Fermi velocity has been set to unity). A similar singularity had already been found by Dyson in the analysis of disordered linear chains [Dyson 1953]. On the other hand, the reference [Motrunich, Damle e Huse 2001] found through a general analysis using strong-disorder renormalization group (RG) that systems of classes D and DIII exhibit localization and an average DOS that vanishes as a power law $\rho(\varepsilon) \sim |\varepsilon\tau|^{\delta-1}$ with $\delta > 0$, as $\varepsilon \to 0$. Remarkably, at certain critical points obtained by fine-tuning the disorder, both delocalization and Dyson's divergence can be present. The authors of the reference [Motrunich, Damle e Huse 2001] were also among the first to relate this special type of criticality to transitions between topological phases and also to point out that it could be a signature of the existence of Majorana zero modes. The reference [Gruzberg, Read e Vishveshwara 2005] confirmed these results and presented evidence that the delocalization at critical points is well described by the DMPK equation of superconductors. Furthermore, they claimed that there may be a "superuniversality" combining the chiral class and the superconducting classes D and DIII, since they have certain similar characteristics in regards to these critical points. Later, the authors of the references [Mudry 2017, Morimoto, Furusaki e Mudry 2015] argued that the diverging nature of the average density of states at the band centre is a signature

of topologically protected zero modes bound to point defects. As discussed in the subsection 2.5.2, there is a correspondence between delocalization, Dyson divergence and topologically Majorana zero modes in the superconducting classes D and DIII.

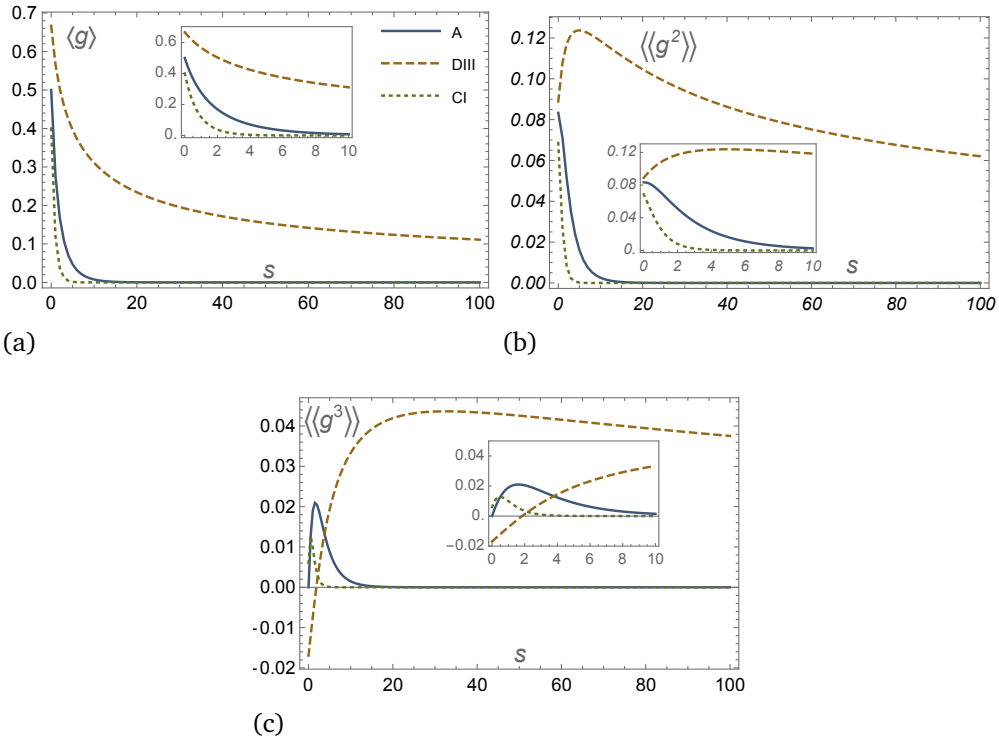

Figure 13 – First three cumulants of the thermal conductance for the WD class A (full line) and BdG classes DIII (dashed line) and CI (dotted line) with a single open channel: $N_1 = N_2 = 1$. The insets show the small s behaviors. Note the qualitative difference of the class DIII BdG system. (Color online)

In the long length limit, $s \gg 1$, we may use the saddle-point method in the equation 3.32 to obtain more explicit analytic expressions for each class. For the class AI, we get

$$\langle g \rangle = 4\langle g^2 \rangle = \frac{64}{9}\langle g^3 \rangle = 2c_{00}^{(0)}(N_1)c_{00}^{(0)}(N_2)\left(\frac{\pi}{s}\right)^{3/2} e^{-s/4}, \tag{3.34}$$

whilst for classes DIII and CI we find respectively

$$\langle g\rangle = \frac{3}{2}\langle g^2\rangle = \frac{15}{8}\langle g^3\rangle = \frac{2}{\sqrt{\pi s}}, \tag{3.35}$$

$$\langle g\rangle = s\langle g^2\rangle = 3s\langle g^3\rangle = 4c_{00}^{(1/2)}(N_1)c_{00}^{(1/2)}(N_2)\frac{e^{-s}}{\sqrt{\pi s}}. \tag{3.36}$$

From these equations, we see that the BdG DIII class shows anomalous power law behaviors in all three moments. In contrast, the other two classes (WD and CI) show a rapid exponential decay of the moments as a function of s, which is a common signature of Anderson localization. The significant attenuation in the decay of the moments for the DIII class as a function of the system's length is thus a kind of delocalization effect, which can be interpreted as indicating a type of anomalous metallic behavior. Since a normal disordered quantum wire shows exponential localization when its length exceeds the localization length, we must conclude that the localization length vanishes for a class DIII BdG system. A similar conclusion has been reached in [Macêdo 2002] for a thick quantum wire in series with a quantum point contact, which can be described by a DMPK Fokker-Planck equation with a delta function initial condition.

Another noteworthy feature comes from the fact that $c_{nk}^{(\nu)}(N) = 1$ when $N \to \infty$. Using this property we can recover several previous results of the literature. The most interesting cases are: (a) thick wire: we take $N_1 \to \infty$ and $N_2 \to \infty$, which reproduces the results found in the reference [Mirlin, Mullergroeling e Zirnbauer 1994] and (b) the disordered quantum wire limit: we take $N_1 \to \infty$ with N_2 fixed or $N_2 \to \infty$ with N_1 fixed, which reproduces the results shown in the reference [Macêdo 2002].

It is also useful to investigate the system's behavior close to the ballistic limit, i.e. when $s \ll 1/g_c$, where $g_c = N_1N_2/(N_1 + N_2)$. For that, we expand the equation 3.32 around $s = 0$ to obtain

$$\langle g\rangle = \frac{N_1N_2}{N_1 + N_2 + \nu}\left(1 - \frac{(N_1 + \nu)(N_2 + \nu)(N_1 + N_2 + 2\nu)}{(N_1 + N_2 + \nu)^2 - 1}s + ...\right) \tag{3.37}$$

and

$$\langle\langle g^2\rangle\rangle = \frac{N_1(N_1+\nu)N_2(N_2+\nu)}{(N_1+N_2+\nu)^2((N_1+N_2+\nu)^2-1)}(1 + \frac{2((N_1-N_2)^2-\nu^2)(N_1+N_2+2\nu)}{(N_1+N_2+\nu)^2-4}s+...). \tag{3.38}$$

Note that the zero-order terms reproduce the results of the quantum dot for the three classes [Souza e Macedo-Junior 2015], as expected. The correction terms are new predictions that may be useful for comparison with alternative techniques, such as the trajectory-based semiclassical approach.

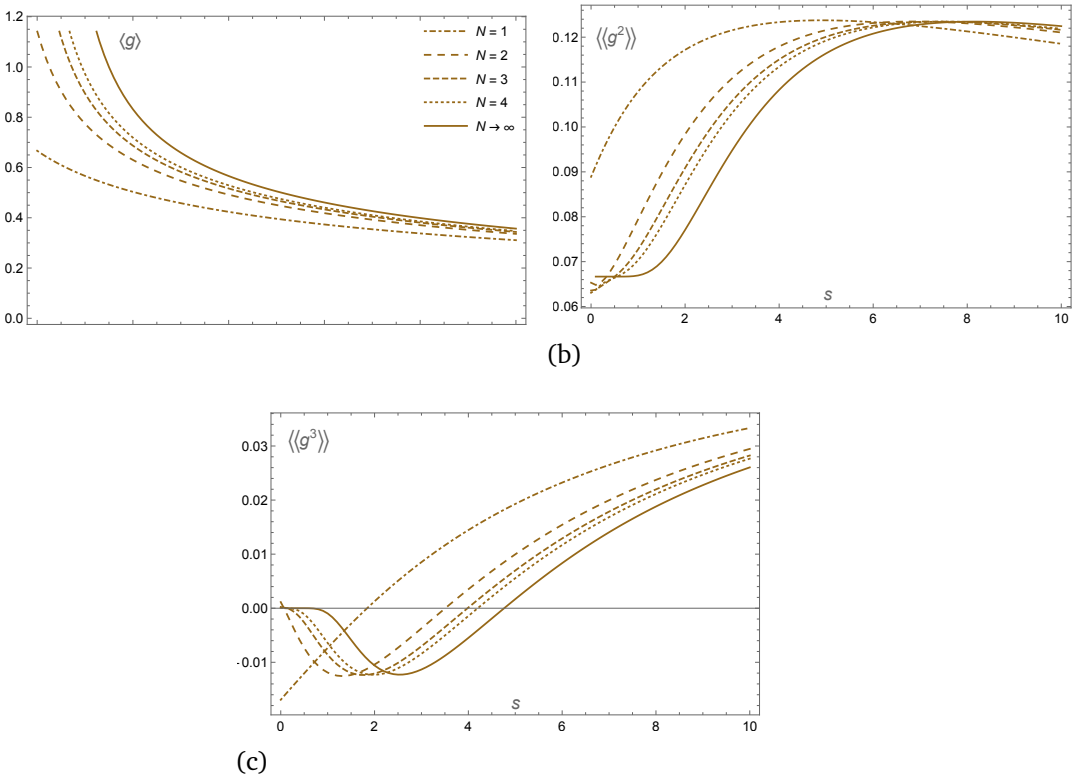

Figure 14 – Variation of the first three cumulants of the thermal conductance for the DIII class with different numbers of channels N. $N_1 = N_2 = N$

Finally, in the figure 14 we show the behavior of the first three cumulants of the DIII class as a function of the number of channels in each lead. We keep $N_1 = N_2$ and compare the result with the thick-wire limit $N \to \infty$. We observe

that said limit is reached quickly after an increase of a few channels. The same is also true for the WD and CI classes.

4 NON-EQUILIBRIUM OPEN QUANTUM SYSTEMS

As we have seen in the previous chapters, scattering matrix theory (SMT) has had great success in describing quantum transport phenomena, not only for complex systems (using the RMT) but also with simple systems [Blanter e Büttiker 2000]. However, SMT says nothing about the interactions inside the system, because by construction, it only relates the wave functions in the leads, before and after the scattering, without concern for the interactions inside the sample. In contrast, the formalism of the master equation has a microscopic construction starting from the Hamiltonian of the system. It therefore can describe the interactions of particles within the sample, which is useful in the study of phenomena related to quantum control operations in simple transport systems, and the thermodynamics associated with them.

The master equations, originally formulated to the study of quantum optics systems [Breuer, Petruccione et al. 2002], were adapted to describe solid-state systems [Kulik e Shekhter 1975, Gurvitz e Prager 1996]. The best known and used is the master equation type Lindblad, which besides the Markovian property, it is also consistent with the rotating wave approximation, thus providing it with a conceptually coherent theoretical framework. Lindblad master equation is usually derived from a second order perturbative treatment of the coupling between the system and the environment. Various improvements have been proposed, such as taking into account higher orders in perturbation theory [Zedler 2011], using Liouvillian form of perturbation theory [Schoeller 2009, Emary 2010], or including memory effects. This latter generates non-Markovian master equations [Braggio, König e Fazio 2006], which may also have consistency and interpretation problems, such as the fact that it may yield negative probabilities. In this Thesis, we use the Lindblad master equation because it allows making a consistent thermodynamic construction and to make extensions in a simple way, such as including the Full Counting Statistics.

4.1 Master equation and full counting statistics

The dynamic evolution of open quantum systems is non-unitary. This is either due to the interaction with measuring instruments (measurement problem) or the interaction with the environment (reservoirs for example). Open quantum systems do not follow the unitary dynamic evolution of closed systems, which follow the von-Neumann equation

$$\dot{\rho}(t) = -i[H(t), \rho(t)], \tag{4.1}$$

whose formal solution can be written as

$$\rho(t) = U(t)\rho(0)U^{\dagger}(t), \tag{4.2}$$

with the unitary time evolution operator

$$U(t) = \hat{\tau} \exp\left(-i \int_0^t H(t')dt'\right), \tag{4.3}$$

where $\hat{\tau}$ is the time-ordering operator. The von-Neumann equation describes the unitary evolution of the density matrix of a closed system and preserves all its intrinsic properties, such as self-adjointness, unit trace, and positivity. So a general non-unitary evolution of open systems should ideally also preserve these properties.

The map that represents the most general evolution that preserves the above cited properties of the density matrix is the Kraus map [Kraus 1983]

$$\rho(t + \Delta t) = \sum_{\alpha} K_{\alpha}(t, \Delta t)\rho(t)K_{\alpha}^{\dagger}(t, \Delta t), \tag{4.4}$$

where the Kraus operators $K_{\alpha}(t, \Delta t)$ are defined as

$$\sum_{\alpha} K_{\alpha}(t, \Delta t)K_{\alpha}^{\dagger}(t, \Delta t) = 1. \tag{4.5}$$

The von-Neumann unitary evolution is a particular case of a Kraus map, but a direct interpretation of the Kraus operators for open systems is not so direct.

If we are led by certain restrictions that may be reasonable for certain physical systems, it is possible to obtain more practical and simple solutions. This

is the case of the Lindblad equation, which can be obtained by imposing a locality in time property and to have constant coefficients. So, under these considerations, the Lindblad equation is the most general master equation that preserves the self-adjointness, unit trace, and positivity of the density matrix [Lindblad 1976].

In an N-dimensional Hilbert space, the Lindblad master equation has the form

$$\dot{\rho} = \mathcal{W}\rho = -i[H,\rho] + \sum_{\alpha,\beta} \gamma_{\alpha,\beta} \left(A_\alpha \rho A_\beta^\dagger - \frac{1}{2}\{A_\beta^\dagger A_\alpha, \rho\} \right), \tag{4.6}$$

where $H = H^\dagger$ and $\gamma_{\alpha,\beta} = \gamma_{\beta,\alpha}^\dagger$ is a positive semidefinite matrix, i.e. all eigenvalues of $\gamma_{\alpha,\beta}$ are non-negative. Note that this equation is composed of a unitary part (von-Neumann type) and another non-unitary part driven by the damping matrix $\gamma_{\alpha,\beta}$. This damping matrix can be diagonalized using unitary transformations such that $\sum_{\alpha,\beta} U_{\alpha,\alpha'} \gamma_{\alpha,\beta} U_{\beta,\beta'}^\dagger = \delta_{\alpha',\beta'}\gamma_{\alpha'}$. These unitary operations can be used to define a new set of operators $A_\alpha = \sum_{\alpha'} U_{\alpha,\alpha'} L_{\alpha'}$ so that the Lindblad equation can be rewritten in a simplified way [Schaller 2014]

$$\dot{\rho} = -i[H,\rho] + \sum_{\alpha} \gamma_{\alpha} \left(L_\alpha \rho L_\alpha^\dagger - \frac{1}{2}\{L_\alpha^\dagger L_\alpha, \rho\} \right). \tag{4.7}$$

It is possible to make a rigorous derivation of the Lindblad equation from a few assumptions and approximations considering that the system of interest is coupled to the environment through a reservoir typically much larger than the system. The central point of the derivation lies in the consideration that the coupling between the system and the reservoir is weak, so it will be considered a perturbative expansion on the environment. The total Hamiltonian is composed by the Hamiltonian of the system $\mathcal{H}_S$, the Hamiltonian of the bath $\mathcal{H}_B$ and the Hamiltonian of interaction $\mathcal{H}_I$ that directly connects the observables of the system and reservoir respectively, thus

$$H = \mathcal{H}_S \otimes \mathbf{1} + \mathbf{1} \otimes \mathcal{H}_B + \mathcal{H}_I, \tag{4.8}$$

and

$$\mathcal{H}_I = \sum_{\alpha} A_\alpha \otimes B_\alpha. \tag{4.9}$$

The size of the reservoir is always considered much larger than the size of the system (see figure 15). For completeness, a deduction of the Lindblad equation

will be shown below. It is not intended to be rigorous or step-by-step guided, but will help us discuss the physical aspects of the approximations used in its derivation.

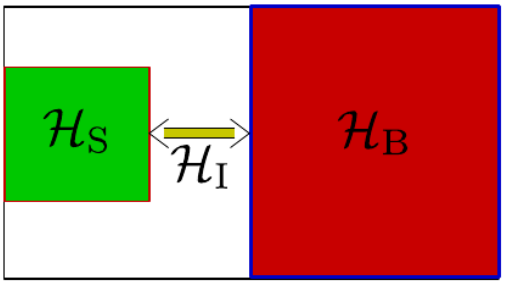

Figure 15 – An open system (S) can be considered as a small part of a system coupled to a much larger bath (B) by means of an interaction described by $\mathcal{H}_I$ [Schaller 2014].

4.1.1 Born approximation

For convenience, we are going to work in the interaction picture, where the symbols will be written in bold characters as is usually done. Thus, we may write the density operator

$$\boldsymbol{\rho}(t) = e^{i(H_S+H_B)t}\rho(t)e^{-i(H_S+H_B)t}, \tag{4.10}$$

which evolves in time according to

$$\dot{\boldsymbol{\rho}} = -i[\boldsymbol{\mathcal{H}_I}(t), \boldsymbol{\rho}] \tag{4.11}$$

where

$$\boldsymbol{\mathcal{H}_I} = \sum_\alpha \boldsymbol{A_\alpha}(t) \otimes \boldsymbol{B_\alpha}(t). \tag{4.12}$$

Without loss of generality, the operators in $\mathcal{H}_I$ are considered to be hermitian $A_\alpha^\dagger = A_\alpha$ and $B_\alpha^\dagger = B_\alpha$. Iterating the formal general solution of equation 4.11 with itself and doing the partial trace on the Hilbert space of the bath to discard its degrees of freedom, we obtain

$$\dot{\boldsymbol{\rho}}_S = -i\,\mathrm{Tr}_B\{[\boldsymbol{\mathcal{H}_I}(t), \boldsymbol{\rho}]\} - \int_0^t \mathrm{Tr}_B\{[\boldsymbol{\mathcal{H}_I}(t), [\boldsymbol{\mathcal{H}_I}(t'), \boldsymbol{\rho(t')}]]dt'\}. \tag{4.13}$$

Here we make the Born approximation namely, the assumption that the reservoir are much larger than the system, so that the system hardly affects the reservoir. It is then is possible to expand the total density matrix as

$$\boldsymbol{\rho}(t) = \boldsymbol{\rho}_S(t) \otimes \rho_B + \mathcal{O}\{\lambda\}, \tag{4.14}$$

where λ is the coupling parameter between the system and the reservoir $\boldsymbol{\mathcal{H}_I} \sim \mathcal{O}\{\lambda\}$, which is assumed small and dimensionless. So the equation 4.13 is interpreted as a second order expansion

$$\dot{\boldsymbol{\rho}}_S = -i\,\mathrm{Tr}_B\{[\boldsymbol{\mathcal{H}_I}(t), \boldsymbol{\rho}]\} - \int_0^t \mathrm{Tr}_B\{[\boldsymbol{\mathcal{H}_I}(t), [\boldsymbol{\mathcal{H}_I}(t'), \boldsymbol{\rho}_S(t') \otimes \rho_B]]\}dt' + \mathcal{O}\{\lambda^3\}. \tag{4.15}$$

Substituting the equations 4.12 and 4.14 into 4.15 yields

$$\dot{\boldsymbol{\rho}}_S = -i \sum_{\alpha} (\boldsymbol{A_\alpha}(t)\rho_S^0(t)\,\mathrm{Tr}\{\boldsymbol{B_\alpha}(t)\rho_B\} - \rho_S^0(t)\boldsymbol{A_\alpha}(t)\,\mathrm{Tr}\{\boldsymbol{\rho_B}\boldsymbol{B_\alpha}(t)\}) \tag{4.16}$$

$$\begin{aligned} -\sum_{\alpha,\beta} \int_0^t \big(&+ \boldsymbol{A_\alpha}(t)\boldsymbol{A_\beta}(t')\boldsymbol{\rho}_S(t')\,\mathrm{Tr}\{\boldsymbol{B_\alpha}(t)\boldsymbol{B_\beta}(t')\rho_B\} \\ &- \boldsymbol{A_\alpha}(t)\boldsymbol{\rho}_S(t')\boldsymbol{A_\beta}(t')\,\mathrm{Tr}\{\boldsymbol{B_\alpha}(t)\rho_B\boldsymbol{B_\beta}(t')\} \\ &- \boldsymbol{A_\beta}(t)\boldsymbol{\rho}_S(t')\boldsymbol{A_\alpha}(t')\,\mathrm{Tr}\{\boldsymbol{B_\beta}(t)\rho_B\boldsymbol{B_\alpha}(t')\} \\ &+ \boldsymbol{\rho}_S(t')\boldsymbol{A_\beta}(t)\boldsymbol{A_\alpha}(t')\,\mathrm{Tr}\{\rho_B\boldsymbol{B_\beta}(t)\boldsymbol{B_\alpha}(t')\}\,\big)\,dt', \end{aligned} \tag{4.17}$$

where $\rho_S^0(t)$ is the initial density matrix of the system, which is also decorrelated from the reservoir density matrix $\rho = \rho_S^0 \otimes \rho_B$. Without loss of generality we assume that the reservoir operators satisfy

$$\mathrm{Tr}\{\boldsymbol{B_\alpha}(t)\rho_B\} = 0, \tag{4.18}$$

then, equation 4.16 can be rewritten in a more compact way as

$$\begin{aligned} \dot{\boldsymbol{\rho}}_S = -\sum_{\alpha,\beta} \int_0^t dt' \,(&C_{\alpha,\beta}(t,t')[\boldsymbol{A_\alpha}(t), \boldsymbol{A_\beta}(t')\rho_S(t')] \\ &+ C_{\beta,\alpha}(t',t)[\rho_S(t')\boldsymbol{A_\beta}(t'), \boldsymbol{A_\alpha}(t)])\,, \end{aligned} \tag{4.19}$$

where

$$C_{\alpha,\beta}(t_1,t_2) = \mathrm{Tr}\{\boldsymbol{B_\alpha}(t_1)\boldsymbol{B_\beta}(t_2)\rho_B\} \tag{4.20}$$

is the bath correlation function. This integer-differential equation is non-Markovian because the matrix density depends on all previous times. Although the equation preserves trace and hermiticity, it does not necessarily preserve positivity [Schaller 2014], so other approximations are necessary.

4.1.2 Markov approximation

Markov approach relies on the fact that the whole system can be separated into two parts with well separated time scales: the relaxation time of the bath, which is much shorter than, the relaxation time of the system. Because it is assumed that the size of the bath is much larger than the size of the system, the changes induced in the bath by the weak coupling with the system are considered small. Thus, it is natural to assume that the bath quickly reaches its equilibrium state. Then we can say that the dynamics of the density matrix varies very slowly with respect to the decay times of the correlation function of the bath, so we can insert $\boldsymbol{\rho}(t') \to \boldsymbol{\rho}(t)$ into equation 4.15 to obtain

$$\dot{\boldsymbol{\rho}}_S = -\int_0^t \mathrm{Tr}_B\{[\boldsymbol{\mathcal{H}_I}(t), [\boldsymbol{\mathcal{H}_I}(t'), \boldsymbol{\rho}_S(t) \otimes \rho_B]]\}dt'. \tag{4.21}$$

This is the Born-Redfield equation, which is local in time and preserves trace and hermiticity. However, it still has a complicated time dependence, which is why ideally time independent coefficients should be imposed. Note that when the Hamiltonian of the bath commutes with its matrix density $[\mathcal{H}_B, \rho_B] = 0$, the bath correlation function depends only on the difference of times

$$C_{\alpha,\beta}(t_1, t_2) = C_{\alpha,\beta}(t_2 - t_1) = \mathrm{Tr}\{e^{i\mathcal{H}_B(t_2-t_1)} B_\alpha e^{-i\mathcal{H}_B(t_2-t_1)} B_\beta \rho_B\}, \tag{4.22}$$

generating the following symmetry

$$C_{\alpha,\beta}(\tau) = C^*_{\beta,\alpha}(-\tau). \tag{4.23}$$

Now we set $\tau = t - t'$ and make the limit of integration go to infinity in equation 4.21. This does not significantly change the value of the integral, because the decay time of the bath correlation function is short (see equation 4.19). Then we are left with

$$\dot{\boldsymbol{\rho}}_S = -\int_0^\infty \mathrm{Tr}_B\{[\boldsymbol{\mathcal{H}_I}(t), [\boldsymbol{\mathcal{H}_I}(t'), \boldsymbol{\rho}_S(t) \otimes \rho_B]]\}dt', \tag{4.24}$$

or, returning to the Schrödinger picture

$$\dot{\rho}_S = -i[\mathcal{H}_S, \rho_S(t)] - \sum_{\alpha,\beta} \int_0^\infty C_{\alpha,\beta}(\tau)[A_\alpha, e^{-i\mathcal{H}_S\tau} A_\beta e^{i\mathcal{H}_S\tau} \rho_S(t)] d\tau$$
$$- \sum_{\alpha,\beta} \int_0^\infty C_{\beta,\alpha}(-\tau)[\rho_S(t) e^{-i\mathcal{H}_S\tau} A_\beta e^{i\mathcal{H}_S\tau}, A_\alpha] d\tau. \tag{4.25}$$

This equation can be rewritten in a compact form

$$\dot{\rho}_S = -i[\mathcal{H}_S, \rho_S(t)] - \sum_\alpha ([A_\alpha, \Lambda_\alpha \rho_S(t)] + [\rho_S(t)\Lambda_\alpha^\dagger, A_\alpha]) d\tau, \tag{4.26}$$

with

$$\Lambda_\alpha = \sum_\beta \int_0^\infty C_{\alpha,\beta}(\tau) e^{-i\mathcal{H}_S\tau} A_\beta e^{i\mathcal{H}_S\tau} d\tau. \tag{4.27}$$

This equation is called the Markovian master equation, it contains constant coefficients, is local in time and preserves two desired properties of the density matrix: hermiticity and unit trace. However, it does not necessarily ensure the positivity of the density matrix, so it can lead to non-physical results such as negative probabilities. Therefore, another approximation must be considered to arrive at the Lindblad equation. Nonetheless, there are simple examples where the Markov master equation, and the Redfield equation, has been successfully applied, making microscopic considerations to the bath correlation function without generating negative probabilities [Whitney 2008].

4.1.3 Secular approximation

Going back to the interaction picture, we can see that there are several oscillating terms in the dynamics of the density matrix. The secular approximation or rotating wave approximation (RWA) averages out most of the rapidly oscillating dynamic terms. This is justified by the fact that, if we have different scales of oscillation, the fastest oscillating terms can be discarded because their average is zero. So, the equation 4.25 written in the interaction picture and expanded into

the basis of the eigenvectors of the system Hamiltonian $\mathcal{H}_S |a\rangle = E_a |a\rangle$ gives

$$\dot{\boldsymbol{\rho}}_S = -\sum_{\alpha,\beta} \int_0^\infty (C_{\alpha,\beta}(\tau)[\boldsymbol{A_\alpha}(t), \boldsymbol{A_\beta}(t-\tau)\boldsymbol{\rho}_S(t)] + \text{h.c.})d\tau$$

$$= \sum_{\alpha,\beta} \int_0^\infty C_{\alpha,\beta}(\tau) \sum_{a,b,c,d} (|a\rangle \langle a| \boldsymbol{A_\beta}(t-\tau) |b\rangle \langle b| \boldsymbol{\rho}_S(t) |d\rangle \langle d| \boldsymbol{A_\alpha}(t) |c\rangle \langle c|$$

$$- |d\rangle \langle d| \boldsymbol{A_\alpha}(t) |c\rangle \langle c|a\rangle \langle a| \boldsymbol{A_\beta}(t-\tau) |b\rangle \langle b| \boldsymbol{\rho}_S(t))d\tau + \text{h.c.}. \quad (4.28)$$

Making explicit the time dependence of the coupling operators and abbreviating $A_\alpha^{a,b} = \langle a| A_\alpha |b\rangle$ and $L_{a,b} = |a\rangle \langle b|$, we find

$$\dot{\boldsymbol{\rho}}_S = \int_0^\infty \sum_{\alpha,\beta} C_{\alpha,\beta}(\tau) \sum_{a,b,c,d} (e^{i(E_b-E_a)(t-\tau)} e^{i(E_d-E_c)t} A_\beta^{a,b} A_\alpha^{d,c} L_{a,b} \boldsymbol{\rho}_S(t) L_{c,d}^\dagger$$

$$- e^{i(E_b-E_a)(t-\tau)} e^{i(E_d-E_c)t} A_\beta^{a,b} A_\alpha^{d,c} L_{c,d}^\dagger L_{a,b} \boldsymbol{\rho}_S(t))d\tau + \text{h.c.}$$

$$= \sum_{\alpha,\beta} \sum_{a,b,c,d} e^{-i(E_b-E_a-(E_d-E_c))t} \int_0^\infty C_{\alpha,\beta}(\tau) e^{i(E_b-E_a)\tau} A_\beta^{a,b} (A_\alpha^{d,c})^* d\tau$$

$$\times (L_{a,b} \boldsymbol{\rho}_S(t) L_{c,d}^\dagger - L_{c,d}^\dagger L_{a,b} \boldsymbol{\rho}_S(t)) + \text{h.c.} \quad (4.29)$$

Denoting $w = E_b - E_a$ and $w' = E_d - E_c$; the secular approximation discards the oscillating terms in t, keeping only those which $e^{-i(w-w')t} \approx \delta_{w,w'}$, since when $w \neq w'$, the oscillation is considered fast enough to average to zero, regarding the slow dynamics of the density matrix [Breuer, Petruccione et al. 2002, Harbola, Esposito e Mukamel 2006]:

$$\dot{\boldsymbol{\rho}}_S = \sum_{\alpha,\beta} \sum_{a,b,c,d} \Gamma_{\alpha,\beta}(E_b - E_a) \delta_{E_b-E_a, E_d-E_c} A_\beta^{a,b} (A_\alpha^{c,d})^* (L_{a,b} \boldsymbol{\rho}_S(t) L_{c,d}^\dagger - L_{c,d}^\dagger L_{a,b} \boldsymbol{\rho}_S(t))$$

$$+ \sum_{\alpha,\beta} \sum_{a,b,c,d} \Gamma_{\alpha,\beta}^*(E_b - E_a) \delta_{E_b-E_a, E_d-E_c} (A_\beta^{a,b})^* A_\alpha^{c,d} (L_{c,d} \boldsymbol{\rho}_S(t) L_{a,b}^\dagger - \boldsymbol{\rho}_S(t) L_{a,b}^\dagger L_{c,d}), \quad (4.30)$$

where

$$\Gamma_{\alpha,\beta}(w) = \int_0^\infty C_{\alpha,\beta}(\tau) e^{iw\tau} d\tau \quad (4.31)$$

corresponds to the Fourier transform of the bath correlation function. Doing the transformation $\alpha \leftrightarrow \beta$, $a \leftrightarrow c$ and $b \leftrightarrow d$ in the second line of the equation 4.30,

and grouping similar terms, we arrive at

$$\begin{aligned}\dot{\boldsymbol{\rho}}_S = \sum_{\alpha,\beta}\sum_{a,b,c,d}(\Gamma_{\alpha,\beta}(E_b-E_a)+\Gamma^*_{\beta,\alpha}(E_b-E_a))\delta_{E_b-E_a,E_d-E_c}A^{a,b}_\beta(A^{c,d}_\alpha)^* L_{a,b}\boldsymbol{\rho}_S(t)L^\dagger_{c,d}\\ -\sum_{\alpha,\beta}\sum_{a,b,c,d}\Gamma_{\alpha,\beta}(E_b-E_a)\delta_{E_b-E_a,E_d-E_c}A^{a,b}_\beta(A^{c,d}_\alpha)^* L^\dagger_{c,d}L_{a,b}\boldsymbol{\rho}_S(t)\\ -\sum_{\alpha,\beta}\sum_{a,b,c,d}\Gamma^*_{\beta,\alpha}(E_b-E_a)\delta_{E_b-E_a,E_d-E_c}A^{a,b}_\beta(A^{c,d}_\alpha)^* \boldsymbol{\rho}_S(t)L^\dagger_{c,d}L_{a,b}.\end{aligned} \tag{4.32}$$

It is possible to split the Γ factor into an hermitian and an anti-hermitian part

$$\Gamma_{\alpha,\beta}(w) = \frac{1}{2}\gamma_{\alpha,\beta}(w) + \frac{1}{2}\sigma_{\alpha,\beta}(w), \tag{4.33}$$

$$\Gamma^*_{\beta,\alpha}(w) = \frac{1}{2}\gamma_{\alpha,\beta}(w) - \frac{1}{2}\sigma_{\alpha,\beta}(w), \tag{4.34}$$

with $\gamma_{\alpha,\beta}(w) = \gamma^*_{\beta,\alpha}(w)$ being the hermitian part, and $\sigma_{\alpha,\beta}(w) = -\sigma^*_{\beta,\alpha}(w)$ the anti-hermitian part. These functions are the full, even and odd, Fourier transform of the bath correlation function respectively

$$\gamma_{\alpha,\beta}(w) = \Gamma_{\alpha,\beta}(w) + \Gamma^*_{\beta,\alpha}(w) = \int_{-\infty}^{\infty} C_{\alpha,\beta}(\tau)e^{iw\tau}d\tau, \tag{4.35}$$

$$\sigma_{\alpha,\beta}(w) = \Gamma_{\alpha,\beta}(w) - \Gamma^*_{\beta,\alpha}(w) = \int_{-\infty}^{\infty} C_{\alpha,\beta}(\tau)\,\mathrm{sgn}(\tau)e^{iw\tau}d\tau. \tag{4.36}$$

It can be showed that

$$\sigma_{\alpha,\beta}(w) = \frac{i}{\pi}\mathcal{P}\int_{-\infty}^{\infty}\frac{\gamma_{\alpha,\beta}(w)}{w-\Omega}d\Omega. \tag{4.37}$$

So, the master equation becomes

$$\begin{aligned}\dot{\boldsymbol{\rho}}_S &= \sum_{\alpha,\beta}\sum_{a,b,c,d}\gamma_{\alpha,\beta}(E_b-E_a)\delta_{E_b-E_a,E_d-E_c}A^{a,b}_\beta(A^{c,d}_\alpha)^*\left(L_{a,b}\boldsymbol{\rho}_S(t)L^\dagger_{c,d} - \frac{1}{2}\{L^\dagger_{c,d}L_{a,b},\boldsymbol{\rho}_S(t)\}\right)\\ &\quad -\sum_{\alpha,\beta}\sum_{a,b,c,d}\frac{1}{2i}\sigma_{\alpha,\beta}(E_b-E_a)\delta_{E_b-E_a,E_d-E_c}A^{a,b}_\beta(A^{c,d}_\alpha)^*[L^\dagger_{c,d}L_{a,b},\boldsymbol{\rho}_S(t)]\\ &= \sum_{\alpha,\beta}\sum_{a,b,c,d}\gamma_{\alpha,\beta}(E_b-E_a)\delta_{E_b-E_a,E_d-E_c}A^{a,b}_\beta(A^{c,d}_\alpha)^*\left(L_{a,b}\boldsymbol{\rho}_S(t)L^\dagger_{c,d} - \frac{1}{2}\{L^\dagger_{c,d}L_{a,b},\boldsymbol{\rho}_S(t)\}\right)\\ &\quad -\sum_{\alpha,\beta}\sum_{a,b,c}\frac{1}{2i}\sigma_{\alpha,\beta}(E_b-E_a)\delta_{E_b,E_a}A^{c,b}_\beta(A^{c,a}_\alpha)^*[L_{a,b},\boldsymbol{\rho}_S(t)].\end{aligned} \tag{4.38}$$

Usually the term

$$H_{LS} = \sum_{\alpha,\beta} \sum_{a,b,c} \frac{1}{2i} \sigma_{\alpha,\beta} (E_b - E_a) \delta_{E_b,E_a} A_\beta^{c,b} (A_\alpha^{c,a})^* \left|a\right\rangle \left\langle b\right| \tag{4.39}$$

is called the Lamb-Shift Hamiltonian because it can be included in the system Hamiltonian as a renormalization caused by the interaction with the reservoir, whereas $H_{LS} = H_{LS}^\dagger$ and $[H_{LS}, \mathcal{H}_S] = 0$. Then we can finally write the master equation in the Lindblad form, in the Schrödinger picture, putting together the above definitions

$$\begin{aligned} \dot{\rho}_S = & -i \left[\mathcal{H}_S + \sum_{\alpha,\beta} \sigma_{\alpha,\beta} \left|a\right\rangle \left\langle b\right| , \rho_S(t) \right] \\ & + \sum_{a,b,c,d} \gamma_{ab,cd} \left(\left|a\right\rangle \left\langle b\right| \rho_S(t) (\left|c\right\rangle \left\langle d\right|)^\dagger - \frac{1}{2} \{ (\left|c\right\rangle \left\langle d\right|)^\dagger \left|a\right\rangle \left\langle b\right| , \rho_S(t) \} \right) \end{aligned} \tag{4.40}$$

where we used the new definitions

$$\gamma_{ab,cd} = \sum_{\alpha,\beta} \gamma_{\alpha,\beta} (E_b - E_a) \delta_{E_b - E_a, E_d - E_c} \left\langle a\right| A_\beta \left|b\right\rangle \left\langle c\right| A_\alpha \left|d\right\rangle^* , \tag{4.41}$$

and

$$\sigma_{ab} = \sum_{\alpha,\beta} \sum_{c} \frac{1}{2i} \sigma_{\alpha,\beta} (E_b - E_a) \delta_{E_b,E_a} \left\langle c\right| A_\beta \left|b\right\rangle \left\langle c\right| A_\alpha \left|a\right\rangle^* . \tag{4.42}$$

This equation is equivalent to the equation 4.6, preserves the hermiticity, trace and positivity of the density matrix, as was desired. The positivity comes from the fact that any equation with the Lindblad form preserves the positivity together with the fact that the $\gamma_{ab,cd}$ matrix can be shown to be non-negative, i.e. $\sum_{a,b,c,d} x_{a,b}^* \gamma_{ab,cd} x_{c,d} \geq 0$ for all $x_{a,b}$.

4.1.4 Thermalization and multi-terminal coupling

In the derivation of the master equation in the Lindblad form, the only assumptions made on the reservoirs were that its number of freedom degrees are much greater than the number of freedom degrees in the system and the requirements $[\mathcal{H}_B, \rho_B] = 0$ and $\mathrm{T}r\{B_\alpha \rho_B\} = 0$ (see equation 4.18). Then, it is

reasonable to assume that the reservoir states are close to thermal equilibrium since the system hardly modifies the bath states, Thus, we may write

$$\rho_B = \frac{e^{-\beta \mathcal{H}_B}}{\mathrm{T}r(e^{-\beta \mathcal{H}_B})}. \tag{4.43}$$

With this thermal state, the bath correlation function fulfills the Kubo-Martin-Schwinger (KMS) condition

$$C_{\alpha,\beta}(\tau) = C_{\beta,\alpha}(-\tau - i\beta), \tag{4.44}$$

which leads to

$$\gamma_{\alpha,\beta}(-w) = \gamma_{\beta,\alpha}(w)e^{-\beta w}, \tag{4.45}$$

or equivalently (from the equation 4.41)

$$\frac{\gamma_{ab,ab}}{\gamma_{ba,ba}} = e^{-\beta(E_a - E_b)}. \tag{4.46}$$

This equation is known as the detailed balance relation and establishes the general relation between the transition rates. Equation 4.45 can be used to show the stationary solution of the master equation when the system is coupled to one single reservoir, so that

$$\rho_s = \frac{e^{-\beta \mathcal{H}_S}}{\mathrm{T}r(e^{-\beta \mathcal{H}_S})}, \tag{4.47}$$

i.e., the system is in thermal equilibrium with the reservoir. If the reservoir exchanges particles with the system, it is in a grand-canonical state

$$\rho_B = \frac{e^{-\beta(\mathcal{H}_B - \mu N_B)}}{\mathrm{T}r(e^{-\beta(\mathcal{H}_B - \mu N_B)})}, \tag{4.48}$$

where μ is the chemical potential, and $N = N_S + N_B$ is the total number of particles in the system and the bath respectively, which is a conserved quantity since $[\mathcal{H}, N] = 0$; and the master equation solution is

$$\rho_B = \frac{e^{-\beta(\mathcal{H}_S - \mu N_S)}}{\mathrm{T}r(e^{-\beta(\mathcal{H}_S - \mu N_S)})}. \tag{4.49}$$

The case of a system coupled to several reservoirs is very interesting in the sense that, if each reservoir has a different temperature or chemical potential, the

system will be carried to different states of thermal equilibrium. So, in general the stationary state of the system will be a non-equilibrium state. Considering that the different reservoirs do not interact directly, we have

$$\mathcal{H}_B = \sum_{l=1}^{K} \mathcal{H}_B^{(l)} \tag{4.50}$$

and naturally $[\mathcal{H}_B^{(l)}, \mathcal{H}_B^{(k)}] = 0$. If each reservoir has a certain temperature and chemical potential, then

$$\rho_B = \frac{e^{-\beta(\mathcal{H}_B^{(1)} - \mu N_B^{(1)})}}{\mathrm{T}r\big(e^{-\beta(\mathcal{H}_B^{(1)} - \mu N_B^{(1)})}\big)} \otimes ... \otimes \frac{e^{-\beta(\mathcal{H}_B^{(K)} - \mu N_B^{(K)})}}{\mathrm{T}r\big(e^{-\beta(\mathcal{H}_B^{(K)} - \mu N_B^{(K)})}\big)}, \tag{4.51}$$

and the system is coupled directly to each reservoir

$$\mathcal{H}_I = \sum_{\alpha} A_\alpha \otimes \sum_{l=1}^{K} B_\alpha^K. \tag{4.52}$$

Since we are assuming $\mathrm{Tr}\{B_\alpha^{(l)}(t)\rho_B\} = \langle B_\alpha^{(l)} \rangle = 0$ from the beginning, the bath correlation function (see equation 4.20) is also additive

$$C_{\alpha,\beta}(\tau) = \sum_{l=1}^{K} C_{\alpha,\beta}^{(l)}(\tau), \tag{4.53}$$

which implies that the correlation function between different reservoirs is zero

$$C_{\alpha,\beta}^{(k,l)}(\tau) = \delta_{k,l} C_{\alpha,\beta}(\tau) \tag{4.54}$$

and therefore, such additivity is transferred via Fourier Transform (see equations 4.35 and 4.40) to the master equation. This can be written in a compact way using the notation of the master equation in Liouville space:

$$\mathcal{W} = \mathcal{W}^{(0)} + \sum_{l=1}^{K} \mathcal{W}^{(l)}, \tag{4.55}$$

where $\mathcal{W}$ corresponds to the Liouvillian of the Markovian master equation

$$\dot{\rho} = \mathcal{W}\rho. \tag{4.56}$$

Here we introduced the notation in the Liouville space. As we have seen, a Markovian master equation is composed of a unitary evolution $\mathcal{W}_0\rho = -i[\mathcal{H}, \rho]$, and non-unitary evolutionary terms $\mathcal{W}^{(l)}$ which are independent of each other for the different (l) reservoirs. The density matrices are rewritten in the Lioville space, as a mapping from the Hilbert space such that

$$\hat{\rho} = \begin{pmatrix} \rho_{1,1} & \cdots & \rho_{1,N} \\ \vdots & \ddots & \vdots \\ \rho_{N,1} & \cdots & \rho_{N,N} \end{pmatrix} \Leftrightarrow |\rho\rangle = \begin{pmatrix} \rho_{1,1} \\ \vdots \\ \rho_{N,N} \\ \rho_{1,2} \\ \rho_{2,1} \\ \vdots \\ \rho_{N-1,N} \\ \rho_{N,N-1} \end{pmatrix}, \tag{4.57}$$

conventionally by first placing the N populations, and then the $N(N-1)$ coherences. So in Liouville space, the density matrix is a vector of dimension N^2 and the Liouvillian, a matrix $N^2 \times N^2$.

4.1.5 Full counting statistics

The simplest multi-terminal case is the two-terminal coupling, in which the reservoirs are at different temperatures and/or chemical potential. In general, the system will achieve a non-equilibrium stationary state in the presence of transport of particles and heat. Understanding transport properties is fundamental to understanding processes that typically occur out of equilibrium, such as thermal machines or molecular processes. A powerful tool in the study of transport properties is the Full Counting Statistics, which allows the calculation of all the moments or cumulants of transport observables. Roughly, it gives the statistics of the number of particles that enter or leave one or more reservoirs, in a specific process during an interval of time [Esposito, Harbola e Mukamel 2009, Schaller 2014]. We will illustrate the counting or monitoring process, on a master equation with one single reservoir, albeit it can easily be generalized to more reservoirs.

The structure of the master equation makes it possible to identify "jump" terms responsible for increasing or decreasing the number of particles in the system. It is possible to write a n-resolved master equation at time t, as follows

$$\dot{\rho}^{(n)} = \mathcal{W}_0\rho^{(n)} + \mathcal{W}_+\rho^{(n-1)} + \mathcal{W}_-\rho^{(n+1)}, \tag{4.58}$$

where $\mathcal{W}_+$ increases by one the number of particles in the reservoir, and $\mathcal{W}_-$ decreases it by one. All the other processes are described in $\mathcal{W}_0$. Thus, the complete Liouvillian is

$$\mathcal{W} = \mathcal{W}_0 + \mathcal{W}_+ + \mathcal{W}_-. \tag{4.59}$$

Making use of the discrete Fourier transform, we can write

$$\rho(\chi, t) = \sum_n \rho^{(n)}(t)e^{in\chi}, \tag{4.60}$$

that generates the following master equation

$$\dot{\rho}(\chi, t) = (\mathcal{W}_0 + e^{i\chi}\mathcal{W}_+ + e^{-i\chi}\mathcal{W}_-)\rho(\chi, t) = \mathcal{W}(\chi)\rho(\chi, t). \tag{4.61}$$

The last equation is written in terms of a χ parameter, which is known as the counting field. The general solution to this master equation is

$$\rho(\chi, t) = e^{\mathcal{W}(\chi)t}\rho(\chi, 0) = e^{\mathcal{W}(\chi)t}\rho_0, \tag{4.62}$$

in which $\rho^{(0)}(0) = \delta_{n,0}\rho_0$ is conventionally assumed as the initial condition. Note from the equation 4.60 that we can recover the original master equation taking $\chi = 0$

$$\rho(t) = \sum_n \rho^{(n)}(t). \tag{4.63}$$

The probability distribution of the number of particles in a interval of time can be obtained as

$$P_n(t) = \mathrm{Tr}\big(\rho^{(n)}(t)\big). \tag{4.64}$$

The decomposition of the master equation into its n-resolved equations (also called conditional equations), increases the number of equations to solve, so it is not very practical to work with it. However, there is a more direct way to evaluate the counting statistics, using the fact that

$$\mathrm{Tr}(\rho(\chi, t)) = \mathrm{Tr}\big(e^{\mathcal{W}(\chi)t}\rho_0\big) = \sum_n P_n(t)e^{in\chi}, \tag{4.65}$$

then is possible evaluate the moments simply by calculating the derivatives with respect to the counting field

$$\langle n^k(t)\rangle = \sum_n n^k P_n(t) = (-i\partial_\chi)^k \sum_n P_n(t) e^{in\chi}\Big|_{\chi=0}. \tag{4.66}$$

Defining the moment generating function as

$$\mathcal{M}(\chi,t) = \mathrm{Tr}(\rho(\chi,t)) = \mathrm{Tr}\big(e^{\mathcal{W}(\chi)t}\rho_0\big), \tag{4.67}$$

the moments can be computed as

$$\langle n^k(t)\rangle = (-i\partial_\chi)^k \mathcal{M}(\chi,t)\Big|_{\chi=0}. \tag{4.68}$$

Generically, the initial condition is set to the steady state solution $\rho_0 = \bar{\rho_0}$, where $\mathcal{W}(0)\bar{\rho_0} = 0$. In the same way it is possible to define a cumulant generating function as

$$\mathcal{C}(\chi,t) = \ln \mathcal{M}(\chi,t) = \ln \mathrm{Tr}\big(e^{\mathcal{W}(\chi)t}\rho_0\big), \tag{4.69}$$

then the cumulants can be calculated as

$$\langle\langle n^k(t)\rangle\rangle = (-i\partial_\chi)^k \mathcal{C}(\chi,t)\Big|_{\chi=0}. \tag{4.70}$$

We can also define the k-th order zero frequency current correlation as

$$\left\langle S^{(k)}\right\rangle = \frac{\mathrm{d}}{\mathrm{d}t}\frac{\partial^k}{\partial\,(i\chi)^k}\mathcal{C}\,(\chi,t)|_{\chi=0,t\to\infty} = \frac{\mathrm{d}}{\mathrm{d}t}\langle\langle n^k(t)\rangle\rangle|_{t\to\infty}, \tag{4.71}$$

and the zero-frequency Fano factors as

$$F^{(k)} = \frac{\left\langle S^{(k)}\right\rangle}{\left\langle S^{(1)}\right\rangle}. \tag{4.72}$$

It can be shown that in the long-time limit, the cumulant generating function only depends on the dominant eigenvalue $\lambda(\chi)$ of the Liouvillian $\mathcal{W}(\chi)$ [Esposito, Harbola e Mukamel 2009]

$$\mathcal{C}(\chi,t) \approx \lambda(\chi)t. \tag{4.73}$$

Remarkably, this result simplifies the calculations significantly.

4.2 Feedback in quantum systems

Quantum control refers to the ability to drive a quantum system to a desired state. Various theoretical and experimental models have been successful in this effort [Zhang et al. 2017, Emary 2016]. Typically what is needed is a controller to act on the system. If the controller does not do a feedback process, the operation is called open loop control. Otherwise, a feedback process is an operation in which the controller uses output information from the system, as input for the modification of the system itself. This type of operation is called closed loop control or feedback control. However, in the realm of quantum, we have to differentiate between two types of feedback. If the controller uses classical information from a measurement process, the process is called measurement feedback quantum control. However it may be the case where the information processed by the controller is of quantum nature, i.e. information that does not come from a measurement process, but from a type of quantum signal (such as light polarization or spin). This type of control is known as coherent feedback control. In the figure 16 these different types of control are shown schematically [James e Nurdin 2015]. In this Thesis we will study systems under Wiseman-Milburn feedback control, which is a measurement feedback quantum control.

4.2.1 Wiseman-Milburn feedback

The quantum control scheme proposed by Wiseman and Milburn, originally for quantum optical systems [Wiseman 1994, Wiseman e Milburn 2009], has been extended to mesoscopic systems, where it has been applied in the stabilization and purification of quantum states [Pöltl, Emary e Brandes 2011], the design of thermal machines [Strasberg et al. 2013] and the freezing of current fluctuations [Brandes 2010], among others. This scheme is based on the possibility of detecting jumps triggered by the reservoirs in the quantum system. Immediately after the detection of a jump, the control operation generally unitary is applied so that, depending on the parameters of the control operation, a desired state can be obtained. We will now explain each of the steps of this control scheme.

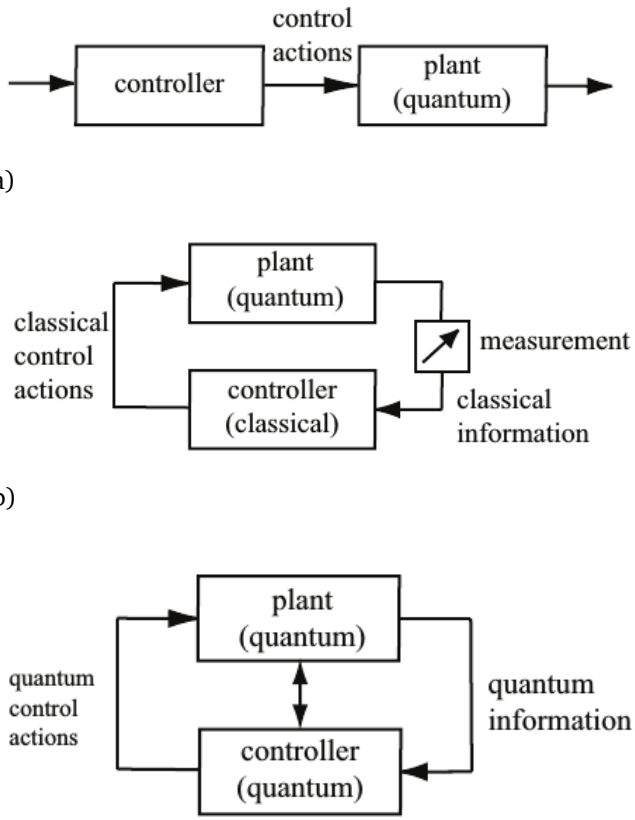

Figure 16 – Schemes of the different types of quantum control (a) open loop control, (b) measurement feedback control, (c) coherent feedback control [James e Nurdin 2015].

In general, a Markovian master equation can be written in Liouville space as

$$\dot{\rho}(t) = \mathcal{W}\rho(t). \tag{4.74}$$

In the system Hamiltonian eigenbasis, the Liouvillian has the following block structure

$$\mathcal{W} = \begin{pmatrix} \mathcal{W}_{pop} & 0 \\ 0 & \mathcal{W}_{coh}, \end{pmatrix} \tag{4.75}$$

which means that on the Hamiltonian eigenbasis, populations and coherences evolve independently. Populations have their own evolution equation

$$\dot{\rho}_{pop}(t) = \mathcal{W}_{pop}\rho_{pop}(t), \tag{4.76}$$

while the coherences are exponentially damped until they disappear in the steady state. It is known that the Liouvillian in Lindblad equations such as 4.7 and 4.40, can be interpreted as the sum of two terms: the first describes the smooth evolution of the system, and the second describes an evolution by jumps

$$\mathcal{W}_{pop} = \mathcal{W}_0 + \sum_{\nu} \sum_{i>j} (\mathcal{J}^{\nu}_{j\to i} + \bar{\mathcal{J}}^{\nu}_{i\to j}), \tag{4.77}$$

where $\mathcal{J}^{\nu}_{j\to i}$ and $\bar{\mathcal{J}}^{\nu}_{i\to j}$ are the superoperators responsible for the quantum jumps $j \to i$, $i \to j$ in the system triggered by the ν reservoir. Defining $|i\rangle\rangle$ and $|j\rangle\rangle$ as system states in Liouville space such that $E_i - E_j > 0$, the jump superoperators are

$$\mathcal{J}^{\nu}_{j\to i} = \gamma^{\nu}_{j\to i} \, |i\rangle\rangle\langle\langle j| \, , \qquad \bar{\mathcal{J}}^{\nu}_{i\to j} = \bar{\gamma}^{\nu}_{i\to j} \, |j\rangle\rangle\langle\langle i| \, , \tag{4.78}$$

with the transition rates satisfying the local detailed balance

$$\ln\left(\frac{\gamma^{\nu}_{j\to i}}{\bar{\gamma}^{\nu}_{i\to j}}\right) = -\beta_{\nu}(E_i - E_j) \tag{4.79}$$

such as in equation 4.46. Then, the smooth evolution is

$$\mathcal{W}_0 = -\sum_{\nu} \sum_{i>j} (\gamma^{\nu}_{j\to i} \, |j\rangle\rangle\langle\langle j| + \bar{\gamma}^{\nu}_{i\to j} \, |i\rangle\rangle\langle\langle i|). \tag{4.80}$$

Here we have the same Markovian master equation studied before, unravelled in terms of jumps and smooth transitions in the Liouville space. Now we can introduce the Wiseman-Milburn control scheme preserving the Markovianity and other desirable properties in a master equation, as was discussed before. Assuming a system coupled to two reservoirs, the control scheme can be understood in three steps:

- Jump detection: A given reservoir, the one on the left, induces a jump in the system by transferring a particle to the system: $\mathcal{J}^{L}_{j\to i} \, |j\rangle\rangle = \gamma^{L}_{j\to i} \, |i\rangle\rangle$.
- Control operation: Immediately after the jump, the control operation is applied, establishing certain parameters to obtain the desired state: $\mathcal{C}^{L}_{j\to i}\mathcal{J}^{L}_{j\to i} \, |j\rangle\rangle = \gamma^{L}_{j\to i} \, |k\rangle\rangle$.

- Relaxation: The system jumps from the last state to the original state, emitting the particle to the right reservoir, so that a new process can start: $\mathcal{J}^R_{i\to j}\left|k\right\rangle\rangle = \gamma'^R_{i\to j}\left|j\right\rangle\rangle$.

Note from the first and second step that the control scheme is doing the operation $\mathcal{C}^L_{j\to i}\left|i\right\rangle\rangle = \left|k\right\rangle\rangle$. This can be done by a unitary operation, such that in the Hilbert space is (now we can denote ϱ as density matrix acting in Hilbert space and ρ, the corresponding vector in Liouville space)

$$\mathcal{C}\rho \leftrightarrow U_C \varrho U_C^\dagger \qquad \hat{U}_C = e^{-i\theta_c \vec{n}\vec{\sigma}}. \tag{4.81}$$

The unitary operation rotates the state around the unit vector $\vec{n} = (\sin\theta, 0, \cos\theta)$. In the third step, the transition rate is indicated as $\gamma'^R_{i\to j}$, which is modified with respect to the original rate $\gamma^R_{i\to j}$, because the transition makes the jump $k \to j$, not $i \to j$. Taking into account all possible transitions in all possible reservoirs, we can write the master equation of the control process in the Liouville space as

$$\mathcal{W}^C = \mathcal{W}_0 + \sum_\nu \sum_{i>j} \left(\mathcal{C}^\nu_{j\to i}\mathcal{J}^\nu_{j\to i} + \overline{\mathcal{C}}^\nu_{i\to j}\overline{\mathcal{J}}^\nu_{i\to j}\right), \tag{4.82}$$

which has the following block structure

$$\mathcal{W}^C = \begin{pmatrix} \mathcal{W}^C_{pop} & 0 \\ \mathcal{W}^C_{cp} & \mathcal{W}_{coh} \end{pmatrix}. \tag{4.83}$$

This equation maintains the independence of the populations, but unlike equation 4.75, it couples the coherencies to the populations, so the control operation can be used to stabilize coherent states. Then the Liouvillian of populations can be written as

$$\begin{aligned} \mathcal{W}^C_{pop} = &\sum_\nu \sum_{i>j} \gamma^\nu_{j\to i} \left(\sum_k \left(\mathcal{C}^\nu_{j\to i}\right)_{ki} \left|k\right\rangle\rangle\langle\langle j| - \left|j\right\rangle\rangle\langle\langle j| \right) \\ &+ \sum_\nu \sum_{i>j} \overline{\gamma}^\nu_{i\to j} \left(\sum_k \left(\overline{\mathcal{C}}^\nu_{i\to j}\right)_{kj} \left|k\right\rangle\rangle\langle\langle i| - \left|i\right\rangle\rangle\langle\langle i| \right). \end{aligned} \tag{4.84}$$

Notice that that the matrix elements of this equation no longer satisfy the detailed balance condition and in the absence of feedback $\left(\mathcal{C}^\nu_{j\to i}\right)_{ki} = \delta_{ik}$, thus recovering equation 4.77.

4.2.2 Delayed feedback

The feedback scheme originally proposed by Wiseman and Milburn considers that immediately upon detecting a jump induced by a reservoir, the control operation is activated. In a realistic scheme, there is a time interval between the detection of the jump and the implementation of the control operation. Therefore, a delay time was included in the scheme and its consequences were studied. The delay time τ is introduced into formalism under a hypothesis called "control-skipping assumption" [Emary 2013, Strasberg et al. 2013]. It establishes that if the delay time is greater than the time between two consecutive jumps, there will be no control operation. This hypothesis is reasonable insofar as it makes sense to assume that if the delay time triggered by a jump is greater than the time where the next jump emerges, the control operation is canceled, since otherwise it would be executed in a time after the next jump (see figure 17). We will see that as consequence, a non-Markovian master equation will be obtained.

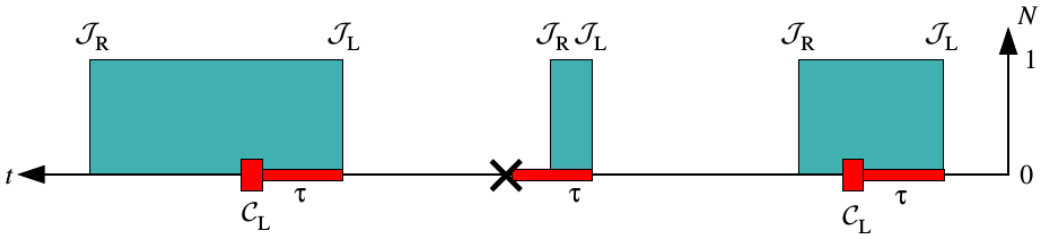

Figure 17 – Control-skipping assumption system scheme. Time flows from right to left. The control operation is canceled when the delay time is greater than the time between jumps, as represented by the cross, in the second activation of the operation [Emary 2013].

We know that the Lindblad master equation can be unraveled in terms of jumps and smooth evolution, so, within a quantum trajectory interpretation, the solution of the master equation can be written as [Carmichael 2009]

$$\rho(t) = \sum_{n=0}^{\infty} \int_0^t \mathrm{d}t_n \ldots \int_0^{t_2} \mathrm{d}t_1 \underbrace{\Omega_0\left(t_n - t_{n-1}\right)\mathcal{J}\ldots\mathcal{J}\Omega_0\left(t_2 - t_1\right)\mathcal{J}\Omega_0\left(t_1\right)}_{n \text{ jumps}}\rho(0) \tag{4.85}$$

with $\Omega_0(t) = e^{\mathcal{W}_0 t}$. This is a sum over all possible paths along the system evolution. From this perspective it is clear that one should introduce the "control-skipping

assumption" as follows

$$\Omega_0(t)\mathcal{J}_\alpha \to \Omega_0^C(t)\mathcal{J}_\alpha = \begin{cases} \Omega_0(t)\mathcal{J}_\alpha, & t < \tau_\alpha \\ \Omega_0\left(t-\tau_\alpha\right)\mathcal{C}_\alpha\Omega_0\left(\tau_\alpha\right)\mathcal{J}_\alpha, & t \geq \tau_\alpha \end{cases} \tag{4.86}$$

where, the first condition is the non-execution of the control operation when the delay time τ is greater than the time between jumps, and the second condition is the effective application of the control. This substitution preserves the structure of the equation 4.85, which in the Laplace space is

$$\rho(z) = \int_0^\infty \mathrm{d}t \mathrm{e}^{-zt}\rho(t) = \frac{1}{z - \mathcal{W}_0 - \sum_\alpha \mathcal{D}_\alpha(z)\mathcal{J}_\alpha}\rho_0, \tag{4.87}$$

with a delayed-control operator

$$\mathcal{D}_\alpha(t) = \delta(t) + \left(\mathcal{C}_\alpha - \mathbb{1}\right)\mathrm{e}^{\mathcal{W}_0\tau_\alpha}\delta\left(t-\tau_\alpha\right). \tag{4.88}$$

Returning to the time domain, we find

$$\dot{\rho}(t) = \left(\mathcal{W}_0 + \sum_\alpha \mathcal{J}_\alpha\right)\rho(t) + \sum_\alpha \left(\mathcal{C}_\alpha - 1\right)\mathrm{e}^{\mathcal{W}_0\tau_\alpha}\mathcal{J}_\alpha\theta\left(t-\tau_\alpha\right)\rho\left(t-\tau_\alpha\right). \tag{4.89}$$

This is a non-Markovian equation, since it depends on time in the past $(t-\tau_\alpha)$. Note that if there is no control operation $\mathcal{C} = 1$, the master equation without feedback is recovered, and if the delay time is zero $\tau = 0$, we go back to the master equation with feedback but without delay. At the limit when the delay time is infinite $\lim_{\tau_\alpha\to\infty} e^{\mathcal{W}_0\tau_\alpha} = 0$, the master equation without feedback is recovered, which makes sense since the control operation would never be executed. Returning to the Laplace space, can be written

$$z\hat{\rho}(z) - \rho(0) = \mathcal{W}_{\text{delay}}(z)\hat{\rho}(z), \tag{4.90}$$

where

$$\mathcal{W}_{\text{delay}}(z) = \mathcal{W}_0 + \sum_\alpha \left[1 + \left(\mathcal{C}_\alpha - 1\right)e^{(\mathcal{W}_0 - z)\tau_\alpha}\right]\mathcal{J}_\alpha. \tag{4.91}$$

In this Thesis we will focus on steady states $\rho = \lim_{z\to 0} z\hat{\rho}(z) = \lim_{t\to\infty}\rho(t)$, so that when $t \to \infty$, $\rho\left(t-\tau_\alpha\right) \approx \rho(t)$ and $\theta\left(t-\tau_\alpha\right) = 1$ for all τ_α. Thus

$$0 \approx \frac{\partial}{\partial t}\rho(t) = \mathcal{W}_{\text{delay}}(0)\rho(t), \tag{4.92}$$

where $\mathcal{W}_{\text{delay}}(0)$ is a Markovian superoperator.

4.3 Stochastic thermodynamics

In general, the term "stochastic thermodynamics" refers to theoretical descriptions of small-scale thermodynamic systems where the effects of fluctuations are relevant. Traditionally, classical thermodynamics is restricted to the description of macroscopic systems in equilibrium or transformations between equilibrium states. The pioneering works of Onsager and Prigogine [Lebon, Jou e Casas-Vázquez 2008, Kondepudi e Prigogine 2014] extended such a description to non-equilibrium systems, which together with the advent of the so-called fluctuation theorems [Bustamante, Liphardt e Ritort 2005], raised the need for a theory that systematically describe these emerging phenomena. Diverse approaches at different levels of sofistication have been proposed, including the field of quantum thermodynamics [Funo e Quan 2018]. Here we work with the formulation of stochastic thermodynamics that was built into master equations, since it offers a consistent theoretical framework for describing small-scale non-equilibrium systems in the Markovian regime [Broeck e Esposito 2015, Esposito e Mukamel 2006]. This theory reproduces well several important results, such as fluctuation theorems and the laws of thermodynamics. It has also been successful in describing nano-thermal engines and molecular machines [Seifert 2012]. In this section we briefly review the fundamentals of macroscopic non-equilibrium thermodynamics, and then address the formulation of stochastic thermodynamics.

4.3.1 Non-equilibrium thermodynamics

The classical theory of thermodynamics only accounts for systems in global equilibrium or in quasi-static transformations (all the time the system is close to equilibrium infinitesimally). However, the inherent irreversibility in any natural process made it necessary the formulation of a non-equilibrium theory. This was carried out under the hypothesis of local equilibrium: *the local and instantaneous relations between thermodynamic quantities in a system out of equilibrium are the same as for a uniform system in equilibrium.* This hypothesis states that locally, in a sufficiently small space or cell, the system quickly reaches the equilibrium, being large enough to opose microscopic fluctuations. A pioneer of these investigations was Onsager who raised the problem for systems close to equilibrium, but in non-

quasi-static transformations, which in a first approximation led him to propose linear relations between the so-called fluxes J_i and the forces X_i that cause the fluxes. The latter are, in general, time derivatives of extensive quantities like mass, heat or charge, whereas the forces are gradients of intensive quantities like concentration, temperature or electrical potential. Some examples of this linear dependence were already known before the Onsager's developments, and therefore were taken as starting points, such as

- Fourier law of heat conduction: $J_Q = -\kappa \frac{\partial T}{\partial x}$. J_Q is the heat flux caused by the temperature T gradient, and κ is the thermal conductivity constant of the material.
- Ohm's law of electrical conduction: $J = -\sigma \frac{\partial V}{\partial x}$. J is the charge flux by the potential V gradient, σ is the electrical conductivity constant.
- Fick's law of diffusion: $J_i = -D \frac{\partial C_i}{\partial x}$. J_i is the matter flux of a species i cause a concentration C_i gradient, and D is the diffusion constant.

Then the following general relation was proposed

$$J = LX, \tag{4.93}$$

where L is a transport coefficient. There may be several forces that put the system out of equilibrium in a linear way, so there are cross effects between fluxes and forces. If the process is close to equilibrium, new terms can be added to the equation 4.93 and coupled fluxes appear. Denoting J_1 and J_2 two coupled fluxes, and X_1 and X_2 the forces originating the fluxes, assuming linearity, the relations are

$$\begin{aligned} J_1 &= L_{11}X_1 + L_{12}X_2, \\ J_2 &= L_{21}X_1 + L_{22}X_2, \end{aligned} \tag{4.94}$$

where L_{11}, L_{21}, L_{12}, L_{22} are phenomenological coefficients. These equations, called linear phenomenological relations, can be written in a most general way

$$J_i = L_{i1}X_1 + L_{i2}X_2 + ... + L_{in}X_n = \sum_{k=1}^{n} L_{ik}X_k \quad (i = 1, 2..., n), \tag{4.95}$$

where the transport coefficients $L_{ik} = (\partial J_i/\partial X_k)_{X_i}$ are generalized conductances. In vector notation, we may write

$$\begin{pmatrix} J_1 \\ J_2 \\ \vdots \\ J_n \end{pmatrix} = \begin{pmatrix} L_{11} & L_{12} & \cdots & L_{1n} \\ L_{21} & L_{22} & \cdots & L_{2n} \\ \vdots & \vdots & \ddots & \vdots \\ L_{n1} & L_{n2} & \cdots & L_{nn} \end{pmatrix} \begin{pmatrix} X_1 \\ X_2 \\ \vdots \\ X_n \end{pmatrix}. \tag{4.96}$$

Phenomenological coefficients of type L_{ii} correspond to direct effects, and the coefficients of type L_{ik} with $i \neq k$ correspond to crossed effects. The Onsager theorem states that the couplings are symmetric. That is, given the set of fluxes J_i and the associated forces X_k, the matrix of the phenomenological coefficients is symmetric or antisymmetric

$$L_{ik} = \pm L_{ki} \quad (i \neq k). \tag{4.97}$$

depending of the parity of the time-reversal symmetry of the fluctuations of extensive state variables with respect to their equilibrium values [Lebon, Jou e Casas-Vázquez 2008]. Usually the forces have its origin in the environment, or external reservoirs to the system, so a thermodynamic description of open systems was put forward. For this, Prigogine introduced the concepts of entropy flux and production entropy from the second law of thermodynamics. For the whole system-environment, the increase in total entropy must be equal to or greater than zero.

$$\Delta S_{tot} = \Delta S + \Delta S_r \geq 0, \tag{4.98}$$

where ΔS is the entropy generated by the system and $\Delta S_r = \Delta Q_r/T$ the entropic contribution of the environment, which comes exclusively from the heat Q_r flowing to/from the system. If the environment provides heat to the system, then $Q_r = -Q$, or

$$\Delta S \geq -\Delta S_r = \frac{Q}{T}. \tag{4.99}$$

Then the entropy flux that enters to the system is defined as $\Delta_e S = -\Delta S_r$ and the entropy production is defined as the total entropy generated $\Delta_i S = \Delta S_{tot}$, so

the second law of thermodynamics for a non-isolated system can be written as

$$\Delta S = \Delta_i S + \Delta_e S \quad \Delta_i S \geq 0, \tag{4.100}$$

$$dS = d_i S + d_e S \quad d_i S \geq 0, \tag{4.101}$$

$$\dot{S} = \dot{S}_i + \dot{S}_e \quad \dot{S}_i \geq 0. \tag{4.102}$$

As the traditional formulation of the second law of thermodynamics, the production of entropy (total entropy) is inherently irreversible, achieving equality only for reversible quasistatic processes. Prigogine established for steady states ($\dot{S} = 0$), that irreversible stationary states produce entropy at a minimal rate. This is known as Prigogine's theorem. It can also be shown that the entropy production can be written as the sum of fluxes times the corresponding forces

$$\dot{S}_i = \sum_{i=1}^{N} J_i X_i \geq 0. \tag{4.103}$$

There is another way to write the laws of thermodynamics in terms of the free energy state function defined as $F = E - TS$. In the canonical ensemble $\Delta F = \Delta E - T\Delta S$, the first law of thermodynamics is

$$\Delta E = Q + W = T\Delta_e S + W. \tag{4.104}$$

Combining this with $\Delta_i S = \Delta S - \Delta_e S \geq 0$, the second law can be rewritten as

$$T\Delta_i S = W - \Delta F \geq 0. \tag{4.105}$$

This equation establishes a minimum limit on the work done to make possible a given transformation. If ΔF is negative, it means that the work can also be negative, or in other words, work can be extracted from the system. Note that this reformulation of thermodynamics for non-equilibrium open systems is not restricted to the linear regime. It is valid for any system arbitrarily out of the equilibrium.

With the advent of the study of small nano-size systems, it became evident that fluctuations are important, even determinant in some cases. The consolidation of the fluctuation theorems, in a regime of nonequilibrium beyond the linear, helped to understand the relations between thermodynamics and fluctuations.

One of the first fluctuation theorem was found by Gallavotti and Cohen [Gallavotti e Cohen 1995], and establishes the relation between the straight and inverse entropy flux distribution in a steady state process

$$\lim_{t\to\infty} \frac{k_B}{t} \ln\left(\frac{P(\dot{S}_i)}{P(-\dot{S}_i)}\right) = \dot{S}_i. \tag{4.106}$$

This relationship shows a privileged entropy flux direction, which is the same direction of heat flux. Nevertheless, there may be fluctuations of flux in the opposite direction. For macroscopic systems, the relationship between probability distributions of the previous equation grows exponentially, since the entropy is an extensive magnitude, becoming the fluctuations insignificant. Another fluctuation theorem is the Jarzynski equality [Jarzynski 1997], that relates the free energy of a irreversible process between two equilibrium states, with their related work.

$$e^{(-\beta\Delta F)} = \left\langle e^{-\beta W} \right\rangle. \tag{4.107}$$

This equation have as a consequence $\langle W\rangle \geq \Delta F$ which is the second law referred to in equation 4.105. Again, this theorem states that there may be fluctuations in work, so for certain trajectories $W < \Delta F$, but on average the second law must be maintained. A generalized fluctuation theorem was introduced by Crooks [Crooks 1999], in a theorem that relates the distribution of work produced by a irreversible non-equilibrium process forward in time $P_F(W)$, and the respective backward process, that is, the time-reversed trajectory $P_R(W)$.

$$\frac{P_F(W)}{P_R(-W)} = e^{\beta(W-\Delta F)} \tag{4.108}$$

. Through this Crooks theorem it is possible to deduce the Jarzynski equality and the Gallavotti-Cohen fluctuation theorem in steady states.

4.3.2 The formulation of stochastic thermodynamics

In the section 4.1 we saw the general form of a Markovian master equation in Liouville space:

$$\dot{\rho} = \mathcal{W}\rho. \tag{4.109}$$

Can be shown that a Markovian master equation can be written on the diagonal basis of the density matrix as [Esposito e Mukamel 2006]

$$\begin{aligned}\dot{p}_m(t) &= \sum_{m'} \mathcal{W}_{m,m'}(t)p_{m'}(t) \\ &= \sum_{m' \neq m} (\mathcal{W}_{m,m'}(t)p_{m'}(t) - \mathcal{W}_{m',m}(t)p_m(t)) \\ &= \sum_{m' \neq m} J_{m,m'}(t). \end{aligned} \tag{4.110}$$

with the probability current defined as

$$J_{m,m'}(t) = \mathcal{W}_{m,m'}(t)p_{m'}(t) - \mathcal{W}_{m',m}(t)p_m(t), \tag{4.111}$$

where m, m' are the possible states of the density matrix and $\mathcal{W}_{m,m'}$ is the transition probability element from state m to state m', per unit of time. In general, the basis is time-dependent, as the states and the transitions. The conservation of probability impose the condition

$$\sum_{m} \mathcal{W}_{m,m'} = 0, \tag{4.112}$$

so, the diagonal elements of the transition probability rates are

$$\mathcal{W}_{m,m} = -\sum_{m' \neq m} \mathcal{W}_{m',m}. \tag{4.113}$$

In the section 4.1 it was also established that a Lindblad equation has constant coefficients, that is, $\mathcal{W}_{m',m}$ are independent of time. Each state m can be associated to the energy ϵ_m, and a number of particles n_m. The average of the energy and the number of particles are respectively

$$E = \sum_{m} \epsilon_m p_m, \tag{4.114}$$

$$N = \sum_{m} n_m p_m. \tag{4.115}$$

The first law of thermodynamics can be formulated as

$$\dot{E} = \dot{W} + \dot{Q} + \dot{W}_{chem}, \tag{4.116}$$

where the work and heat fluxes are defined as

$$\dot{W} = \sum_m \dot{\epsilon}_m p_m, \tag{4.117}$$

and

$$\dot{Q} + \dot{W}_{chem} = \sum_m \epsilon_m \dot{p}_m. \tag{4.118}$$

This means that changes in the work cause changes in the energy levels, as well as changes in the heat causes changes in the states of the system, that is, jumps between states. Chemical work is included into the changes of the states because it can induce jumps, changing the occupation numbers. The generalization to multiple reservoirs is straightforward since it is assumed that the transition rates matrix is additive

$$\boldsymbol{\mathcal{W}} = \sum_\nu \boldsymbol{\mathcal{W}}^{(\nu)}, \tag{4.119}$$

The other quantities are also additives. We thus have

$$\dot{Q} = \sum_\nu \dot{Q}^{(\nu)}, \tag{4.120}$$

$$\dot{N} = \sum_\nu \dot{N}^{(\nu)}, \tag{4.121}$$

$$\dot{W}_{chem} = \sum_\nu \dot{W}^{(\nu)}_{chem}, \tag{4.122}$$

$$J_{m,m'} = \sum_\nu J^{(\nu)}_{m,m'}. \tag{4.123}$$

Now we introduce the condition of local detailed balance, which is equivalent to the local equilibrium assumption, and assumes that each transition rate $\boldsymbol{\mathcal{W}}^{(\nu)}$ at each moment, obeys a detailed balance with respect to the corresponding equilibrium distribution of the corresponding reservoir ν

$$\mathcal{W}^{(\nu)}_{m,m'}(t) p^{eq,v}_{m'}(t) = \mathcal{W}^{(\nu)}_{m',m}(t) p^{eq,v}_{m}(t). \tag{4.124}$$

The equilibrium distribution in the canonical ensemble is

$$p^{eq,v}_m(t) = \exp\Big(-\beta^{(\nu)}\big(\epsilon_m(t) - F^{eq,v}(t)\big)\Big), \tag{4.125}$$

where

$$\exp\left(-\beta^{(\nu)}F^{eq,v}(t)\right) = \sum_{m} \exp\left(-\beta^{(\nu)}\epsilon_m(t)\right). \tag{4.126}$$

In the grand canonical ensemble ($G = E - TS - \mu N$) and we get

$$p_m^{eq,v}(t) = \exp\Big(- \beta^{(\nu)}\big(\epsilon_m(t) - \mu^{(\nu)}n_m(t) - G^{eq,v}(t)\big)\Big), \tag{4.127}$$

where

$$\exp\left(-\beta^{(\nu)}G^{eq,v}(t)\right) = \sum_{m} \exp\left(-\beta^{(\nu)}(\epsilon_m(t) - \mu^{(\nu)}n_m(t))\right). \tag{4.128}$$

Defining the difference in energy and number of particles in a transition as

$$\epsilon_{m,m'} = \epsilon_m - \epsilon'_m, \tag{4.129}$$

$$n_{m,m'} = n_m - n'_m, \tag{4.130}$$

we may use the equation 4.110 to write the rates of thermodynamic quantities, induced for each coupling reservoir, in terms of the probability current $J_{m,m'}$ (Note that $J_{m,m'} = -J_{m',m}$ and the external work is zero $\dot{W} = 0$). We get

$$\dot{E}^{(\nu)} = \frac{1}{2}\sum_{m,m'} \epsilon_{m,m'}J^{(\nu)}_{m,m'}, \tag{4.131}$$

$$\dot{N}^{(\nu)} = \frac{1}{2}\sum_{m,m'} n_{m,m'}J^{(\nu)}_{m,m'}, \tag{4.132}$$

$$\begin{aligned}\dot{W}^{(\nu)}_{chem} &= \frac{1}{2}\sum_{m,m'} \mu^{(\nu)}n_{m,m'}J^{(\nu)}_{m,m'},\\ &= \mu^{(\nu)}\dot{N}^{(\nu)},\end{aligned} \tag{4.133}$$

$$\begin{aligned}\dot{Q}^{(\nu)} &= \frac{1}{2}\sum_{m,m'} q^{(\nu)}_{m,m'}J^{(\nu)}_{m,m'},\\ &= \dot{E}^{(\nu)} - \mu^{(\nu)}\dot{N}^{(\nu)},\end{aligned} \tag{4.134}$$

where

$$q^{(\nu)}_{m,m'} = \epsilon_{m,m'} - \mu^{(\nu)}n_{m,m'}. \tag{4.135}$$

From the equation 4.127 the "local detailed balance assumption" results in

$$\ln \frac{\mathcal{W}^{(\nu)}_{m,m'}}{\mathcal{W}^{(\nu)}_{m',m}} = \ln \frac{p^{eq,v}_{m}}{p^{eq,v}_{m'}} = -\beta^{(v)} q_{m,m'} = \beta^{(v)} q_{m',m}. \tag{4.136}$$

This relation is equivalent to the equations 4.46 and 4.79, and allows a direct connection between the stochastic dynamics of the system with well-established thermodynamic quantities. The "local detailed balance" assumption describe the coupling of the system with the reservoirs, however there is no assumption about the state of the system itself, so it may be arbitrarily far from equilibrium.

Shannon entropy was used to describe entropy, since, because of the structure of the equation 4.75, in the stationary state the coherences disappear, and we are left with

$$S = -k_\beta \sum_m p_m \ln p_m. \tag{4.137}$$

It is straightforward to show that the rate of change of the entropy can be split as the contribution of two terms

$$\dot{S} = k_\beta \sum_{m,m',\nu} \mathcal{W}^{(v)}_{m,m'} p_{m'} \ln \frac{\mathcal{W}^{(\nu)}_{m,m'} p_{m'}}{\mathcal{W}^{(\nu)}_{m',m} p_m} + k_\beta \sum_{m,m',\nu} \mathcal{W}^{(v)}_{m,m'} p_{m'} \ln \frac{\mathcal{W}^{(\nu)}_{m,m'}}{\mathcal{W}^{(\nu)}_{m',m}}, \tag{4.138}$$

from which the entropy production was identified as

$$\dot{S}_i = k_\beta \sum_{m,m',\nu} \mathcal{W}^{(v)}_{m,m'} p_{m'} \ln \frac{\mathcal{W}^{(\nu)}_{m,m'} p_{m'}}{\mathcal{W}^{(\nu)}_{m',m} p_m} \geq 0, \tag{4.139}$$

and the entropy flux as

$$\dot{S}_e = k_\beta \sum_{m,m',\nu} \mathcal{W}^{(v)}_{m,m'} p_{m'} \ln \frac{\mathcal{W}^{(\nu)}_{m,m'}}{\mathcal{W}^{(\nu)}_{m',m}}. \tag{4.140}$$

This identification was chosen because it is consistent with the usual form of thermodynamics. The entropy production is always positive because $(x-y)\ln x/y \geq 0$ and it can be written as the sum of products between fluxes and forces, as the equation 4.103

$$\frac{d_i S}{dt} = \frac{1}{2} \sum_{m,m',\nu} J^{(v)}_{m,m'} X^{(v)}_{m,m'} \geq 0, \tag{4.141}$$

where $J^{(v)}_{m,m'}$ is the probability current flux and

$$X^{(v)}_{m,m'} = k_\beta \ln \frac{\mathcal{W}^{(\nu)}_{m,m'} p_{m'}}{\mathcal{W}^{(\nu)}_{m',m} p_m} \tag{4.142}$$

is the force causing the flux. From the equation 4.136, the entropy flux is

$$\frac{d_e S}{dt} = \frac{k_\beta}{2} \sum_{m,m',\nu} J^{(v)}_{m,m'} q^{(v)}_{m,m'} = \sum_\nu \frac{\dot{Q}^{(v)}}{T^{(v)}}. \tag{4.143}$$

Both definitions, the equations 4.139 and 4.140 are consistent with the standard formulation of non-equilibrium thermodynamics.

4.3.3 Trajectory stochastic thermodynamics

Up to this point, we have presented the fundamentals of the stochastic thermodynamics from the point of view of ensembles, however, it is also possible to make a formulation in terms of trajectories, that is, in terms of individual realizations. The stochastic nature of the dynamics has their origin in the fluctuations caused by the interaction with the environment, that is, from the heat exchange. However, considering individual realizations, the work becomes stochastic too, so that each realization can generate a different amount of work. This will be reflected in the fluctuation theorems, presented here under the formulation of stochastic thermodynamics. A trajectory, denoted by $\mathit{\Pi}$ corresponds to the state of the system in a specific time interval, *i.e.*, $m(t)$, $t \in [t_i, t_f]$. The initial state is $m_i = m_1 = m(t_i)$, there are $N-1$ jumps from m_j to m_{j+1} at specific instants of time $t_{j+1,j}$, and the final state is $m_f = m_N = m(t_f)$.

For a single realization, the energy is also a state function, being a microstate of the system. Using the notation of lower script to specify the thermodynamic quantities at the trajectory level, we define

$$e = e^{\mathit{\Pi}} = \epsilon_{m(t)}(t). \tag{4.144}$$

The energy difference only depends on the final and initial states

$$\Delta e = e_f - e_i = \epsilon_{m(t_f)}(t_f) - \epsilon_{m(t_i)}(t_i). \tag{4.145}$$

Then, as before, work on a trajectory is related to changes in the energy of a given state; and the heat is related to the jumps between states.

$$\begin{aligned} w =&[\epsilon_{m_1}(t_{2,1}) - \epsilon_{m_1}(t_i)] + [\epsilon_{m_2}(t_{3,2}) - \epsilon_{m_2}(t_{2,1})] \\ &+ ... + [\epsilon_{m_N}(t_f) - \epsilon_{m_N}(t_{N,N-1})], \end{aligned} \tag{4.146}$$

$$q = \sum_{jumps} q_{j+1,j}, \tag{4.147}$$

$$q_{j+1,j} = \epsilon_{m_{j+1}}(t_{j+1,j}) - \epsilon_{m_j}(t_{j+1,j}). \tag{4.148}$$

For multiple reservoirs, it is necessary to specify each reservoir

$$q = \sum_{\nu} q^{(\nu)}, \tag{4.149}$$

It is also possible to formulate the first law of thermodynamics at the trajectory level as

$$\Delta e = w + q. \tag{4.150}$$

Routinely in information theory, the entropy of a single event can be defined as the lack of knowledge or certainty, by Shannon's formula $S = -\ln p_m$. So, for example, the certainty about an event $p_m \to 1$ implies $S \to 0$ and the total uncertainty $p_m \to 0$ leads to entropy growing indefinitely $S \to \infty$. Seifert defined the entropy of a single trajectory in the stochastic thermodynamics [Seifert 2005] as

$$s = s^{\Pi}(t) = -k_\beta \ln p_{m(t)}(t). \tag{4.151}$$

This definition is consistent with the Shannon entropy (see equation 4.137) since it is evident that the average over the ensemble is

$$S = \langle s \rangle = -k_\beta \sum_m p_m \ln p_m. \tag{4.152}$$

Just like energy difference, entropy difference is a state function of the corresponding microstate

$$\Delta s = -k_\beta \ln p_{m_f}(t_f) + k_\beta \ln p_{m_i}(t_i). \tag{4.153}$$

The entropy flux at the trajectory level can be expressed as

$$\Delta_e s = \sum_{jumps} \frac{q^{(\nu)}_{j+1,j}}{T^{(\nu)}}, \tag{4.154}$$

or, from the local detailed balance (see equation 4.136)

$$\Delta_e s = -k_\beta \sum_{jumps} \ln \frac{\mathcal{W}^{(\nu)}_{j+1,j}}{\mathcal{W}^{(\nu)}_{j,j+1}}. \tag{4.155}$$

This leads to the following expression for the entropy production

$$\Delta_i s = \Delta s - \Delta_e s = -k_\beta \ln p_{m_f}(t_f) + k_\beta \ln p_{m_i}(t_i) + k_\beta \sum_{jumps} \ln \frac{\mathcal{W}^{(\nu)}_{j+1,j}}{\mathcal{W}^{(\nu)}_{j,j+1}}. \tag{4.156}$$

This expression for the entropy production of a single realization can be negative. This is kind of expected since the stochastic character of the system can generate trajectories with negative entropy.

Introducing the stochastic free energy

$$f = e - Ts, \tag{4.157}$$

and combining the equations 4.154 and 4.156 with the stochastic first law (equation4.150), we obtain

$$T\Delta_i s = w - \Delta f, \tag{4.158}$$

which corresponds to the analogous expression 4.105 obtained using ensemble statistics. For an equilibrium distribution p^{eq}_m the free energy becomes independent of the state

$$f^{eq} = F^{eq}. \tag{4.159}$$

So, if the initial and final system states are in equilibrium, we get

$$T\Delta_i s = w - \Delta F^{eq}. \tag{4.160}$$

This result is important because it indicates, that apart from a fixed quantity ΔF^{eq}, the stochastic work and the stochastic entropy production behave in the same way.

There is a central result in the theory of stochastic thermodynamics, a fundamental relation for the entropy production [Broeck e Esposito 2015]. Given a trajectory $\mathit{\Pi}$ one can associate it with a probability $\mathcal{P}(\mathit{\Pi})$ of observing it. It is also possible to identify the time reverse path labeled with a "tilde" $\widetilde{\mathit{\Pi}}$, and its

probability $\widetilde{P}(\widetilde{\Pi})$ so that the initial probability of the inverse trajectory is the final probability of the forward trajectory. So, the entropy production along the trajectory Π is

$$\Delta_i s = k_\beta \ln \frac{\mathcal{P}(\Pi)}{\widetilde{\mathcal{P}}(\widetilde{\Pi})}. \tag{4.161}$$

The second law of thermodynamics is immediately recovered from this result, because the ensemble average of the stochastic entropy production is non-negative

$$\Delta_i S = \langle \Delta_i s \rangle = k_\beta \sum_{\Pi} \mathcal{P}(\Pi) \ln \frac{\mathcal{P}(\Pi)}{\widetilde{\mathcal{P}}(\widetilde{\Pi})} \geq 0. \tag{4.162}$$

Another result that can be immediately derived is the integral fluctuation theorem

$$\left\langle \exp\left(\frac{-\Delta_i s}{k_\beta}\right) \right\rangle = \left\langle \frac{\widetilde{\mathcal{P}}}{\mathcal{P}} \right\rangle = \sum_{\Pi} \mathcal{P} \frac{\widetilde{\mathcal{P}}}{\mathcal{P}} = 1. \tag{4.163}$$

which is valid for any initial and final probability. For the special case of transitions between equilibrium states, one can introduce the equation 4.160 in the previous result to obtain the well-known Jarzynski equality (see the equation 4.107)

$$\langle \exp(-\beta w) \rangle = \exp(-\beta \Delta F^{eq}). \tag{4.164}$$

Also from equation the 4.161 it is possible to show that

$$\frac{P(\Delta_i s)}{\widetilde{P}(-\Delta_i s)} = \exp\left(\frac{\Delta_i s}{k_\beta}\right) \tag{4.165}$$

which is the Gallavotti-Cohen theorem or detailed fluctuation theorem referred to in the equation 4.106.

4.3.4 Thermodynamics of feedback

At this point, it is possible to formulate the thermodynamics of the Wiseman-Milburn feedback with the formalism of stochastic thermodynamics. The starting point is the generator of the master equation 4.77 including the counting factors in the jump terms

$$\mathcal{W}(\chi) = \mathcal{W}_0 + \sum_{\nu} \sum_{i>j} (\gamma^{\nu}_{j\to i} e^{i\chi^{\nu}_{j,i}} |i\rangle\rangle\langle\langle j| + \bar{\gamma}^{\nu}_{i\to j} e^{-i\chi^{\nu}_{j,i}} |j\rangle\rangle\langle\langle i|). \tag{4.166}$$

As we saw in the subsection 4.1.5, the net current associated with the transition $j \to i$ triggered by the reservoir ν, can be calculated by taking the time derivative of the first moment of the transport statistic

$$\begin{aligned} I^{\nu}_{(i,j)}(t) &= \frac{\partial}{\partial t}\langle n\rangle^{\nu}_{(i,j)}(t) = \frac{\partial}{\partial t}\frac{\partial}{\partial\left(i\chi^{\nu}_{(i,j)}\right)}\operatorname{tr}(\rho(\chi,t))\Big|_{\chi=0} \\ &= \operatorname{tr}\left(\mathcal{W}'(0)e^{\mathcal{W}(0)t}\rho(0) + \mathcal{W}(0)\left(e^{\mathcal{W}(0)t}\right)'\rho(0)\right), \end{aligned} \tag{4.167}$$

where $'$ is the notation of the derivative with respect to $(i\chi^{\nu}_{(i,j)})$ evaluated at $\chi = 0$. The second term vanish because of the condition $\sum_i \mathcal{W}_{i,j} = 0$. Thus, we get

$$I^{\nu}_{(i,j)}(t) = \operatorname{tr}\left(\mathcal{W}'(0)\rho(t)\right). \tag{4.168}$$

So, the probability current associated with the transition $(i,j)^{\nu}$ is

$$I^{\nu}_{(i,j)}(t) = \gamma^{\nu}_{j\to i}p_j(t) - \bar{\gamma}^{\nu}_{i\to j}p_i(t). \tag{4.169}$$

Note that this current is the same defined in the equation 4.111. Following this same procedure, when the feedback is applied, we start from the generator of the equation 4.82

$$I^{\nu}_{(i,j)}(t) = \operatorname{tr}\left[\left(\mathcal{C}^{\nu}_{j\to i}\mathcal{J}^{\nu}_{j\to i} - \overline{\mathcal{C}}^{\nu}_{i\to j}\overline{\mathcal{J}}^{\nu}_{i\to j}\right)\rho(t)\right] \tag{4.170}$$

it can be shown that the equation 4.169 is recovered. That is, the probability current does not change when the control operation is applied. So, in consistence with the equation 4.134, the heat transfer is defined as

$$\dot{Q}^{(\nu)}(t) = \sum_{i>j}\left(E_i - E_j - \mu^{\nu}\right)I^{\nu}_{(i,j)}(t). \tag{4.171}$$

Each time a jump is detected by the control operation, the feedback is implemented with an energy injection that can be written as

$$\left(\dot{\mathcal{F}}^{(\nu)}_{E}(t)\right)_{(i,j)} = \operatorname{tr}\left[\mathcal{H}_S\left(\mathcal{C}^{\nu}_{j\to i} - 1\right)\mathcal{J}^{\nu}_{j\to i}\rho(t)\right] + \operatorname{tr}\left[\mathcal{H}_S\left(\overline{\mathcal{C}}^{\nu}_{i\to j} - 1\right)\overline{\mathcal{J}}^{\nu}_{i\to j}\rho(t)\right]. \tag{4.172}$$

This quantity is positive if the energy of the system increases, and zero if no control operation is implemented ($\mathcal{C}^{\nu}_{j\to i}, \overline{\mathcal{C}}^{\nu}_{i\to j} = 1$). So, the first law of thermodynamics with feedback is

$$\dot{E}(t) = \sum_{\nu}\left(\dot{Q}^{(\nu)}(t) + \dot{\mathcal{F}}^{(\nu)}_{E}(t)\right) + \dot{W}_{chem}, \tag{4.173}$$

with

$$\dot{\mathcal{F}}_E^{(\nu)}(t) = \sum_{i>j} \left(\dot{\mathcal{F}}_E^{(\nu)}(t) \right)_{(i,j)}. \tag{4.174}$$

The control operation also modifies the entropy production and flux adding new entropy to the system. From the definitions of entropy of stochastic thermodynamics 4.139, 4.140, one can identify the corresponding entropies in the presence of feedback as

$$\dot{S}_{\mathbf{i}}(t) = \sum_{\nu} \sum_{i,j} \left(\mathcal{W}^C \right)_{ij}^{(\nu)} p_j(t) \ln \frac{\left(\mathcal{W}^C \right)_{ij}^{(\nu)} p_j(t)}{(\mathcal{W})_{ji}^{(\nu)} p_i(t)} \geqslant 0, \tag{4.175}$$

$$\dot{S}_{\mathbf{e}}(t) = \sum_{v} \sum_{i,j} \left(\mathcal{W}^C \right)_{ij}^{(\nu)} p_j(t) \ln \frac{\left(\mathcal{W}^C \right)_{ji}^{(\nu)}}{\left(\mathcal{W}^C \right)_{ij}^{(\nu)}}, \tag{4.176}$$

where the superscript C refers to the application of control in the master equation. After some algebraic manipulations, the entropy flow reads [Strasberg et al. 2013]

$$\dot{S}_{\mathrm{e}}(t) = \sum_{\nu} \frac{\dot{Q}^{(\nu)}(t)}{T_\nu} - \dot{\mathcal{F}}_S(t), \tag{4.177}$$

where $\dot{\mathcal{F}}_S(t)$ characterizes the entropy injection. Hence, the second law of thermodynamics is given by

$$\dot{S}_{\mathbf{i}} = \dot{S} - \dot{S}_{\mathrm{e}} = \dot{S} - \sum_{\nu} \frac{\dot{Q}^{(\nu)}}{T_\nu} + \dot{\mathcal{F}}_S \geq 0. \tag{4.178}$$

This reformulation of the thermodynamic laws shows that the control operation can inject both energy and entropy into the system, being both additive

$$\dot{\mathcal{F}}_{E,S} = \sum_{\nu} \mathcal{F}_{E,S}^{(v)}. \tag{4.179}$$

From this point of view a Maxwell demon could be understood as a feedback operation where the injected energy flux is zero $\dot{\mathcal{F}}_E = 0$, but injected entropy flux is non-zero $\dot{\mathcal{F}}_E > 0$.

5 THERMODYNAMICS OF FEEDBACK CONTROLLED DYNAMICS WITH FERMIONIC AND BOSONIC RESERVOIRS

The non-equilibrium thermodynamics of small quantum systems have been a subject of great recent interest, because the exchange of energy in both, molecular (biological) machines and thermal engines, occurs far from equilibrium [Bustamante, Liphardt e Ritort 2005]. Fluctuations play a relevant role in the dynamics of these small systems, so the development of the fluctuation theorems [Evans, Cohen e Morriss 1993, Evans e Searles 2002], the Jarzynski's equality [Jarzynski 1997], and the Crocks theorem [Crooks 1999], and their experimental tests [Ritort 2004], are fundamental steps in the understanding of such thermodynamic processes.

More recently, the use of quantum control operations to create feedback protocols, which use information of the system to modify the system itself in a closed loop, has proved useful and efficient in the execution of tasks that could be difficult to achieve otherwise. The reduction of noise and quantum decoherence rate, quantum error correction, the purification and stabilization of quantum states [Zhang et al. 2017], and the implementation of heat engines [Strasberg et al. 2013] are examples of the possibilities of application of quantum feedback control.

The theoretical formulation of stochastic thermodynamics provides a simple and coherent framework to study the non-equilibrium thermodynamic processes for small systems [Broeck e Esposito 2015, Seifert 2012, Esposito, Harbola e Mukamel 2009]. Assuming that the process is Markovian and under the rotating wave approximation (RWA), it is possible to obtain a Lindblad type master equation for the dynamic evolution, and from the formulation of stochastic thermodynamics we obtain the relevant thermodynamic quantities, even if the dynamic is modified by a feedback operation.

We are going to study a qubit system coupled with two bosonic and fermionic reservoirs respectively. Such systems may correspond, in the bosonic case, to the absorption/emission of photons of a two-level system, from/to coupled

photon reservoirs, and in the fermionic case, to the transport of electrons through a quantum point coupled to electron reservoirs.

5.1 Qubit system

A two-level system coupled to two boson reservoirs at different temperatures absorbs and emits bosons to and from each reservoir. The system as a whole can be understood as a system of bosons transport through the two-level system, from the hot reservoir to the cold reservoir. A quantum dot coupled to two electron reservoirs at different temperatures and/or chemical potential is a fermionic transport system through the quantum dot. Both correspond to qubit systems whose Hamiltonian is composed of the Hamiltonian of the qubit, the Hamiltonian of the reservoirs and a term describing the interaction between the system and the reservoirs. We may thus write

$$H = H_S + H_B + V, \tag{5.1}$$

$$H_S = \frac{\epsilon}{2}\sigma_z, \tag{5.2}$$

$$H_B = \sum_{\nu\in\{L,R\}} \sum_k \omega_{k\nu} b^\dagger_{k\nu} b_{k\nu}, \tag{5.3}$$

$$V = \sum_{\nu\in\{L,R\}} \sum_k T_{k\nu}(b^\dagger_{k\nu} c_s + b_{k\nu} c^\dagger_s). \tag{5.4}$$

where $\epsilon, \omega_{k\nu}, T_{k\nu} \geq 0$ are the eigenenergy difference in the qubit levels, the normal modes energy in the reservoirs, and the coupling energy respectively. The system operators in the eigen-basis are $\sigma_z = |1\rangle\langle 1| - |0\rangle\langle 0|$, $c_s = |0\rangle\langle 1|$, $c^\dagger_s = |1\rangle\langle 0|$, and $b_{k\nu}, b^\dagger_{k\nu}$ denotes the annihilation and creation reservoir operators. Each reservoir is independent and does not interact directly with the other reservoir, and its operators obey the following (anti-)commutation relations

$$b_{k\nu} b^\dagger_{l\nu'} \pm b^\dagger_{l\nu'} b_{k\nu} = \delta_{kl}\delta_{\nu\nu'}, \tag{5.5}$$

where the anticommutation relation reveals the fermionic character of the operators, and the commutation, the bosonic character.

This type of transport system has been widely studied due to its simplicity. Specifically, for a weak bath-system coupling, under the Markovian and RWA

approximations, corresponds to a Lindblad master equation [Gurvitz e Prager 1996, Harbola, Esposito e Mukamel 2006, Harbola, Esposito e Mukamel 2007]

$$\dot{\rho}(t) = -i[H_s, \rho(t)] + \left(\sum_{\nu \in \{L,R\}} \gamma_\nu \right) \left(c_s^\dagger \rho(t) c_s - \frac{1}{2} \rho(t) c_s c_s^\dagger - \frac{1}{2} c_s^\dagger c_s \rho(t) \right) + \left(\sum_{\nu \in \{L,R\}} \overline{\gamma}_\nu \right) \left(c_s \rho(t) c_s^\dagger - \frac{1}{2} \rho(t) c_s^\dagger c_s - \frac{1}{2} c_s c_s^\dagger \rho(t) \right), \tag{5.6}$$

where the transition rates

$$\gamma_\nu = \Gamma_\nu n_\nu(\epsilon), \qquad \overline{\gamma}_\nu = \Gamma_\nu (1 \mp n_\nu(\epsilon)), \tag{5.7}$$

are determined by the Fermi or Bose distributions as

$$n_\nu(\epsilon) = (e^{\beta_\nu(\epsilon - \mu_\nu)} \pm 1)^{-1}, \tag{5.8}$$

depending on whether the reservoirs are fermionic or bosonic. The convention is that the upper sign in the equations 5.7,5.8 is maintained for the fermionic case, and the lower sign for the bosonic case. The tunnel rates Γ_ν are calculated assuming a constant density of states σ in the leads (see figure 2): $\Gamma_\nu = \frac{2\pi}{\hbar} \sigma \sum_k |T_{k\nu}|^2$. It is well known that the dynamics in a Lindblad equation can be separated in terms of jumps and continuous evolution. Note that the terms with factors $c_s^\dagger \rho(t) c_s$ and $c_s \rho(t) c_s^\dagger$ correspond to the jumps in the evolution, since they represent transitions between the states $0 \leftrightarrow 1$, and the rest of the terms correspond to the smooth or continuous evolution.

The master equation 5.6 can be written in the Liouville basis $\{p_0, p_1, \rho_{0,1}, \rho_{1,0}\}$ as

$$\dot{\rho}(t) = \mathcal{W} \rho(t), \tag{5.9}$$

with $\mathcal{W}$ having the block structure

$$\mathcal{W} = \begin{pmatrix} \mathcal{W}_{pop}^C & 0 \\ 0 & \mathcal{W}_{coh} \end{pmatrix}, \tag{5.10}$$

where

$$\mathcal{W}_{pop} = \sum_\nu \begin{pmatrix} -\gamma_\nu & \overline{\gamma}_\nu \\ \gamma_\nu & -\overline{\gamma}_\nu \end{pmatrix}, \tag{5.11}$$

$$\mathcal{W}_{coh} = \begin{pmatrix} i\epsilon - \sum_\nu \frac{\gamma_\nu + \bar{\gamma}_\nu}{2} & 0 \\ 0 & -i\epsilon - \sum_\nu \frac{\gamma_\nu + \bar{\gamma}_\nu}{2} \end{pmatrix}. \tag{5.12}$$

The populations and coherences are decoupled, and the coherences decay exponentially. In the steady state the populations are

$$p_0 = 1 - p_1 = \frac{\sum_\nu \gamma_\nu}{\sum_\nu (\gamma_\nu + \bar{\gamma}_\nu)}, \tag{5.13}$$

and the coherences vanish $\rho_{0,1}, \rho_{1,0} = 0$. So, as seen in the subsection 4.3.4, we have that the probability current and the heat flow are respectively

$$I^\nu = \gamma_\nu p_0 - \bar{\gamma}_\nu p_1, \qquad \dot{Q}^{(\nu)} = (\epsilon - \mu_\nu) I^\nu. \tag{5.14}$$

Then, the first and second law of thermodynamics are given respectively by

$$\dot{E} = \dot{Q}_L + \dot{Q}_R, \qquad \dot{S}_i = \dot{S} - (\beta_L - \beta_R)\dot{Q}_L \geqslant 0. \tag{5.15}$$

5.2 Qubit system with feedback

As we have seen in section 4.2.1, the Wiseman-Milburn feedback is a protocol implemented by detecting the particles exchanged between the reservoirs and the system. Immediately after the detection a unitary control operation is implemented, to drive the system to the desired state. Denoting ϱ as the density matrix acting in Hilbert space and ρ, the corresponding vector in Liouville space, the unitary operator $\mathcal{C}\rho \leftrightarrow U_C \varrho U_C^\dagger$ in the basis $\{|0\rangle, |1\rangle\}$ is

$$U_\nu^\pm \equiv e^{-i\alpha_\nu^\pm (|0\rangle\langle 1| + |1\rangle\langle 0|)} = \begin{pmatrix} \cos(\alpha_\nu^\pm) & -i\sin(\alpha_\nu^\pm) \\ -i\sin(\alpha_\nu^\pm) & \cos(\alpha_\nu^\pm) \end{pmatrix}. \tag{5.16}$$

This operation corresponds to a rotation of $\alpha_\nu^\pm$ around the x-axis of the Bloch sphere, and is implemented over the jumps terms of the master equation. The $+/-$ labels, refer to the triggered operation by the absorption/emission of a particle in the system from/into the ν reservoir. Under this scheme, the feedback master equation has the following block structure (the superscript C refers to the application of control):

$$\dot{\rho}(t) = \mathcal{W}^C \rho(t), \tag{5.17}$$

$$\mathcal{W}^C = \begin{pmatrix} \mathcal{W}^C_{pop} & 0 \\ \mathcal{W}^C_{cp} & \mathcal{W}_{coh} \end{pmatrix}. \tag{5.18}$$

with

$$\mathcal{W}^C_{\rm pop} = \sum_v \begin{pmatrix} -\gamma_v \cos^2\alpha^v_+ & \overline{\gamma}_v \cos^2\alpha^v_- \\ \gamma_v \cos^2\alpha^v_+ & -\overline{\gamma}_v \cos^2\alpha^v_- \end{pmatrix}, \tag{5.19}$$

$$\mathcal{W}^C_{cp} = \frac{i}{2}\sum_\nu \begin{pmatrix} -\gamma_v \sin 2\alpha^\nu_+ & \overline{\gamma}_v \sin 2\alpha^\nu_- \\ \gamma_v \sin 2\alpha^v_+ & -\overline{\gamma}_v \sin 2\alpha^v_- \end{pmatrix}, \tag{5.20}$$

and $\mathcal{W}_{coh}$ being the same as the equation 5.12. Again, occupations are not coupled to coherences, but coherences are coupled to occupations through $\mathcal{W}^C_{cp}$ terms. This means that coherent states can also be stabilized by the control operation because, in the presence of feedback, coherences do not vanish in the steady state. The solution of the equation 5.17 for the steady state is

$$p_0 = 1 - p_1 = \frac{\overline{\gamma}_L \cos^2\alpha^L_- + \overline{\gamma}_R \cos^2\alpha^R_-}{\gamma_L \cos^2\alpha^L_+ + \overline{\gamma}_L \cos^2\alpha^L_- + \gamma_R \cos^2\alpha^R_+ + \overline{\gamma}_R \cos^2\alpha^R_-} \tag{5.21}$$

$$\begin{aligned}\rho_{01} = \rho^*_{10} = &\frac{2i\gamma_L \cos\alpha^L_+ \left[\overline{\gamma}_L \cos\alpha^L_- \sin\left(\alpha^L_- - \alpha^L_+\right) + \overline{\gamma}_R \cos\alpha^R_- \sin\left(\alpha^R_- - \alpha^L_+\right)\right]}{\mathcal{N}} \\ &+\frac{2i\gamma_R \cos\alpha^R_+ \left[\overline{\gamma}_L \cos\alpha^L_- \sin\left(\alpha^L_- - \alpha^R_+\right) + \overline{\gamma}_R \cos\alpha^R_- \sin\left(\alpha^R_- - \alpha^R_+\right)\right]}{\mathcal{N}},\end{aligned} \tag{5.22}$$

with

$$\begin{aligned}\mathcal{N} = &\left(\gamma_L \cos^2\alpha^L_+ + \overline{\gamma}_L \cos^2\alpha^L_- + \gamma_R \cos^2\alpha^R_+ + \overline{\gamma}_R - \overline{\gamma}_R \sin^2\alpha^R_-\right) \\ &\times \left(-2i\Omega + \gamma_L + \overline{\gamma}_L + \gamma_R + \overline{\gamma}_R\right).\end{aligned} \tag{5.23}$$

Now we can formulate the stochastic thermodynamics of the system in the presence of feedback, from the definitions established in the section 4.3. The first law of thermodynamics becomes

$$\dot{E}(t) = \dot{Q}^L(t) + \dot{\mathcal{F}}^L_E(t) + \dot{Q}^R(t) + \dot{\mathcal{F}}^R_E(t) + \dot{W}_{chem}, \tag{5.24}$$

where the injected energy rate by the feedback is

$$\dot{\mathcal{F}}^{(v)}_E(t) = \epsilon\left(I^v_F(t) - I^v(t)\right), \tag{5.25}$$

and $I_F^v(t)$ is the effective current of the feedback generator of the equation 5.19

$$I_F^v(t) = \cos^2 \alpha_+^\nu \gamma_v p_0(t) - \cos^2 \alpha_-^\nu \overline{\gamma}_\nu p_1(t). \tag{5.26}$$

In the steady state $\dot{E}(t) = 0$, and therefore $I_F^L + I_F^R = 0$, or equivalently $\dot{\mathcal{F}}_E = -\dot{Q}^L - \dot{Q}^R - \dot{W}$. In the same way, the injected entropy rate can be found from the equation 4.177 and the *local detailed balance* condition

$$\dot{\mathcal{F}}_S = \sum_v \frac{\dot{Q}^{(v)}}{T_v} + \left(-\frac{\epsilon - \mu_L}{T_L} + \frac{\epsilon - \mu_R}{T_R} + f_L - f_R \right) I_F^L \tag{5.27}$$

with $f_v = \ln \frac{\cos^2 \alpha_+^\nu}{\cos^2 \alpha_-^\nu}$. The second law of thermodynamics has the form

$$\dot{S}_i = \dot{S} - \dot{S}_e = \dot{S} - \sum_\nu \frac{\dot{Q}^{(\nu)}}{T_\nu} + \dot{\mathcal{F}}_S \geq 0. \tag{5.28}$$

It is feasible to write an integral fluctuation theorem at the trajectory level, when the feedback protocol is implemented. In the same way as in the section 4.3.3, reformulating all quantities at the level of trajectories, from the equation 4.163 we have

$$\left\langle \exp\left(\frac{-\Delta s + \sum_\nu \frac{\dot{q}^{(\nu)}}{T_\nu} - f_S}{k_\beta} \right) \right\rangle = 1, \tag{5.29}$$

where f_S is the integral injected entropy flux. From this, it is possible to derive Jarzynski's equality for the case of a coupling with a single reservoir, and the detailed fluctuation theorem for stationary states [Esposito e Schaller 2012].

5.3 Qubit system with time-delayed feedback

As was shown in the section 4.2.2, the condition for applying the control operation instantaneously after the detection of a jump, was relaxed in order to describe more realistic systems. A time delay τ was introduced under the "control-skipping assumption" which states that if the delay time is greater than the time between two consecutive jumps, there will be no control operation. The generator of the master equation with time-delayed feedback $\mathcal{W}_{\text{delay}}(0)$ in the

steady state (see equation 4.92), has the following block form in the Liouville basis

$$\mathcal{W}_{\rm delay}(0) = \begin{pmatrix} \mathcal{W}_{pop}^{delay} & 0 \\ \mathcal{W}_{cp}^{delay} & \mathcal{W}_{coh} \end{pmatrix}, \tag{5.30}$$

with

$$\mathcal{W}_{\rm pop}^{delay} = \sum_{v} \begin{pmatrix} -\gamma_v(1-\exp\left(\sum_\nu \overline{\gamma}_v\tau_-^v\right)\sin^2\alpha_+^v) & \overline{\gamma}_v(1-\exp\left(\sum_\nu \gamma_v\tau_+^v\right)\sin^2\alpha_-^v) \\ \gamma_v(1-\exp\left(\sum_\nu \overline{\gamma}_v\tau_-^v\right)\sin^2\alpha_+^v) & -\overline{\gamma}_v(1-\exp\left(\sum_\nu \gamma_v\tau_+^v\right)\sin^2\alpha_-^v) \end{pmatrix}, \tag{5.31}$$

$$\mathcal{W}_{cp}^{delay} = \frac{i}{2}\sum_{y} \begin{pmatrix} -\gamma_v\exp\left(\sum_\nu \overline{\gamma}_v\tau_-^v\right)\sin 2\alpha_+^\nu & \overline{\gamma}_v\exp\left(\sum_\nu \gamma_v\tau_+^v\right)\sin 2\alpha_-^\nu \\ \gamma_v\exp\left(\sum_\nu \overline{\gamma}_v\tau_-^v\right)\sin 2\alpha_+^v & -\overline{\gamma}_v\exp\left(\sum_\nu \gamma_v\tau_+^v\right)\sin 2\alpha_-^v \end{pmatrix}, \tag{5.32}$$

and $\mathcal{W}_{coh}$ unmodified. The parameter $\tau_\pm^\nu$ is the delay time for each of the related control operations $U_\nu^\pm$. Notice that the delay time introduces a damping, both, in populations and coherences as it increases. The laws and the equations of stochastic thermodynamics remain the same as in the previous section, where the time delay vanishes. Only few changes must be introduced: for the first law of thermodynamics, the equation 5.24 is maintained, changing I_F^v for

$$I_F^v(t) = (1-e^{(\sum_\nu \overline{\gamma}_v\tau_-^v)}\sin^2\alpha_+^v)\gamma_v p_0(t) - (1-e^{(\sum_\nu \gamma_v\tau_+^v)}\sin^2\alpha_-^v)\overline{\gamma}_\nu p_1(t), \tag{5.33}$$

which is the effective current of the feedback generator of the equation 5.31. For the law second law of thermodynamics, the equation 5.27 is maintained too, introducing a new f_v

$$f_v = \ln\frac{1-e^{(\sum_\nu \overline{\gamma}_v\tau_-^v)}\sin^2\alpha_+^v}{1-e^{(\sum_\nu \gamma_v\tau_+^v)}\sin^2\alpha_-^v}. \tag{5.34}$$

5.4 Applications: Heat pump

Simple transport systems with a feedback operation can be used to generate a heat pump. This is a device that, working between two reservoirs at different temperatures, delivers heat to the hotter reservoir using a given external work. The efficiency of a conventional heat pump can be characterized by the coefficient of performance, which quantifies the heat delivered to the hotter reservoir, with

respect to the used total work. Assuming that the left reservoir is the hotter reservoir $T_L > T_R$, the coefficient of performance is

$$\kappa_C \equiv \frac{-\dot{Q}_L}{\dot{W}} \leq \frac{T_L}{T_L - T_R} \equiv \frac{1}{\eta_C}, \tag{5.35}$$

where η_C is the Carnot coefficient and hence κ_C is always positive and less than $1/\eta_C$. Strasberg et al [Strasberg et al. 2013] showed that it is possible to design a heat pump with a two-level system between two reservoirs of phonons at different temperatures using a Wiseman-Milburn type feedback as an external source of work since this feedback injects both energy and entropy into the system. They showed that it is not enough just to take into account the work injected by the feedback, since a correct description must take into account the work produced by the entropy injection. From the first and second law of thermodynamics written in the equations 5.24 and 5.28, for stationary states ($\dot{E} = 0$, $\dot{S} = 0$), it is easy to show

$$T_R \dot{S}_i = \dot{\mathcal{F}}_E + T_R \dot{\mathcal{F}}_S + \dot{W}_{chem} + \dot{Q}_L \eta_C \geq 0. \tag{5.36}$$

where $\dot{W}_{chem} = (\mu_L - \mu_R) I^L$ is the work induced by the difference between chemical potentials in the reservoirs (electrochemical potential, see equation 4.133). If $\dot{W}_{chem}$ is assumed positive, then

$$\dot{\mathcal{F}}_E + T_R \dot{\mathcal{F}}_S + \dot{W}_{chem} \geq -\dot{Q}_L \eta_C \geq 0. \tag{5.37}$$

So, as the heat delivered to the left reservoir is negative, the device works as a heat pump. The performance coefficient is

$$\kappa_C = \frac{-\dot{Q}_L}{\dot{\mathcal{F}}_E + T_R \dot{\mathcal{F}}_S + \dot{W}_{chem}} = \frac{1}{\eta_C} \left(1 - \frac{T_R \dot{S}_i}{\dot{\mathcal{F}}_E + T_R \dot{\mathcal{F}}_S + \dot{W}_{chem}} \right) \leq \frac{1}{\eta_C}. \tag{5.38}$$

The fact of considering $\dot{W}_{chem} \neq 0$, will allow us to extend the analysis done in [Strasberg et al. 2013] for bosonic reservoirs (which typically have zero chemical potential), to systems with fermionic reservoirs. It is possible to change the difference between chemical potentials simply by applying a potential difference $V = \mu_L - \mu_R$ between the reservoirs, such as $\dot{W}_{chem} = V I^L$. We will show the analysis corresponding to a quantum dot coupled to two electron reservoirs,

and we will make the comparative analysis with the analog system with bosonic reservoirs.

The efficiency of the heat pump is maximal, when the parameters minimize the negative heat flux (see equation 5.14) $\dot{Q}^{(\nu)} = (\epsilon - \mu_\nu)(\gamma_\nu p_0 - \bar{\gamma}_\nu p_1^\nu)$. This is true when the occupations are $p_0 \to 0$ and $p_1 \to 1$; which is fulfilled by the parameters $\alpha_+^\nu = 0$, $\alpha_-^\nu = \pi/2$ (see equation 5.21).

The analysis of the Full Counting Statistic shows us a clear signature on the efficiency of the system. We allow the free variation of the parameter α_-^ν, keeping $\alpha_+^\nu = 0$, and plot the related Fano factors (see equation 4.72), calculated with the approximation referred to in the equation 4.73, assuming zero delay time. We see the Fano factors converging to unity when $\alpha_-^\nu = \pi/2$, that is to say, when the system has maximum efficiency. In the figure 18 we see such behavior for the fermionic system, being the behavior of the bosonic system very similar.

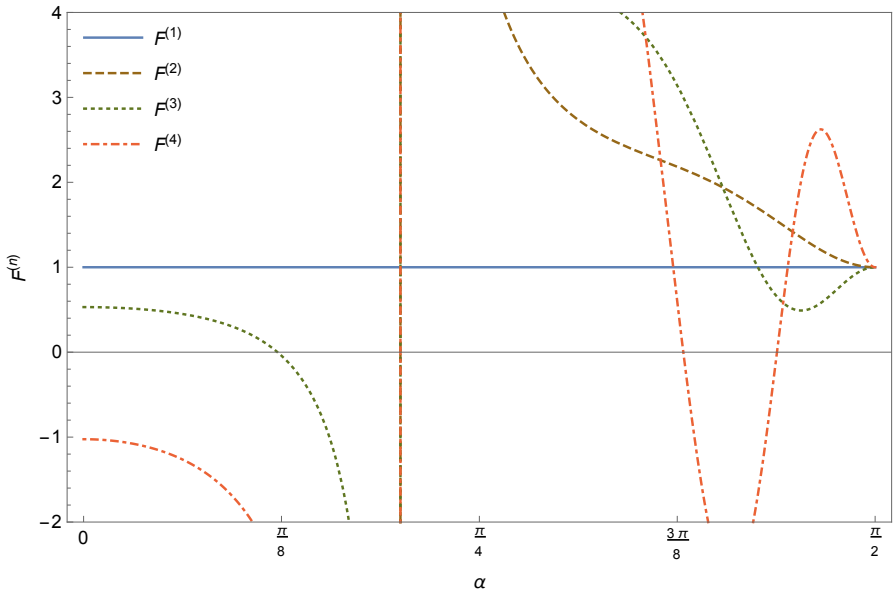

Figure 18 – Variation of the values of the Fano factors with respect to the feedback parameter α_-^ν for the fermionic system. System parameters: $\Gamma_L = 1$, $\Gamma_R = 1$, $\epsilon = 1$, $T_L = 1$, $T_R = 0.5$ $V = 0$ ($\eta_C = 2$). Feedback parameters: $\alpha_+^\nu = 0$.

This behavior can be understood since when the system has maximum efficiency, the state of the system is pure and without coherence $p_0 \to 0$, $p_1 \to 1$, $\rho_{0,1} = \rho_{1,0}^* = 0$. For this reason, it is expected that these states have classical

statistics, which corresponds to a cumulant generating function of a Poisson process, where all Fano factors are equal to unity.

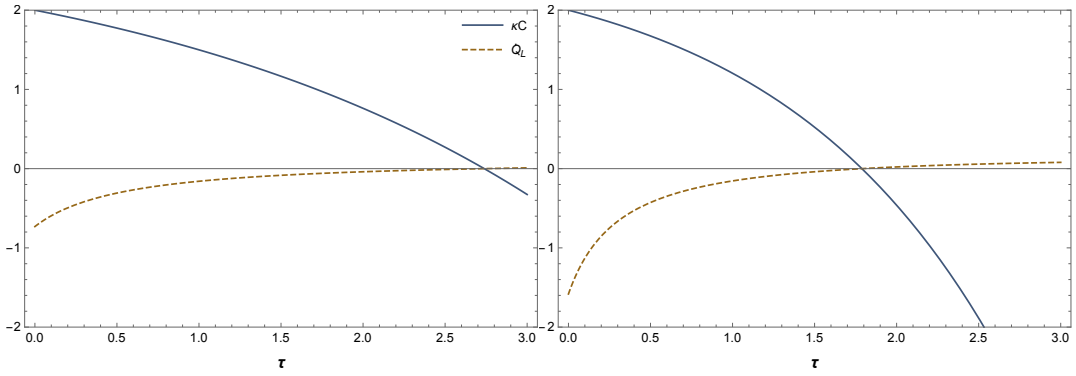

(a) (b)

Figure 19 – Influence of the delay time on the efficiency of the heat pump. System parameter: $\Gamma_L = 1$, $\Gamma_1 = 1$, $\epsilon = 1$, $T_L = 1$, $T_R = 0.5$ $V = 0$ ($\eta_C = 2$). Feedback parameters: $\alpha_+^\nu = 0$, $\alpha_-^\nu = \pi/2$. (a) Fermionic reservoirs, (a) Bosonic reservoirs.

Let us try and figure out what happens when the delay time is finite. In the figure 19, maintaining the maximum efficiency parameters, we see how the delay time decreases the efficiency of the heat pump, as well as the heat flow transferred to the hotter reservoir, for both, fermionic and bosonic reservoirs respectively. It was assumed that all possible control operations have the same delay time $\tau = \tau_\pm^\nu$ and there is not potential difference $V = 0$. For $\tau = 0$ the efficiency is maximum $\kappa_C = \frac{1}{\eta_C}$, as expected, regardless of the type of reservoir. For small τ the transfer of heat to the hotter reservoir is higher when the reservoirs are bosonic, however, this heat exchange survives for longer delay times in the fermionic case. It can be seen that for a specific τ, the machine ceases to function as a heat pump, since the direction of the heat transfer changes its direction $\dot{Q}_L \geq 0$, at the moment when the coefficient of efficiency is zero.

An exponential decay occurs in the behavior of the energy and entropy fluxes injected by the feedback, as shown in the figure 20. The reason is that longer delay times imply fewer control operations implemented, by the “control-skipping assumption”.

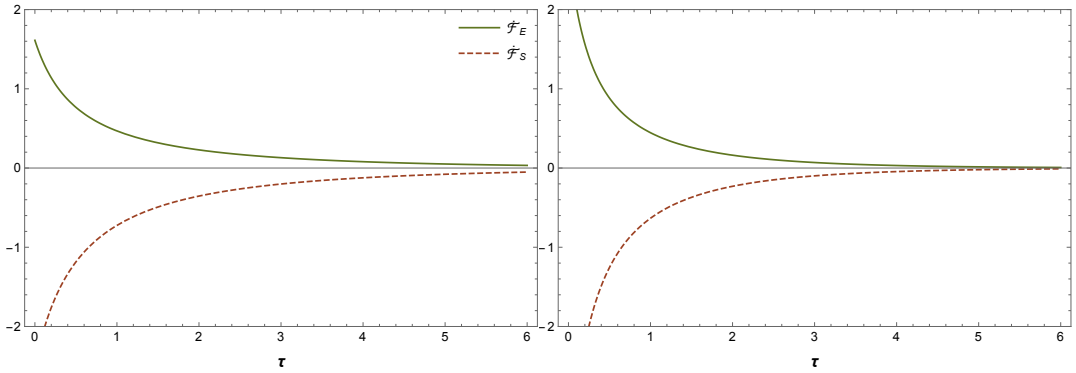

(a) (b)

Figure 20 – Influence of the delay time on feedback and entropy fluxes. The parameters are the same as the figure 19 (a) Fermionic reservoirs, (a) Bosonic reservoirs.

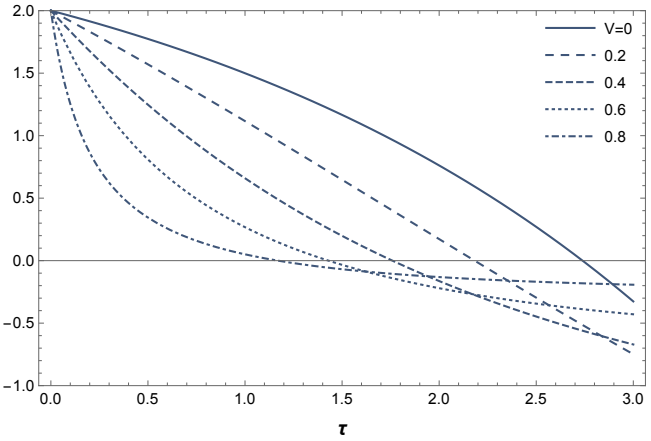

Figure 21 – Influence of potential difference on efficiency of fermionic heat pump. The parameters are again the same as the figure 19 but varying V.

In the case of fermionic reservoirs, it is interesting to see how the efficiency of the heat pump is affected when we vary the chemical potential difference between the reservoirs. In the figure 21 one can observe that when the potential difference increases, the process reduces its efficiency more quickly, as delay times grow, which is somehow expected because the negative heat transfer goes against the temperature difference, as well as the potential difference in the reservoirs. In other words, a positive potential difference is an additional barrier to the heat flow provided to the hotter reservoir. In fact, the heat flow is maximized when the

delay time and potential difference are close to zero, as shown in the figure 22.

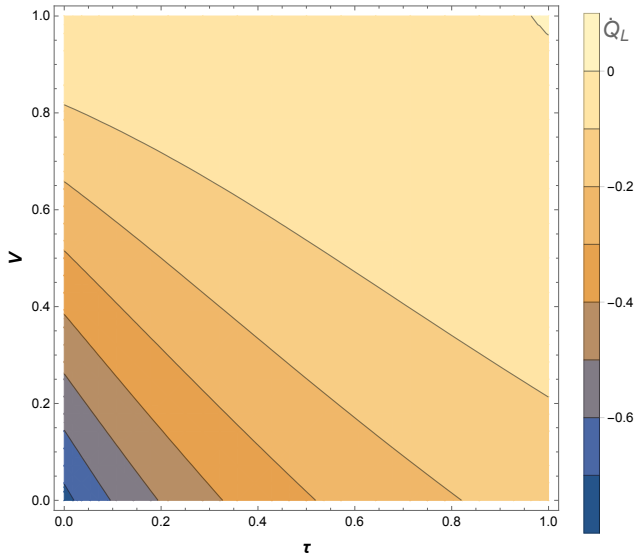

Figure 22 – Influence of potential difference and time delay on heat flux. The parameters are the same as the figure 19 but varying V.

5.5 Purification of quantum states

The quantum states of open systems become mixed when they interact with their environment (see figure 15). Some quantum feedback protocols have been effective in keeping pure the states in open quantum systems. Poltl et al. [Pöltl, Emary e Brandes 2011] applied the Wiseman-Milburn feedback to purify the states of a two quantum point system between two reservoirs, at zero temperature in the high-bias limit; and they analyze the Full Counting Statistics of the electron transport. Strasberg et al. [Strasberg et al. 2013] applied the same feedback protocol to purify the states of a qubit coupled to two phonon reservoirs. They analyze the thermodynamics of the transport system with reservoirs at finite temperature. We extend these analyzes by studying the application of the Wiseman-Milburn feedback to the purification of quantum states in a quantum dot coupled to two electron reservoirs, and we extend the analysis of the Full Counting Statistics to finite temperatures. The control operation is chosen to point

to the following target pure state

$$\rho_{target} = \begin{pmatrix} \cos^2\alpha & i\cos\alpha\sin\alpha \\ -i\cos\alpha\sin\alpha & \sin^2\alpha \end{pmatrix}. \tag{5.39}$$

This state is in a general representation of a pure qubit in terms of the polar angle with constant azimuthal angle, in the Bloch sphere. With the choice of the control parameters $\alpha_+^\nu = \alpha$, $\alpha_-^\nu = \alpha + \pi/2$ (see equation 5.16), all possible jumps will point to the target state

$$\mathcal{C}_+^\nu \mathcal{J}_+^\nu |0\rangle\rangle = \rho_{target}, \qquad \mathcal{C}_-^\nu \mathcal{J}_-^\nu |1\rangle\rangle = \rho_{target}. \tag{5.40}$$

It is possible to know how far away is any state ρ from the target state ρ_{target}, using the *trace distance* defined by:

$$\mathcal{D}(\rho, \rho_{target}) = \frac{1}{2}\,\mathrm{tr}\sqrt{(\rho - \rho_{target})^2} = \frac{1}{2}\sum_i |\lambda_i| \tag{5.41}$$

where $|\lambda_i|$ are the eigenvalues of $\rho - \rho_{target}$. $\mathcal{D}$ varies between 0 and 1, being $\mathcal{D} = 0$ the value for indistinguishable states.

In the figure 23 we evaluate the numerical exploration of $\mathcal{D}$, as a measurement of purification, for the variation of the feedback parameter α. In the reference [Strasberg et al. 2013] it had already been inferred, for the bosonic system, that at high temperatures ($\beta \to 0$) the purification is always reached for arbitrary α (see figure 23 (b)). For the fermionic system, such purification is not always reached even at high temperatures (see figure 23 (a)). Nevertheless, for both cases, the feedback achieves the purification with the parameter $\alpha = \pi/2$, at any temperature. In the figure 23 (c),(d) it is shown the behaviour of some specific values of the parameter α.

In the figure 24 we estimate the variation of the thermodynamic quantities corresponding to the energy and entropy fluxes, for different temperature values. From this we emphasize that, for the feedback parameter $\alpha = \pi/4$, the fluxes disappear, which indicates that the control operation generates an equilibrium steady state, where the fluxes and currents are balanced by canceling each other out. This is why the feedback protocol cannot function as a Maxwell daemon, since if the energy injected into the system disappears, so will the injected entropy.

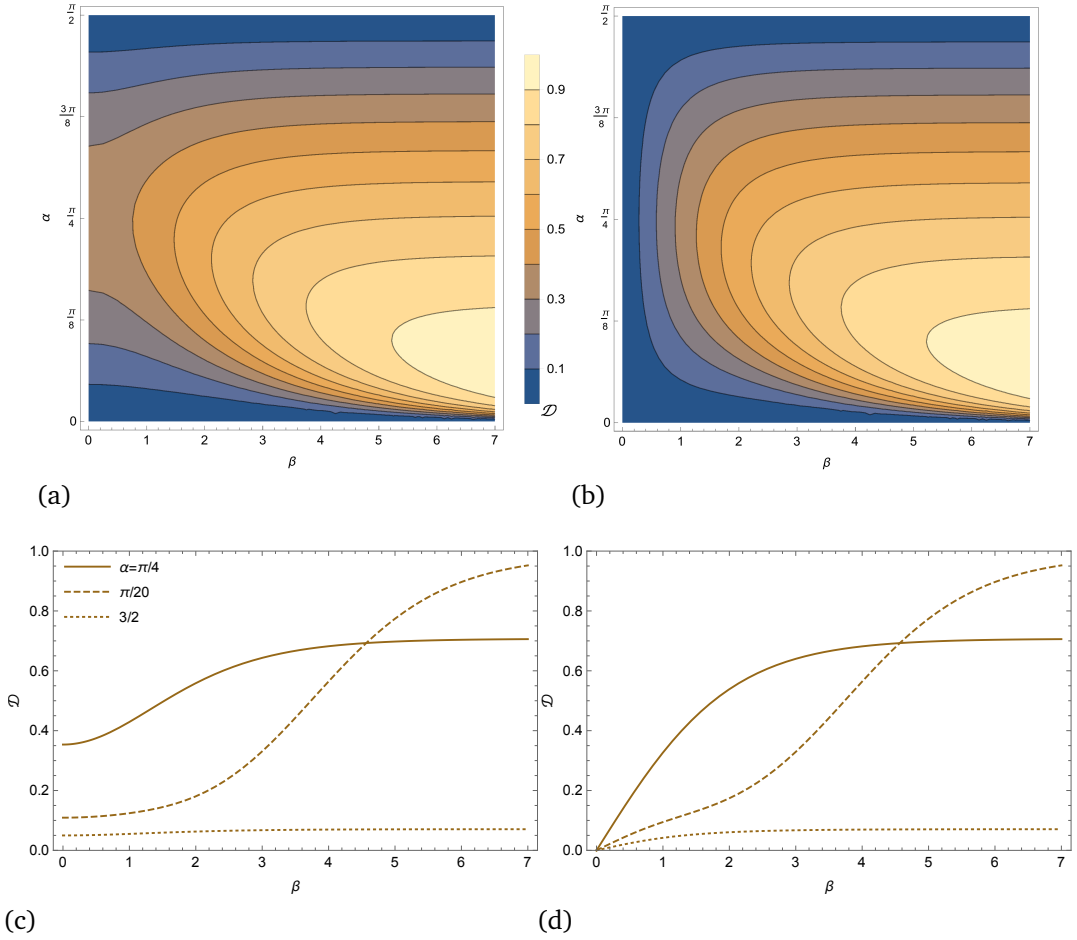

Figure 23 – Trace distance between the quantum states and the target state. To the left the fermionic system and to the right the bosonic system. Below some specific values of the feedback parameters α referenced in the figure. System parameters: $\Gamma_L = 1$, $\Gamma_R = 1$, $V = 0$, $\beta = \beta_L = \beta_R$. Feedback parameters: $\alpha_+^\nu = \alpha$, $\alpha_-^\nu = \alpha + \pi/2$.

On the other hand, the analysis of the Full Counting Statistics (see figure 25) shows that Fano factors converge to the unity when the states reach the purity, that is, when the feedback parameter is $\alpha = \pi/2$. In this parameter, the target state is pure and without coherences (see equation 5.39). So, in the same way that the heat pump, it is expected that the states obey a classical statistic, with a Poisson cumulant generating function.

Knowing the signature of a specific operation on the full counting statistics,

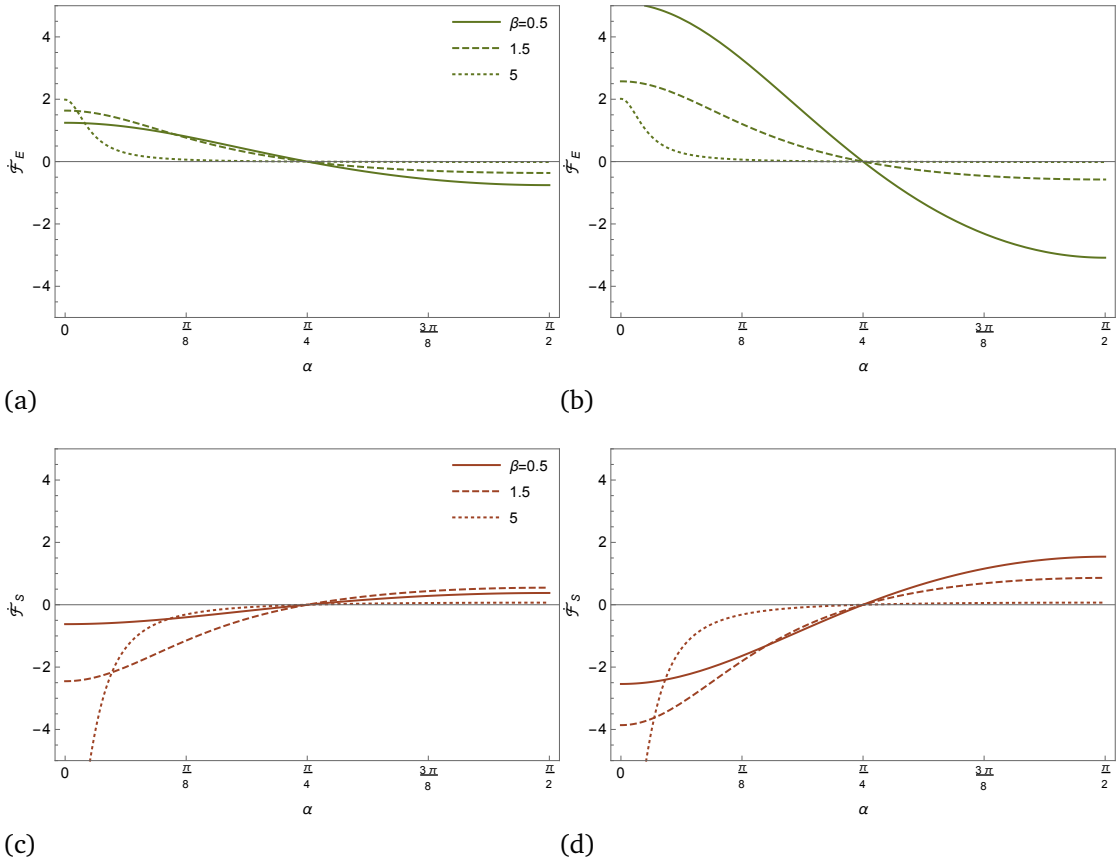

Figure 24 – Variation of the feedback entropy fluxes with respect to the feedback parameter α, for some values of $\beta = \beta_L = \beta_R$ referenced in the graph. To the left the fermionic system and to the right the bosonic system. System and feedback parameters are the same as the figure 23.

can be useful experimentally to tune the parameters of the operation by comparison with the signature [Pöltl, Emary e Brandes 2011]. In the case of a Poissonian process, the signature corresponds to the convergence of the Fano factors to unity, however other signatures of other statistics of possible transport systems can be compared, taking advantage of the fact that high orders in counting statistics are nowadays experimentally accessible [Flindt et al. 2009].

As can be seen from the equation 5.22, it is also possible to stabilize coherent quantum states with an adequate choice of feedback parameters. The question arises whether it is possible to purify such states. The answer given by

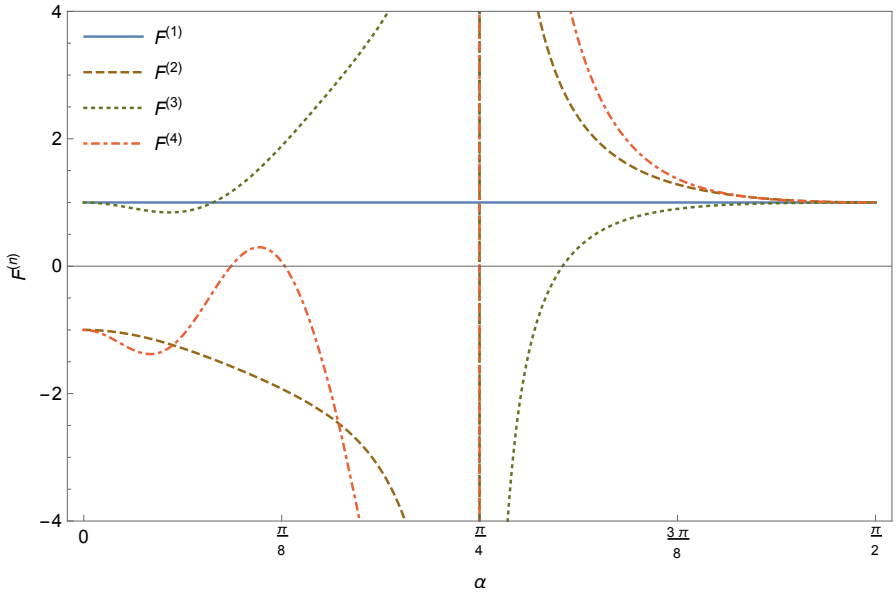

Figure 25 – Variation of the Fano factors with respect to the feedback parameter α, for $\beta_L = \beta_R = 1$. System and feedback parameters are the same as the figure 23.

Strasberg [Strasberg et al. 2013] is affirmative for high temperatures, insofar as, when the temperature of the reservoirs rises, the action of feedback also increases due to the increasing frequency and detection of jumps, which generates a more intensive purification process. We do not expect the transport statistics in these cases to be Poissonian since the states are not classical, however, the study of the statistics of such quantum states is of special interest and will be addressed in future work.

6 SUMMARY AND CONCLUSIONS

In the first part of the Thesis, we employed random-matrix theory and matrix-valued Brownian motion models to study two classes of superconducting quantum chains. In the continuum dot-wire limit, we find an exact description of the crossover in thermal conduction between a superconducting chaotic ballistic cavity (a quantum dot) and a disordered multichannel superconducting quantum wire. We obtained exact expressions for the first three moments of the heat conductance of two classes of superconducting dot-wire systems with time-reversal symmetry. The analytic solution describes in detail various types of smooth transitions as a function of the systems' length, which include ballistic-metallic and metallic-insulating transitions. Interestingly, in the single channel case, if the system is realized experimentally as a topological superconductor, we can interpret the total suppression of the insulating regime in class DIII as a signature of the presence of condensed matter Majorana fermions. The results were contrasted with those already known in the literature for normal class AI.

In the second part of the Thesis, we made a comparative analysis of non-equilibrium stochastic thermodynamics of a qubit system coupled to two reservoirs, fermionic and bosonic respectively; subjected to a Wiseman-Milburn quantum delayed feedback. Two concrete applications of the feedback were studied: the implementation of a heat pump and the purification of the system states. The extension of these applications to a fermionic transport system (a quantum point of a level coupled to two electron reservoirs) was studied, showing the influence of increasing delay times on the efficiency of the heat pump, with respect to what is reported in the literature for a bosonic transport system (a two-level system coupled to two phonon reservoirs). The differences between applying the purification protocol in the fermionic system and the bosonic system, with zero delay times, were reported. In both applications, the Full Counting Statistics analysis leaves a Poissonian statistics signature, when the tasks achieve their highest performance, i.e., when the heat pump reaches its maximum efficiency, and when the purification process is achieved.

REFERENCES

ABRAHAMS, E. et al. Scaling theory of localization: Absence of quantum diffusion in two dimensions. *Physical Review Letters*, APS, v. 42, n. 10, p. 673, 1979. Citado 2 vezes nas páginas 25 and 26.

ALTLAND, A.; ZIRNBAUER, M. R. Nonstandard symmetry classes in mesoscopic normal-superconducting hybrid structures. *Physical Review B*, APS, v. 55, n. 2, p. 1142, 1997. Citado 2 vezes nas páginas 37 and 52.

ALTSHULER, B. Fluctuations in the extrinsic conductivity of disordered conductors. *JETP lett*, v. 41, n. 12, p. 648–651, 1985. Citado na página 21.

ANDERSON, P. W. Absence of diffusion in certain random lattices. *Physical review*, APS, v. 109, n. 5, p. 1492, 1958. Citado na página 25.

ASHCROFT, N. W.; MERMIN, N. D. *Solid state physics*. [S.l.]: New York: Holt, Rinehart and Winston., 1976. Citado 2 vezes nas páginas 22 and 23.

AVRON, J. E.; OSADCHY, D.; SEILER, R. A topological look at the quantum hall effect. *Physics today*, American Institute of Physics, v. 56, n. 8, p. 38–42, 2003. Citado na página 32.

BARANGER, H. U.; MELLO, P. A. Mesoscopic transport through chaotic cavities: A random s-matrix theory approach. *Physical review letters*, APS, v. 73, n. 1, p. 142, 1994. Citado na página 36.

BATEMAN, H.; ERDELYI, A. *Higher transcendental functions*. [S.l.]: McGraw-Hill New York, 1953. Citado na página 135.

BEENAKKER, C. Quantum transport in semiconductor-superconductor microjunctions. *Physical Review B*, APS, v. 46, n. 19, p. 12841, 1992. Citado na página 30.

BEENAKKER, C. Andreev billiards. In: *Quantum Dots: a Doorway to Nanoscale Physics*. [S.l.]: Springer, 2005. p. 131–174. Citado 2 vezes nas páginas 30 and 31.

BEENAKKER, C. et al. Random-matrix theory of andreev reflection from a topological superconductor. *Physical Review B*, APS, v. 83, n. 8, p. 085413, 2011. Citado na página 30.

BEENAKKER, C.; HOUTEN, H. van. Quantum transport in semiconductor nanostructures. In: *Solid state physics*. [S.l.]: Elsevier, 1991. v. 44, p. 1–228. Citado na página 13.

BEENAKKER, C. W. J. Random-matrix theory of quantum transport. *Reviews of modern physics*, APS, v. 69, n. 3, p. 731, 1997. Citado 6 vezes nas páginas 22, 33, 36, 41, 52, and 55.

BEENAKKER, C. W. J. Random-matrix theory of majorana fermions and topological superconductors. *Reviews of Modern Physics*, APS, v. 87, n. 3, p. 1037, 2015. Citado 5 vezes nas páginas 32, 37, 38, 53, and 55.

BERGMANN, G. Localization in thin films—a time-of-flight-experiment with conduction electrons. *Physica B+ C*, Elsevier, v. 126, n. 1-3, p. 229–234, 1984. Citado na página 25.

BERKOLAIKO, G.; KUIPERS, J. Universality in chaotic quantum transport: The concordance between random-matrix and semiclassical theories. *Physical Review E*, APS, v. 85, n. 4, p. 045201, 2012. Citado na página 53.

BLANTER, Y. M.; BÜTTIKER, M. Shot noise in mesoscopic conductors. *Physics reports*, Elsevier, v. 336, n. 1-2, p. 1–166, 2000. Citado 3 vezes nas páginas 16, 29, and 68.

BRAGGIO, A.; KÖNIG, J.; FAZIO, R. Full counting statistics in strongly interacting systems: non-markovian effects. *Physical review letters*, APS, v. 96, n. 2, p. 026805, 2006. Citado na página 68.

BRANDES, T. Feedback control of quantum transport. *Physical review letters*, APS, v. 105, n. 6, p. 060602, 2010. Citado na página 83.

BREUER, H.-P.; PETRUCCIONE, F. et al. *The theory of open quantum systems*. [S.l.]: Oxford University Press on Demand, 2002. Citado 2 vezes nas páginas 68 and 75.

BROECK, C. Van den; ESPOSITO, M. Ensemble and trajectory thermodynamics: A brief introduction. *Physica A: Statistical Mechanics and its Applications*, Elsevier, v. 418, p. 6–16, 2015. Citado 3 vezes nas páginas 89, 100, and 104.

BROUWER, P. et al. Delocalization in coupled one-dimensional chains. *Physical review letters*, APS, v. 81, n. 4, p. 862, 1998. Citado na página 42.

BROUWER, P. W. On the random-matrix theory of quantum transport. *Leiden, Universität, Diss*, 1997. Citado 4 vezes nas páginas 17, 33, 39, and 40.

BROUWER, P. W.; ALTLAND, A. Anderson localization from classical trajectories. *Physical Review B*, APS, v. 78, n. 7, p. 075304, 2008. Citado na página 53.

BROUWER, P. W. et al. Localization and delocalization in dirty superconducting wires. *Physical review letters*, APS, v. 85, n. 5, p. 1064, 2000. Citado 3 vezes nas páginas 42, 55, and 63.

BROUWER, P. W. et al. Disorder-induced critical phenomena–new universality classes in anderson localization. *arXiv preprint cond-mat/0511622*, 2005. Citado na página 43.

BURGOS, M. The measurement problem in quantum mechanics revisited. In: *Selected Topics in Applications of Quantum Mechanics*. [S.l.]: InTech, 2015. Citado na página 12.

BUSTAMANTE, C.; LIPHARDT, J.; RITORT, F. The nonequilibrium thermodynamics of small systems. *arXiv preprint cond-mat/0511629*, 2005. Citado 2 vezes nas páginas 89 and 104.

CALOGERO, F. Calogero-Moser system. *Scholarpedia*, v. 3, n. 8, p. 7216, 2008. Revision #91096. Citado na página 47.

CARMICHAEL, H. *An open systems approach to quantum optics: lectures presented at the Université Libre de Bruxelles, October 28 to November 4, 1991*. [S.l.]: Springer Science & Business Media, 2009. Citado na página 87.

CASELLE, M. A new classification scheme for random matrix theories. *arXiv preprint cond-mat/9610017*, 1996. Citado na página 52.

CASELLE, M.; MAGNEA, U. Random matrix theory and symmetric spaces. *Physics reports*, Elsevier, v. 394, n. 2-3, p. 41–156, 2004. Citado na página 35.

CROOKS, G. E. Entropy production fluctuation theorem and the nonequilibrium work relation for free energy differences. *Physical Review E*, APS, v. 60, n. 3, p. 2721, 1999. Citado 2 vezes nas páginas 93 and 104.

DAHLHAUS, J. P. *Random-matrix theory and stroboscopic models of topological insulators and superconductors*. [S.l.]: Lorentz Institute, Faculty of Science, Leiden University, 2012. Citado na página 53.

DAHLHAUS, J. P.; BÉRI, B.; BEENAKKER, C. W. J. Random-matrix theory of thermal conduction in superconducting quantum dots. *Physical Review B*, APS, v. 82, n. 1, p. 014536, 2010. Citado 4 vezes nas páginas 30, 54, 55, and 63.

DATTA, S. *Electronic transport in mesoscopic systems*. [S.l.]: Cambridge university press, 1997. Citado 3 vezes nas páginas 27, 28, and 53.

DENNERY, P.; KRZYWICKI, A. *Mathematics for physicists*. [S.l.]: Courier Corporation, 2012. Citado na página 45.

DOROKHOV, O. Transmission coefficient and the localization length of an electron in n bound disordered chains. *JETP Lett*, v. 36, n. 7, p. 318–321, 1982. Citado na página 42.

DUARTE-FILHO, G.; MACEDO-JUNIOR, A.; MACÊDO, A. Circuit theory and full counting statistics of charge transfer through mesoscopic systems: A random-matrix approach. *Physical Review B*, APS, v. 76, n. 7, p. 075342, 2007. Citado na página 55.

DYSON, F. J. The dynamics of a disordered linear chain. *Physical Review*, APS, v. 92, n. 6, p. 1331, 1953. Citado 2 vezes nas páginas 43 and 63.

EDWARDS, J.; THOULESS, D. Numerical studies of localization in disordered systems. *Journal of Physics C: Solid State Physics*, IOP Publishing, v. 5, n. 8, p. 807, 1972. Citado na página 25.

EFETOV, K. *Supersymmetry in disorder and chaos*. [S.l.]: Cambridge University Press, 1999. Citado na página 53.

ELLIOTT, S. R.; FRANZ, M. Colloquium: Majorana fermions in nuclear, particle, and solid-state physics. *Reviews of Modern Physics*, APS, v. 87, n. 1, p. 137, 2015. Citado 3 vezes nas páginas 31, 32, and 53.

EMARY, C. *Theory of Nanostructures*. [S.l.]: New york: Wiley, 2009. Citado 2 vezes nas páginas 23 and 27.

EMARY, C. Self-consistent electron counting statistics. *Journal of Physics: Condensed Matter*, IOP Publishing, v. 23, n. 2, p. 025304, 2010. Citado na página 68.

EMARY, C. Delayed feedback control in quantum transport. *Phil. Trans. R. Soc. A*, The Royal Society, v. 371, n. 1999, p. 20120468, 2013. Citado na página 87.

EMARY, C. Feedback control in quantum transport. In: *Control of Self-Organizing Nonlinear Systems*. [S.l.]: Springer, 2016. p. 275–287. Citado na página 83.

ESPOSITO, M.; HARBOLA, U.; MUKAMEL, S. Nonequilibrium fluctuations, fluctuation theorems, and counting statistics in quantum systems. *Reviews of modern physics*, APS, v. 81, n. 4, p. 1665, 2009. Citado 3 vezes nas páginas 80, 82, and 104.

ESPOSITO, M.; MUKAMEL, S. Fluctuation theorems for quantum master equations. *Physical Review E*, APS, v. 73, n. 4, p. 046129, 2006. Citado 2 vezes nas páginas 89 and 94.

ESPOSITO, M.; SCHALLER, G. Stochastic thermodynamics for "maxwell demon" feedbacks. *EPL (Europhysics Letters)*, IOP Publishing, v. 99, n. 3, p. 30003, 2012. Citado na página 109.

EVANS, D. J.; COHEN, E. G. D.; MORRISS, G. P. Probability of second law violations in shearing steady states. *Physical review letters*, APS, v. 71, n. 15, p. 2401, 1993. Citado na página 104.

EVANS, D. J.; SEARLES, D. J. The fluctuation theorem. *Advances in Physics*, Taylor & Francis, v. 51, n. 7, p. 1529–1585, 2002. Citado na página 104.

EVERS, F.; MIRLIN, A. D. Anderson transitions. *Reviews of Modern Physics*, APS, v. 80, n. 4, p. 1355, 2008. Citado na página 25.

FLINDT, C. et al. Universal oscillations in counting statistics. *Proceedings of the National Academy of Sciences*, National Acad Sciences, v. 106, n. 25, p. 10116–10119, 2009. Citado na página 118.

FULGA, I. C. et al. *Scattering theory of topological phase transitions*. [S.l.]: Lorentz Institute, Faculty of Science, Leiden University, 2013. Citado na página 44.

FUNO, K.; QUAN, H. Path integral approach to quantum thermodynamics. *Physical review letters*, APS, v. 121, n. 4, p. 040602, 2018. Citado 2 vezes nas páginas 13 and 89.

GALLAVOTTI, G.; COHEN, E. G. D. Dynamical ensembles in nonequilibrium statistical mechanics. *Physical Review Letters*, APS, v. 74, n. 14, p. 2694, 1995. Citado na página 93.

GARRIGUES, A. R. et al. A single-level tunnel model to account for electrical transport through single molecule-and self-assembled monolayer-based junctions. *Scientific reports*, Nature Publishing Group, v. 6, p. 26517, 2016. Citado na página 15.

GOPAR, V. A.; MUTTALIB, K.; WÖLFLE, P. Conductance distribution in disordered quantum wires: Crossover between the metallic and insulating regimes. *Physical Review B*, APS, v. 66, n. 17, p. 174204, 2002. Citado na página 42.

GRADSHTEYN, I. S.; RYZHIK, I. M. *Table of integrals, series, and products*. [S.l.]: Academic press, 2014. Citado na página 135.

GRUZBERG, I. A.; READ, N.; VISHVESHWARA, S. Localization in disordered superconducting wires with broken spin-rotation symmetry. *Physical Review B*, APS, v. 71, n. 24, p. 245124, 2005. Citado 2 vezes nas páginas 44 and 63.

GURVITZ, S.; PRAGER, Y. S. Microscopic derivation of rate equations for quantum transport. *Physical Review B*, APS, v. 53, n. 23, p. 15932, 1996. Citado 2 vezes nas páginas 68 and 106.

HAAKE, F. *Quantum signatures of chaos*. [S.l.]: Springer Science & Business Media, 2013. Citado na página 34.

HARBOLA, U.; ESPOSITO, M.; MUKAMEL, S. Quantum master equation for electron transport through quantum dots and single molecules. *Physical Review B*, APS, v. 74, n. 23, p. 235309, 2006. Citado 2 vezes nas páginas 75 and 106.

HARBOLA, U.; ESPOSITO, M.; MUKAMEL, S. Statistics and fluctuation theorem for boson and fermion transport through mesoscopic junctions. *Physical Review B*, APS, v. 76, n. 8, p. 085408, 2007. Citado na página 106.

HOUTEN, H. van; BEENAKKER, C. Quantum point contacts. *arXiv preprint cond-mat/0512609*, 2005. Citado 2 vezes nas páginas 13 and 15.

IIDA, S.; WEIDENMÜLLER, H.; ZUK, J. Statistical scattering theory, the supersymmetry method and universal conductance fluctuations. *Annals of Physics*, Elsevier, v. 200, n. 2, p. 219–270, 1990. Citado na página 55.

JALABERT, R.; PICHARD, J.-L.; BEENAKKER, C. Universal quantum signatures of chaos in ballistic transport. *EPL (Europhysics Letters)*, IOP Publishing, v. 27, n. 4, p. 255, 1994. Citado na página 36.

JAMES, M. R.; NURDIN, H. I. A tutorial introduction to quantum feedback control. In: IEEE. *Control Applications (CCA), 2015 IEEE Conference on*. [S.l.], 2015. p. 1–12. Citado 2 vezes nas páginas 83 and 84.

JARZYNSKI, C. Nonequilibrium equality for free energy differences. *Physical Review Letters*, APS, v. 78, n. 14, p. 2690, 1997. Citado 2 vezes nas páginas 93 and 104.

KELLER, M. W. et al. Energy-averaged weak localization in chaotic microcavities. *Physical Review B*, APS, v. 53, n. 4, p. R1693, 1996. Citado 2 vezes nas páginas 16 and 17.

KHALAF, E. Mesoscopic phenomena in topological insulators, superconductors and semimetals. 2017. Citado 3 vezes nas páginas 20, 24, and 32.

KITAEV, A. Y. Unpaired majorana fermions in quantum wires. *Physics-Uspekhi*, IOP Publishing, v. 44, n. 10S, p. 131, 2001. Citado na página 32.

KONDEPUDI, D.; PRIGOGINE, I. *Modern thermodynamics: from heat engines to dissipative structures*. [S.l.]: John Wiley & Sons, 2014. Citado na página 89.

KRAUS, K. *States, effects and operations: fundamental notions of quantum theory*. [S.l.]: Springer, 1983. Citado na página 69.

KULIK, I.; SHEKHTER, R. Kinetic phenomena and charge-discreteness effects in granulated media. *Zhur. Eksper. Teoret. Fiziki*, v. 68, n. 2, p. 623–640, 1975. Citado na página 68.

LEBON, G.; JOU, D.; CASAS-VÁZQUEZ, J. *Understanding non-equilibrium thermodynamics*. [S.l.]: Springer, 2008. Citado 2 vezes nas páginas 89 and 91.

LEE, P.; STONE, A. D.; FUKUYAMA, H. Universal conductance fluctuations in metals: Effects of finite temperature, interactions, and magnetic field. *Physical Review B*, APS, v. 35, n. 3, p. 1039, 1987. Citado 2 vezes nas páginas 26 and 27.

LEE, P. A.; STONE, A. D. Universal conductance fluctuations in metals. *Physical review letters*, APS, v. 55, n. 15, p. 1622, 1985. Citado na página 21.

LINDBLAD, G. On the generators of quantum dynamical semigroups. *Communications in Mathematical Physics*, Springer, v. 48, n. 2, p. 119–130, 1976. Citado na página 70.

MACÊDO, A.; CHALKER, J. et al. Effects of spin-orbit interactions in disordered conductors: A random-matrix approach. *Physical Review B*, APS, v. 46, n. 23, p. 14985, 1992. Citado na página 42.

MACÊDO, A. M. S. Quantum dot to disordered wire crossover: A complete solution in all length scales for systems with unitary symmetry. *Physical Review B*, APS, v. 61, n. 7, p. 4453, 2000. Citado 4 vezes nas páginas 55, 56, 59, and 60.

MACÊDO, A. M. S. Nonanalytic scaling of conductance cumulants in dirty superconducting wires. *Physical Review B*, APS, v. 65, n. 13, p. 132510, 2002. Citado na página 65.

MACEDO-JUNIOR, A.; MACÊDO, A. Universal transport properties of quantum dots with chiral symmetry. *Physical Review B*, APS, v. 66, n. 4, p. 041307, 2002. Citado na página 38.

MACEDO-JUNIOR, A. F. Transporte em nanoestruturas: métodos de movimento browniano e teoria de circuitos. Universidade Federal de Pernambuco, 2006. Citado 2 vezes nas páginas 49 and 50.

MACEDO-JUNIOR, A. F.; MACÊDO, A. Brownian-motion ensembles of random matrix theory: A classification scheme and an integral transform method. *Nuclear Physics B*, Elsevier, v. 752, n. 3, p. 439–475, 2006. Citado 7 vezes nas páginas 18, 44, 47, 56, 57, 58, and 60.

MACEDO-JUNIOR, A. F.; MACÊDO, A. M. Quantum transport: A unified approach via a multivariate hypergeometric generating function. *International Journal of Modern Physics B*, World Scientific, v. 28, n. 26, p. 1450178, 2014. Citado na página 53.

MACEDO-JUNIOR, A. F.; MACÊDO, A. M. S. Brownian-motion ensembles: correlation functions of determinantal processes. *Journal of Physics A: Mathematical and Theoretical*, IOP Publishing, v. 41, n. 1, p. 015004, 2007. Citado 4 vezes nas páginas 44, 49, 57, and 135.

MAJORANA, E. Teoria simmetrica dell'elettrone e del positrone. *Il Nuovo Cimento (1924-1942)*, Springer, v. 14, n. 4, p. 171, 1937. Citado na página 32.

MATHAI, A. M.; SAXENA, R. K.; HAUBOLD, H. J. *The H-function: theory and applications*. [S.l.]: Springer Science & Business Media, 2009. Citado na página 135.

MEHTA, M. L. *Random matrices*. [S.l.]: Elsevier, 2004. Citado na página 34.

MELLO, P.; PEREYRA, P.; KUMAR, N. Macroscopic approach to multichannel disordered conductors. *Annals of Physics*, Elsevier, v. 181, n. 2, p. 290–317, 1988. Citado na página 42.

MELLO, P. A. et al. *Quantum transport in mesoscopic systems: complexity and statistical fluctuations, a maximum-entropy viewpoint*. [S.l.]: Oxford University Press on Demand, 2004. Citado 3 vezes nas páginas 13, 20, and 21.

MIRLIN, A. D.; MULLERGROELING, A.; ZIRNBAUER, M. R. Conductance fluctuations of disordered wires: Fourier analysis on supersymmetric spaces. *Annals of Physics*, Elsevier, v. 236, n. 2, p. 325–373, 1994. Citado na página 65.

MORIMOTO, T.; FURUSAKI, A.; MUDRY, C. Anderson localization and the topology of classifying spaces. *Physical Review B*, APS, v. 91, n. 23, p. 235111, 2015. Citado na página 63.

MOTRUNICH, O.; DAMLE, K.; HUSE, D. A. Griffiths effects and quantum critical points in dirty superconductors without spin-rotation invariance: One-dimensional examples. *Physical Review B*, APS, v. 63, n. 22, p. 224204, 2001. Citado 2 vezes nas páginas 43 and 63.

MUDRY, C. Fractional abelian topological phases of matter for fermions in two-dimensional space. *Topological Aspects of Condensed Matter Physics: Lecture Notes of the Les Houches Summer School: Volume 103, August 2014*, Oxford University Press, v. 103, p. 265, 2017. Citado 2 vezes nas páginas 44 and 63.

MUTTALIB, K.; GOPAR, V. A. Generalization of the dmpk equation beyond quasi one dimension. *Physical Review B*, APS, v. 66, n. 11, p. 115318, 2002. Citado na página 42.

NAZAROV, Y. V.; BLANTER, Y. M. *Quantum transport: introduction to nanoscience*. [S.l.]: Cambridge University Press, 2009. Citado na página 20.

OLVER, F. W. J. *NIST handbook of mathematical functions hardback and CD-ROM*. [S.l.]: Cambridge University Press, 2010. Citado na página 136.

PEDROSA, V. et al. Strong and weak localization in a ballistic quantum chain. *Physica Scripta*, IOP Publishing, v. 2015, n. T165, p. 014016, 2015. Citado na página 55.

PÖLTL, C.; EMARY, C.; BRANDES, T. Feedback stabilization of pure states in quantum transport. *Physical Review B*, APS, v. 84, n. 8, p. 085302, 2011. Citado 3 vezes nas páginas 83, 115, and 118.

RICHTER, K.; SIEBER, M. Semiclassical theory of chaotic quantum transport. *Physical review letters*, APS, v. 89, n. 20, p. 206801, 2002. Citado na página 53.

RITORT, F. Work fluctuations, transient violations of the second law and free-energy recovery methods: Perspectives in theory and experiments. In: SPRINGER. *Poincaré Seminar 2003*. [S.l.], 2004. p. 193–226. Citado na página 104.

SCHALLER, G. Non-equilibrium master equations. *Vorlesung gehalten im Rahmen des GRK*, v. 1558, p. 5, 2014. Citado 3 vezes nas páginas 70, 71, and 73.

SCHALLER, G. *Open quantum systems far from equilibrium*. [S.l.]: Springer, 2014. Citado na página 80.

SCHLOSSHAUER, M. Decoherence, the measurement problem, and interpretations of quantum mechanics. *Reviews of Modern physics*, APS, v. 76, n. 4, p. 1267, 2005. Citado na página 12.

SCHOELLER, H. A perturbative nonequilibrium renormalization group method for dissipative quantum mechanics. *The European Physical Journal Special Topics*, Springer, v. 168, n. 1, p. 179–266, 2009. Citado na página 68.

SEIFERT, U. Entropy production along a stochastic trajectory and an integral fluctuation theorem. *Physical review letters*, APS, v. 95, n. 4, p. 040602, 2005. Citado na página 99.

SEIFERT, U. Stochastic thermodynamics, fluctuation theorems and molecular machines. *Reports on progress in physics*, IOP Publishing, v. 75, n. 12, p. 126001, 2012. Citado 2 vezes nas páginas 89 and 104.

SENA-JUNIOR, M.; ALMEIDA, F.; MACÊDO, A. Counting statistics and an anomalous metallic phase in a network of quantum dots. *Journal of Physics A: Mathematical and Theoretical*, IOP Publishing, v. 47, n. 23, p. 235101, 2014. Citado na página 55.

SOUZA, C. E. C.; MACEDO-JUNIOR, A. F. Quantum transport in chaotic ballistic cavity: a brownian-motion approach. *Journal of Physics A: Mathematical and Theoretical*, IOP Publishing, v. 48, n. 41, p. 415101, 2015. Citado 2 vezes nas páginas 57 and 66.

STENBERG, M. *Quantum coherence and mesoscopic fluctuations*. [S.l.]: Helsinki University of Technology, 2007. Citado na página 30.

STONE, A. D.; SZAFER, A. What is measured when you measure a resistance?—the landauer formula revisited. *IBM Journal of Research and Development*, IBM, v. 32, n. 3, p. 384–413, 1988. Citado 2 vezes nas páginas 13 and 29.

STRASBERG, P. et al. Thermodynamics of quantum-jump-conditioned feedback control. *Physical Review E*, APS, v. 88, n. 6, p. 062107, 2013. Citado 8 vezes nas páginas 83, 87, 103, 104, 111, 115, 116, and 119.

TALKNER, P.; HÄNGGI, P. Aspects of quantum work. *Physical Review E*, APS, v. 93, n. 2, p. 022131, 2016. Citado na página 13.

WEES, B. V. et al. Quantized conductance of point contacts in a two-dimensional electron gas. *Physical Review Letters*, APS, v. 60, n. 9, p. 848, 1988. Citado na página 14.

WHARAM, D. et al. One-dimensional transport and the quantisation of the ballistic resistance. *Journal of Physics C: solid state physics*, IOP Publishing, v. 21, n. 8, p. L209, 1988. Citado na página 14.

WHITNEY, R. S. Staying positive: going beyond lindblad with perturbative master equations. *Journal of Physics A: Mathematical and Theoretical*, IOP Publishing, v. 41, n. 17, p. 175304, 2008. Citado na página 74.

Wikipedia contributors. *Drude model — Wikipedia, The Free Encyclopedia*. 2018. [Online; accessed 6-March-2019]. Disponível em: <https://en.wikipedia.org/w/index.php?title=Drude_model&oldid=860257308>. Citado na página 23.

WISEMAN, H. Quantum theory of continuous feedback. *Physical Review A*, APS, v. 49, n. 3, p. 2133, 1994. Citado na página 83.

WISEMAN, H. M.; MILBURN, G. J. *Quantum measurement and control*. [S.l.]: Cambridge university press, 2009. Citado na página 83.

Wolfram Research, Inc. *Mathematica*. Disponível em: <https://www.wolfram.com>. Citado na página 137.

ZEDLER, P. Master equations in transport statistics: Success and failure of non-markovian and higher order corrections. 2011. Citado na página 68.

ZHANG, J. et al. Quantum feedback: theory, experiments, and applications. *Physics Reports*, Elsevier, v. 679, p. 1–60, 2017. Citado 2 vezes nas páginas 83 and 104.

ZIRNBAUER, M. R. Symmetry classes. *arXiv preprint arXiv:1001.0722*, 2010. Citado na página 37.

APPENDIX A – INITIAL CONDITION: THE ANDREEV QUANTUM DOT

The generating function of the Andreev quantum dot can be calculated by means of equation (3.16) and the kernel shown in (3.17). Using the variables $\eta_0 = \frac{3+\nu_o}{1-\nu_o}$ and $\eta_1 = \frac{3+\nu_1}{1-\nu_1}$, we find the effective Hamiltonian

$$\begin{aligned}\mathcal{H} = (1-\eta_0^2)\frac{\partial^2}{\partial\eta_0^2} + (\mu - \frac{\gamma}{2} - (2+\mu+\frac{\gamma}{2})\eta_0)\frac{\partial}{\partial\eta_0} \\ -(1-\eta_1^2)\frac{\partial^2}{\partial\eta_1^2} - (\mu - \frac{\gamma}{2} - (2+\mu+\frac{\gamma}{2})\eta_1)\frac{\partial}{\partial\eta_1}.\end{aligned} \tag{A.1}$$

The stationary solution of the corresponding Fokker-Planck equation can be written in terms of the eigenfunctions of (A.1), which are Jacobi polynomials $P_n^{(a,b)}$ and Jacobi functions of the second type $Q_n^{(a,b)}$. Inserting this result into equation (3.14) we get

$$W(\{\vartheta\},0) = \left(\frac{1-\nu_o}{1-\nu_1}\right)^N \left(1 + 2^{3+2\mu+\gamma/2}\frac{(\nu_0-\nu_1)(1+\nu_1)^{\gamma/2}}{(1-\nu_0)(1-\nu_1)^{\mu+\gamma/2+1}}R\right), \tag{A.2}$$

where

$$R = \sum_{n=0}^{N-1} \frac{1}{h_n^{(\gamma/2,\mu)}} P_n^{(\gamma/2,\mu)}\left(\frac{3+\nu_o}{1-\nu_o}\right) Q_n^{(\gamma/2,\mu)}\left(\frac{3+\nu_1}{1-\nu_1}\right), \tag{A.3}$$

and

$$h_n^{(\alpha,\beta)} = \frac{2^{\alpha+\beta+1}\Gamma(n+\alpha+1)\Gamma(n+\beta+1)}{n!(2n+\alpha+\beta+1)\Gamma(n+\alpha+\beta+1)}, \tag{A.4}$$

which after some simple algebraic manipulations yields equation (3.18).

APPENDIX B – EIGENFUNCTIONS OF THE ANDREEV QUANTUM WIRE

The generating function of the Andreev quantum wire can be calculated by using equation 3.16, which can be written as

$$\mathcal{H} = (\vartheta_0^2 - 1)\frac{\partial^2}{\partial \vartheta_0^2} + 2(\nu+1)\vartheta_0\frac{\partial}{\partial \vartheta_0} - (\vartheta_1^2 - 1)\frac{\partial^2}{\partial \vartheta_1^2} - 2(\nu+1)\vartheta_1\frac{\partial}{\partial \vartheta_1}. \tag{B.1}$$

Note that the first two terms of this equation match with the operator of the Jacobi differential equation with equal parameters $P_n^{(\nu)}(\vartheta_0) \equiv P_n^{(\nu,\nu)}(\vartheta_0)$

$$\left[(\vartheta_0^2 - 1)\frac{\partial^2}{\partial \vartheta_0^2} + 2(\nu+1)\vartheta_0\frac{\partial}{\partial \vartheta_0}\right] P_n^{(\nu)}(\vartheta_0) = n(n+2\nu+1)P_n^{(\nu)}(\vartheta_0). \tag{B.2}$$

On the other hand, the last two terms of equation (B.1) match with the operator of the hypergeometric differential equation for $F_k^{(\nu)}(\vartheta_1)$

$$\left[-(\vartheta_1^2 - 1)\frac{\partial^2}{\partial \vartheta_1^2} - 2(\nu+1)\vartheta_1\frac{\partial}{\partial \vartheta_1}\right] F_k^{(\nu)}(\vartheta_1) = (k^2 + \nu(\nu+1) + 1/4)F_k^{(\nu)}(\vartheta_1). \tag{B.3}$$

The orthogonality and completeness relations are respectively

$$\int_{-1}^{1} d\vartheta_0 (1-\vartheta_0^2)^\nu P_n^{(\nu)}(\vartheta_0) P_{n'}^{(\nu)}(\vartheta_0) = \delta_{nn'} h_n^{(\nu)} \tag{B.4}$$

$$\sum_{n=0}^{\infty} \frac{P_n^{(\nu)}(\vartheta_0) P_n^{(\nu)}(\vartheta_0')}{h_n^{(\nu)}} = \frac{\delta(\vartheta_0 - \vartheta_0')}{(1-\vartheta_0^2)^\nu} \tag{B.5}$$

and

$$\int_{1}^{\infty} d\vartheta_1 (\vartheta_1^2 - 1)^\nu F_k^{(\nu)}(\vartheta_1) F_{k'}^{(\nu)}(\vartheta_1) = \frac{\delta(k-k')}{(A_k^{(\nu)})^2} \tag{B.6}$$

$$\int_{0}^{\infty} dk (A_k^{(\nu)})^2 F_k^{(\nu)}(\vartheta_1) F_k^{(\nu)}(\vartheta_1') = \frac{\delta(\vartheta_1 - \vartheta_1')}{(\vartheta_1^2 - 1)^\nu}, \tag{B.7}$$

where

$$(A_k^{(\nu)})^2 = \frac{|\Gamma(\nu+1/2+ik)|^2}{2^{2\nu}(\Gamma(\nu+1))^2|\Gamma(ik)|^2} \tag{B.8}$$

Then the eigenfunctions and the eigenvalues of $\mathcal{H}$ are given by

$$\varphi_{nk}(\vartheta_0,\vartheta_1) = \frac{A_k^{(\nu)}}{(h_n^{(\nu)})^{1/2}} P_n^{(\nu)}(\vartheta_0) F_k^{(\nu)}(\vartheta_1) \quad \text{and} \quad \varepsilon_{nk} = k^2 + (n+\nu+1/2)^2 \tag{B.9}$$

with $-1 \leq \vartheta_0 \leq 1$ and $1 \leq \vartheta_0 \leq \infty$. For the calculations of the moments of the heat conductance it is convenient to replace $F_k^{(\nu)}(\vartheta_1)$ by the following function in (B.3)

$$\widetilde{F}_k^{(\nu)}(\vartheta_1) \equiv \frac{1}{\omega(\vartheta_1)} \int_0^\infty dx \frac{\omega(x) F_k^{(\nu)}(x)}{x+\vartheta_1} = \frac{1}{\omega(\vartheta_1)} |\Gamma(1/2-\nu+ik)|^2 F_k^{(-\nu)}(\vartheta_1), \tag{B.10}$$

so, the new set of eigenfunctions $\varphi_{nk}(\vartheta_0,\vartheta_1)$ correspond to the equation (3.22).

APPENDIX C – INTEGRALS OF THE ANDREEV DOT-WIRE SYSTEM

Let us now show the equivalence between equations (3.26) and (3.28). First, we calculate the integrals shown in equation (3.26). We know from [Macedo-Junior e Macêdo 2007] that

$$I_{nl}^{(0)} = \frac{(-1)^n 2^{l+2\nu+1} l!\Gamma(l+\nu+1)\Gamma(n+\nu+1)}{(l-n)!n!\Gamma(n+l+2\nu+2)}. \tag{C.1}$$

Using the identity $F(a,b;c;z) = \Gamma(1-a)\Gamma(c)P_{-a}^{(c-1,a+b-c)}(1-2z)/\Gamma(c-a)$ we can write

$$I_{nl}^{(1)} = \frac{\Gamma(1+n')\Gamma(-2n'-\mu-\nu)}{\Gamma(-n'-\mu-\nu)} \int_{-1}^{1} d\vartheta_0 (1-\vartheta_0)^{\nu+l}(1+\vartheta_0)^{\nu} P_n^{(v)}(\vartheta_0) P_{n'}^{(-2n'-\mu-\nu-1,v)}(\vartheta_0), \tag{C.2}$$

where $n' = N - l - 1$. This integral can be solved by means of equation (20) of the chapter 16.4 of [Bateman e Erdelyi 1953]. We find

$$\begin{aligned} I_{nl}^{(1)} =& \frac{2^{2\nu+l+1}\Gamma(-l+n)\Gamma(n+\nu+1)\Gamma(l+\nu+1)}{n!\Gamma(-l)\Gamma(2\nu+n+l+2)} \times \\ & {}_4F_3[-n', -n'-\mu, \nu+l+1, l+1; -2n'-\mu-\nu, 2\nu+l+n+2, -n+l+1; 1]. \end{aligned} \tag{C.3}$$

or after using $\Gamma(a-n) = (-1)^n\Gamma(-a)\Gamma(1+a)/\Gamma(n+1-a)$

$$\begin{aligned} I_{nl}^{(1)} =& (-1)^n \frac{2^{2\nu+l+1}\Gamma(l+1)\Gamma(n+\nu+1)\Gamma(l+\nu+1)}{\Gamma(n-1)\Gamma(1+l-n)\Gamma(2\nu+n+l+2)} \times \\ & {}_4F_3[-n', -n'-\mu, \nu+l+1, l+1; -2n'-\mu-\nu, 2\nu+l+n+2, -n+l+1; 1]. \end{aligned} \tag{C.4}$$

The remaining integrals can be calculated representing the hypergeometric functions as Meijer G functions by using the identity

$$F[a,b,c,z] = \frac{\Gamma(c)}{\Gamma(b)\Gamma(a)} G_{2,2}^{1,2}\left(-z \,\middle|\, \begin{matrix} 1-a, 1-b, \\ 0, 1-c \end{matrix}\right) \tag{C.5}$$

and integration identities of the Meijer G functions [Gradshteyn e Ryzhik 2014, Mathai, Saxena e Haubold 2009]. Performing the change of variables

$-x = (1-\vartheta_1)/2$ and using the identity $F[a,b;c;z] = (1-z)^{c-a-b}F[c-a,c-b;c;z]$ [Olver 2010], we get

$$\begin{aligned}
J_{kl}0 &= \frac{1}{(-1)^{l+1}2^{2\nu+l}}\int_0^\infty dx \frac{x^{-\nu-l-1}}{(x+1)^\nu} F[-\nu+1/2+ik,-\nu+1/2-ik;-\nu+1;-x] \\
&= \frac{1}{(-1)^{l+1}2^{2\nu+l}}\int_0^\infty dx \frac{F[1/2+ik,1/2-ik;-\nu+1;-x]}{x^{\nu+l+1}} \\
&= \frac{\Gamma(-\nu+1)}{(-1)^{l+1}2^{2\nu+l}|\Gamma(1/2+ik)|^2}\int_0^\infty dx \frac{G^{1,2}_{2,2}\left(x\left|\begin{smallmatrix}\frac{1}{2}+ik,\frac{1}{2}-ik,\\ 0,\nu\end{smallmatrix}\right.\right)}{x^{\nu+l+1}} \\
&= \frac{\Gamma(-\nu+1)}{(-1)^{l+1}2^{2\nu+l}|\Gamma(1/2+ik)|^2}\int_0^\infty dx G^{1,2}_{2,2}\left(x\left|\begin{smallmatrix}-\frac{1}{2}+ik-\nu-l,-\frac{1}{2}-ik-\nu-l,\\ -\nu-l-1,-\nu-1\end{smallmatrix}\right.\right) \\
&= \frac{\Gamma(-\nu+1)\Gamma(-\nu-l)|\Gamma(1/2+ik+\nu+l)|^2}{(-1)^{l+1}2^{2\nu+l}|\Gamma(1/2+ik)|^2\Gamma(l+1)} \qquad \text{(C.6)}
\end{aligned}$$

Finally, similarly to (C.6), we get

$$\begin{aligned}
J_{kl}1 =& \frac{1}{(-1)^{l+1}2^{2\nu+l}}\int_0^\infty dx \frac{x^{-\nu-l-1}}{(x+1)^\nu} F[-\nu+1/2+ik,-\nu+1/2-ik;-\nu+1;-x] \\
&\times F[n'+1,n'+1+\mu;2n'+\mu+\nu+2;-x] \\
&= \frac{\Gamma(-\nu+1)}{(-1)^{l+1}2^{2\nu+l}|\Gamma(1/2+ik)|^2}\frac{\Gamma(2n'+\mu+\nu+2)}{\Gamma(n'+1)\Gamma(n'+\mu+1)} \\
&\times \int_0^\infty dx G^{1,2}_{2,2}\left(x\left|\begin{smallmatrix}-\frac{1}{2}+ik-\nu-l,-\frac{1}{2}-ik-\nu-l,\\ -\nu-l-1,-\nu-1\end{smallmatrix}\right.\right) G^{1,2}_{2,2}\left(x\left|\begin{smallmatrix}-n',-n'-\mu,\\ 0,-2n'-\mu-\nu-1\end{smallmatrix}\right.\right) \\
&= \frac{\Gamma(-\nu+1)}{(-1)^{l+1}2^{2\nu+l}|\Gamma(1/2+ik)|^2}\frac{\Gamma(2n'+\mu+\nu+2)}{\Gamma(n'+1)\Gamma(n'+\mu+1)} \\
&\times G^{3,3}_{4,4}\left(1\left|\begin{smallmatrix}\nu+l+1,-n',-n'-\mu,l+1\\ \frac{1}{2}-ik+\nu+l,\frac{1}{2}+ik+\nu+l,0,-2n'-\mu-\nu-1\end{smallmatrix}\right.\right) \qquad \text{(C.7)}
\end{aligned}$$

Once the integrals have been obtained in terms of Meijer G functions, Theorem 1 follows from using the simple identity

$$(A_k^{(-v)})^2\sum_{l=0}^{N-1}(I_{nl}1J_{kl}1 - I_{nl}0J_{kl}0) = \frac{2P_n^{(v)}(1)|\Gamma(1/2-\nu+ik)|^2}{|\Gamma(ik)|^2\varepsilon_{nk}}c_{nk}^{(\nu)}(N_1)c_{nk}^{(\nu)}(N_2). \qquad \text{(C.8)}$$

or equivalently

$$\sum_{l=0}^{N-1}(I_{nl}1J_{kl}1 - I_{nl}0J_{kl}0) = \frac{\Gamma(n+\nu+1)(\Gamma(-\nu+1))^2}{2^{2\nu-1}\Gamma(n+1)\Gamma(\nu+1)}\frac{c_{nk}^{(\nu)}(N_1)c_{nk}^{(\nu)}(N_2)}{k^2+(n+\nu+1/2)^2}. \quad \text{(C.9)}$$

which can be checked with the Meijer G function representation of algebraic computer systems such as Mathematica [Wolfram Research, Inc.].